

May 2014

Quantitative Corrosion Evaluation and Damage Modeling in Ferrous Materials

Eric Walter Plante
Worcester Polytechnic Institute

Jaime Arnon De Souza
Worcester Polytechnic Institute

Joshua Abraham Morales
Worcester Polytechnic Institute

Khalil Fadi Badran
Worcester Polytechnic Institute

Follow this and additional works at: <https://digitalcommons.wpi.edu/mqp-all>

Repository Citation

Plante, E. W., De Souza, J. A., Morales, J. A., & Badran, K. F. (2014). *Quantitative Corrosion Evaluation and Damage Modeling in Ferrous Materials*. Retrieved from <https://digitalcommons.wpi.edu/mqp-all/1664>

This Unrestricted is brought to you for free and open access by the Major Qualifying Projects at Digital WPI. It has been accepted for inclusion in Major Qualifying Projects (All Years) by an authorized administrator of Digital WPI. For more information, please contact digitalwpi@wpi.edu.



Quantitative Corrosion Evaluation and Damage Modeling in Ferrous Materials

A Major Qualifying Project
Submitted to the Faculty
Of the
WORCESTER POLYTECHNIC INSTITUTE
In Partial Fulfillment of the Requirements for the
Degree of Bachelor of Science
By

Khalil Badran

Jaime De Souza

Joshua Morales

Eric Plante

May 1th, 2014

Professor Diana A. Lados, Advisor

Professor Cosme Furlong, Co-Advisor

Abstract

Corrosion is the leading cause of material damage. Quantitatively measuring corrosion effects and understanding the mechanisms are crucial to predicting/modeling this phenomenon and preventing it. The goal of this study is to develop a reliable testing and analysis methodology that allows quantitative evaluation and further prediction of corrosion damage in ferrous materials. To achieve this goal, a testing apparatus was built, and a relationship between corrosion rate and sample volume, environment, temperature, agitation, and time was uniquely created. Stainless steel samples were studied in a saline solution using two standard testing methods with various conditions. The changes in mass were measured, and an original optical methodology for both surface and cross-section damage evaluation was established. Over time, the change in mass showed an asymptotic decrease, whereas surface area damage increased asymptotically. An analytical relationship between corrosion rate and various controlling parameters was ultimately developed for damage prediction in corroded materials. These results and findings will be presented and discussed.

Table of Contents

Abstract	1
Table of Figures	7
Table of Charts.....	11
1.0 Introduction.....	12
1.1 Problem Statement	12
1.2 Key Questions	12
1.3 Methodology Overview.....	13
2.0 Background.....	15
2.1 What is Corrosion?.....	15
2.2 Economics of Corrosion.....	16
2.3 Thermodynamics of Corrosion.....	17
2.3.1 Relating Free Energy to Potential.....	19
2.3.2 Corrosion Induction.....	20
2.3.3 Corrosion Reactions	21
2.4 Forms of Corrosion	23
2.4.1 Intergranular	23
2.4.2 Pitting.....	25
2.4.3 Stress Corrosion Cracking	26
2.5 Corrosion Growth in Steels	27
2.5.1 Atmospheric Corrosion.....	28
2.5.2 Aqueous Corrosion:	29
2.5.3 Pitting in Stainless steels	29
2.6 Types of Corrosion Tests	30

2.6.1 Immersion Testing	30
2.6.2 Cabinet Testing	31
2.6.3 Electrochemical Testing	32
2.7 Corrosion Control.....	33
2.7.1 Iron Carbon Alloy Crystalline Structure	33
2.7.1.1 Sample	33
2.7.2 Heat Treatment of Steels	45
2.7.3 Material Selection.....	49
2.7.4 Passivity.....	49
2.7.5 Films/Coatings.....	50
2.7.6 Metallic Coated Steels	51
2.7.7 Cathode and Anode Protection.....	51
2.8 Background Test Types.....	52
2.8.1 Types of Corrosion Tests.....	52
2.9 Predictive Models.....	59
2.9.1 Mechanical Models.....	59
2.9.2 Electrochemical Models	63
2.9.3 Established Models.....	67
3.0 Methodology	71
3.1 Tests that apply.....	72
3.1.1 Loss/Gain in Weight.....	72

3.1.2 Cross-sectional Corrosion Damage Measurement	72
3.1.3 Surface Area Measurement	73
3.2 Current Testing Standards	73
3.2.1 Important specifications	74
3.2.2 Solution conditions	75
3.2.3 Current Testing Standards	75
3.2.4 Stirring Plate	76
3.3 Fixture	76
3.3.1 Apparatus	77
3.3.2 Initial Fixture Design	77
3.3.3 Secondary Fixture Design	79
3.3.4 Final Fixture Design	82
3.3.5 COMSOL Simulation	86
3.4 Part Drawings	93
3.5 Corrosion Induction	93
3.5.1 Background	94
3.5.1 Pre-Test Procedure	94
3.5.2 Solution Preparation	95
3.5.3 Sample Preparation & Handling	96
3.5.4 Total Immersion Test	97

3.5.5 Alternate Immersion Test	99
3.6 Data Collection.....	100
3.6.1 Mass Measurement.....	101
3.6.2 Surface Area Analysis	102
3.6.3 Cross Sectional Analysis	103
4.0 Results.....	108
4.1 Mass Data Analysis	108
4.1.1 Total Immersion Test 1.....	108
4.1.2 Alternate Immersion Test 1	112
4.1.3 Total Immersion Test 2.....	113
4.1.4 Alternate Immersion Test 2	117
4.1.5 Change in Mass after Sample Removal.....	118
4.2 Surface Area	118
4.2.1 Total Immersion Test 1.....	118
4.2.2 Total Immersion Test 2.....	119
4.3 Cross Section Analysis.....	123
4.3.1 Total Immersion Test 1.....	123
4.3.2 Total Immersion Test 2.....	124
4.4 Equation Formulation.....	126
5.0 Conclusions and Future Work	133
6.0 Recommendations.....	135
7.0 Acknowledgements.....	136
Appendix A: Part Drawings.....	137

Appendix B: Mass Measurement Data Tables.....	139
Works Cited	144

List of Figures

Figure 1: Corrosion on infrastructure.	16
Figure 2: Relative free energy diagram of three systems.	18
Figure 3: Intergranular corrosion.	24
Figure 4: Exfoliation corrosion.	25
Figure 5: Pitting of various depths.	25
Figure 6: Stress corrosion branching.	27
Figure 7: Mechanism of atmospheric corrosion.	29
Figure 8: Pitting corrosion system.	30
Figure 9: Stainless steel phase diagram.	35
Figure 10: Isothermal transformation for 400 steel.	36
Figure 11: Stainless steel cooling chart.	36
Figure 12: Spheroidite microstructure.	38
Figure 13: Bainite microstructure.	39
Figure 14: Martensite microstructure.	40
Figure 15: Various microstructures occurring in Fe-C alloys.	40
Figure 16: Equations on cooling temperature. (altered from [])	42
Figure 17: Cooling rate on a logarithmic time scale.	43
Figure 18: Cooling rate coefficient comparisons.	45

Figure 19: Quenching chart.	46
Figure 20: Anode and cathode current flow.	52
Figure 21: Comparison of EN and ER corrosion monitoring methods.	55
Figure 22: Pitting types.	57
Figure 23: Pourbaix FeO.....	60
Figure 24: Corrosion section Pourbaix.	61
Figure 25: Mixed potential theory.	66
Figure 26: Primary fixture design.	79
Figure 27: Independent rack design.	79
Figure 28: Circular flow apparatus design configuration.	81
Figure 29: Initial inlet and outlet.	81
Figure 30: Alternate inlet configuration.	81
Figure 31: Final flow configuration.	81
Figure 32: Complete assembly.....	82
Figure 33: Slot placement.	84
Figure 34: Tank support rack.	85
Figure 35: Sample rack holder.	85
Figure 36: Tank lid with notches.	86
Figure 37: COMSOL model geometry.	87

Figure 38: Velocity magnitude at t=2 seconds.	89
Figure 39: Velocity magnitude at t=6 seconds.	90
Figure 40: Velocity magnitude at t=10 seconds.	90
Figure 41: Velocity contour plot at 2 inch height.	91
Figure 42: Velocity contour plot with 3 inch height.	92
Figure 43: Contour plot and arrow surface at fixture height of 4 inches.	93
Figure 44: Mounting press.	104
Figure 45: Mounted sample.	105
Figure 46: Etching locations and resulting microstructures.	106
Figure 47: Microstructure of tempered martensite.	107
Figure 48: Small sample mass change.	109
Figure 49: Interval mass change.	110
Figure 50: Rate of interval mass change.	111
Figure 51: Small samples mass measurements.	111
Figure 52: Large sample mass change, initial total immersion test.	112
Figure 53: Total Immersion Test 2 small sample mass measurements.	114
Figure 54: Mass loss over time.	115
Figure 55: Combination of large sample mass change in Total Immersion Test 1 and 2.	116
Figure 56: Total Immersion Test 1 surface area corrosion damage.	119

Figure 57: Combined Total Immersion Surface Area Corrosion Damage.	120
Figure 58: Surface area of damage of Total Immersion Test 1.	121
Figure 59: Surface area of damage for Total Immersion Test 2.	122
Figure 60: Cross section of samples.	123
Figure 61: Cross sectional area for Total Immersion Test 1.....	124
Figure 63: Cross-sectional thresholding at different time steps during Total Immersion Test 1.	124
Figure 63: Cross sectional area for Total Immersion Test 2.....	125
Figure 64: Mass loss over 168 hours.	128
Figure 65: Surface area corroded (%).	129
Figure 66: Cross section corrosion area.....	130
Figure 67: Solved K_1 parameter value.	131

List of Tables

Table 1: Solution composition.....	32
Table 2: Electrochemical test methods	32
Table 3: Total Immersion Test 1 time intervals.....	98
Table 4: Total Immersion Test 2 time intervals.....	99
Table 5: Dip & Rinse time table	100
Table 6: Total Immersion Test 1 mass measurements small samples	139
Table 7: Total Immersion Test 1 mass measurements large samples.....	140
Table 8: Dip & Rinse Test 2 mass measurements large samples	140
Table 9: Dip & Rinse Test 2 mass measurements small samples.....	141
Table 10: Total Immersion Test 2 small samples	142
Table 11: Total Immersion Test 2 large samples.....	143
Table 12: Alternate submersion Test 2 small samples.....	143

1.0 Introduction

1.1 Problem Statement

Corrosion prevention is one of the largest issues in the production of ferrous metals. Any iron or steel product is likely to be affected by corrosion in its life time. Corrosion can be simply a cosmetic issue or it may pose a serious threat to the function of a product. Regardless of the concern, preventing corrosion is still one of the most challenging topics in steel production today. This project focuses on a stainless steel product that faces a harsh environment including above average temperatures and constant moisture with high salinity. In most cases this corrosion is only a cosmetic issue, but still creates a loss for the company in sales.

The sponsoring company has performed corrosion testing on products in the past, only returning comparative information. The challenge this team has been given is to develop a quantitative method for describing the corrosion experienced by the product independent of other products. With this quantitative method the team hopes to provide a groundwork for future testing with specific test procedures and equipment to be used so that a predictive model can be created with relative certainty.

1.2 Key Questions

When beginning this MQP, the group was faced with several questions that were deemed key. These questions were as follows:

- What materials are considered?
- What environments are of concern?

- How do the materials react in these environments?
- What testing type will appropriately address these operating conditions?
- What materials are to be studied (specifically heat treatment, protective coatings, etc.)?
- What is the desired life expectancy & performance of the test samples?
- What are some of the typical performance measures & test parameters used by the sponsoring company (environment & chemical cleaners, stress type/level, temperature)?
- Will we study actual samples or test specimens of similar geometry?
- What type of information/knowledge/methods/tools will be most useful to the sponsor's engineers for the samples design for corrosion resistance?

Each of these questions had a specific goal intended to clarify the objectives of this project. With cooperation from the sponsor's engineers, all of these questions were answered and the objectives that were stated previously were created under their supervision to ensure that the project satisfied all of the initial requirements.

1.3 Methodology Overview

The group researched causes of corrosion in metals and applied that knowledge to study its effects on the provided samples. The group tested all the components of each sample and recorded the effects that corrosion had on them over a predetermined period of time. From that point of study, the results were compared to the results obtained in different test environments and examined the effects on the sample product. The group created a specialized apparatus to conduct tests on the products and all their components. The results were analyzed for the duration of the testing period against ASTM standards. The created methodology differentiates between the separate parts and measures them accordingly.

The ability to evaluate corrosion over time will be of great aid to the engineers working with these specific products. Numerical values for different characteristics of the corrosion

growth and effects on these certain products will give insight to possible ways of improvement. From these numerical analysis', other engineers can grade the effectiveness of the samples against ASTM standards for corrosion. As a result, this study will help create a method of testing corrosion that applies specifically to ASTM standards for any specific product.

2.0 Background

2.1 What is Corrosion?

Corrosion is a chemical or electrochemical reaction between a metal and its environment that degrades or weakens the material. There are a few restrictions on the definition of corrosion. The first restriction is that corrosion does not include reaction on a nonmetal. Corrosion also does not include damage by physical deterioration. The main products in physical wear are metallic, and the products of corrosion are always non-metals formed by chemical reaction. Corrosion alone cannot damage metals, and is often a combination of physical and chemical degradation, which is termed corrosion erosion. The most common form, rust, is a specific form of corrosion involving the deposition of iron oxides on the material surface.

All substances aim to stabilize by achieving a low energy state. Corrosion is a natural process that provides a way for substances to lower their energy state, which is explained further in the following sections. Most metals, with the exception of very noble metals, will corrode under normal environmental conditions.¹ For the non-noble metals that do not corrode, a thin film of oxide products forms on the surface that protects against further corrosion.

Corrosion is always described as a combination of a metal with its environment. In order to fully understand a corrosive system, the effected materials and environment must both be identified. An analysis of the corrosiveness of an environment cannot be made without

¹ Davis

identifying the tested metal. The opposite is also true; an analysis of rate of corrosion of a metal cannot be made without information about the environment.

2.2 Economics of Corrosion

Corrosion is one of the most economically damaging issues that many engineering projects to date face. As such, engineers are confronted with the task of deciding whether the best of way of dealing with corrosion is to protect the subject with control methods, or design the subject so that part replacement is economically worthwhile. However, designing for corrosion resistance is an expensive business as the price includes the prices of resistant metals, the cost of protection, maintenance, and planned amortization.² From this, the initial cost of the structure isn't the only cost that must be considered, but also the maintenance over time as corrosion takes affect and the costs to keep the subject in proper working order increases.



Figure 1: Corrosion on infrastructure.³

² Talbot

³ Frodesiak

In terms of a dollar value, a 2002 study on the cost of corrosion conducted by NACE found the following. “Corrosion Costs and Preventive Strategies in the United States”, backed by the U.S. Federal Highway Administration, estimated annual costs at the time due to corrosion to be at \$276 billion dollars.⁴ For comparison, the Willis Tower cost around \$175 million dollars to build.⁵ Mathematically speaking, the United States could build 1577 Willis towers if corrosion costs were eliminated altogether. This amount puts a number on the issue to show how serious the impact of corrosion is in terms of economics.

2.3 Thermodynamics of Corrosion

Thermodynamics is a branch of chemistry that is helpful in predicting the chemical reactions that are possible based on fundamental natural laws. Thermodynamics provides a relation between the substances involved, and the environmental conditions. In this study, the use of thermodynamic principles has helped to explain test outcomes and support the physical data involved. Thermodynamics indicates whether or not a reaction will occur, but does not provide information about the rate of reaction. A review of the relevant thermodynamic terms and relations is presented in the following section.

Corrosion is a process that changes the chemical properties of a substance. The Second Law of thermodynamics applies in the form the Clausius inequality. The Clausius inequality states that the change in entropy of a system must be greater than or equal to zero. Entropy is a

⁴ Nace

⁵ Willis

measure of the disorder of a system; high entropy corresponds to a system that is in high disorder or is highly random. A process is only spontaneous if the total entropy is increased.

With this entropy principle and the First Law of thermodynamics, it follows that any spontaneous reaction, at constant pressure, must produce a decrease in the Gibbs free energy. The change in Gibbs free energy must be less than or equal to zero for the reaction to proceed in the direction written. The Gibbs free energy is defined as the enthalpy of a system minus the temperature multiplied by the entropy. The physical meaning of the Gibbs free energy of a system is the maximal electrical work which can be obtained from the reaction proceeding². Gibbs free energy¹.

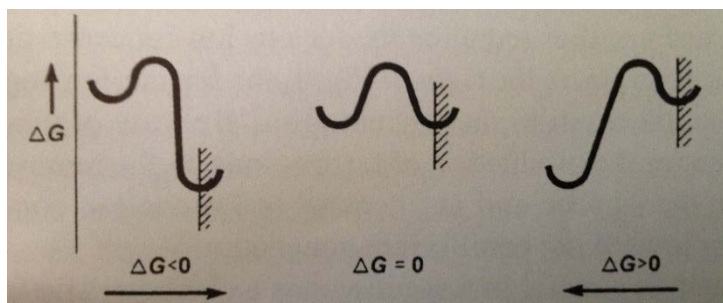


Figure 2: Relative free energy diagram of three systems.⁶

The change in Gibbs free energy of a system is determined by comparing the relative value of Gibbs free energy for the left trough to the relative value at the right trough. Starting from the left, the first diagram shows a process that will lower the Gibbs free energy of the system by proceeding from left to right. The middle curve shows a system in which there is no driving force for reaction in either direction because the start and end values of Gibbs free energy

⁶ Davis

are equal. The right curve represents a system that will produce an increase in Gibbs free energy by proceeding from left to right, so only the reverse reaction will occur. As this diagram shows, the direction of the reaction depends on the relative changes in Gibbs free energy.

All spontaneous processes continue until the change in entropy of the system has reached a maximum and the Gibbs free energy has reached a minimum. These two conditions represent a system that is in equilibrium, when the lowest energy state has been achieved. When a system is in equilibrium, there is no driving force for change.

2.3.1 Relating Free Energy to Potential

During the process of corrosion there is a constant transfer of potential charge within the system. The Gibbs free energy of a system can be related to the cell potential by the following equation₁:

$$\Delta G = -nFE \quad [1]$$

In the Eq. 1, “n” is the number of electrons transferred in the reaction, “F” is the Faraday’s constant ($F=9.649 \times 10^4 \text{ C mol}^{-1}$), and “E” is the electrical potential of the cell. The electrical potential is a measure of the driving force required to transfer electrons in the system. Combining Eq. 1 with knowledge of Gibbs requirements for spontaneity, it can be used to determine if a process will occur as written, or if the reverse reaction will dominate. A large positive potential difference produces a large negative value of Gibbs free energy and means the process is highly spontaneous.

The electrode potential for various metals is tabulated in an electromotive force (emf) series³. These tables typically record the standard reduction potential of a metal. The standard reduction and oxidation potential for a metal have the same magnitude but different signs. The emf series has potentials recorded at standard conditions, which correspond to 1 molar concentration and 1 atm pressure. The Nernst equation, Eq. 2, is used to account for non-standard conditions.

$$E = E^0 - \frac{RT}{nF} \ln Q \quad [2]$$

Metals that are higher up on the emf series represent metals that are more active. The emf series is limited for determining which metal is anodic in respect to the other, because the actual activity of a metal varies depending on the environment³. For this reason, galvanic series have been created that compare potentials in specific environments.

2.3.2 Corrosion Induction

Most corrosion processes are electrochemical, which requires a positive electrode, a negative electrode, and an electrolyte solution. Corrosion in a single material is similar to corrosion in a galvanic cell, which occurs between two separate materials allowing for various types of reactions. There are two parts to the reaction, chemical reduction which occurs at the cathode, and oxidation which occurs at the anode. The process is initiated when a low-resistance metal causes a short-circuit, essentially closing the circuit between the cathode and the anode. Small impurities embedded in the surface of a metal allow for the flow of electricity, creating a local-action cell. The surface of many metals contains a composition of electrodes created by

these surface impurities. As long as the metal stays dry, no current will flow and corrosion does not occur.

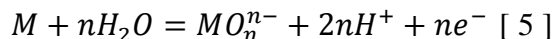
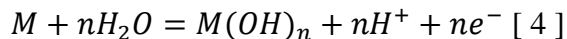
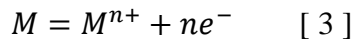
An electrolyte is a solution that contains a compound that dissociates into ions when dissolved by a solvent. For example, sodium chloride (NaCl) when dissolved becomes aqueous Na^+ and Cl^- ions. This ion containing solution carries the electrons that will be transferred from one electrode to the other. When the current is said to flow, the convention assumes the direction of a positive current, flowing from the positive electrode to the negative electrode. However, only negative charges (electrons) move in a metal, moving from the negative electrode to the positive electrode. In the negative electrode, oxidation occurs, which is a loss of electrons. The electrons that are lost in the reaction are now free to move. In the positive electrode, reduction occurs, which results in a gain in electrons. For this reason, electrons flow from the negative electrode that produces electrons to the positive electrode that requires electrons.

Slight differences in the potential of the surface of the metal create a cathode and an anode. Due to the differences in potential, the metal will lose electrons and dissolve in the solution. The electrons will stay behind and move to the anode, and at the cathode, the electrons are then taken up by a depolarizer. The depolarizer reacts with the metal in solution to form corrosion products that bind to the surface.

2.3.3 Corrosion Reactions

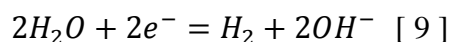
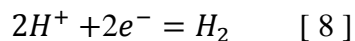
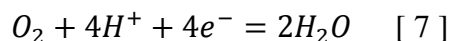
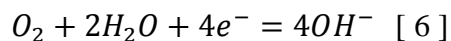
Corrosion reactions can be used to measure corrosion growth by observing the transaction of electrons flowing between the anode and cathode. When monitoring the corrosion

in a galvanic cell, the overall reaction must be split into two half reactions. At the anode, there are three typical oxidations that can occur involving the metal.⁷



In the three reactions, n is the number of electrons. The first oxidation is the production of metal cations where the metal is oxidized into an ion that goes into solution. This reaction frees up electrons that can now move to the cathode. The second reaction displays the formation of oxides or hydroxides which represent the corrosion products that develop on the surface of a metal and can prevent further oxidation. The final reaction represents the metal reacting with water in order to form an anion. These three oxidations all involve the release of electrons.⁸

The other half reaction occurs at the cathode and involves a reduction reaction. There are four typical reductions that occur at the cathode of a galvanic cell.



⁷ Baboian

⁸ Babion

The first reduction is in an aerated, neutral or alkaline solution in which the oxygen is reduced. The second reduction reaction is for an aerated cell with an acidic solution in which the oxygen is also reduced. The third reduction occurs in acidic solution, in which the hydrogen cation is reduced in solution to produce hydrogen gas. The final reduction occurs in neutral or alkaline solution and the hydrogen in water are reduced. As shown, these four reactions need to consume electrons in order to proceed.

2.4 Forms of Corrosion

Though corrosion is seen in many forms, there are two broad classifications: Corrosion that is not influenced by any other processes, and corrosion that is influenced by other processes. Stresses, as well as erosions, are examples of the corrosion that is influenced by another process while pitting is a chemical process separate from other corrosion attacks. The following information characterizes each type of corrosion potentially expected.

2.4.1 Intergranular

Intergranular corrosion is the targeting of the grain boundaries or adjacent areas in a sample. Highly magnified cross sections of a material will show grain boundaries that are distinctly separated by lines or borders. Figure 3 shows an example of the effects of intergranular corrosion. The grain boundaries towards the top of the photo have become much more pronounced where those towards the bottom are barely visible. It appears that the corrosion is making its way downward through the material spreading only by each boundary. This effect occurs when grain boundaries are specifically susceptible to attack, often caused by poor bonds

between grains. To treat or lessen the corrosion that results in grain boundaries heat treatments are often the method, and will be discussed in later sections.

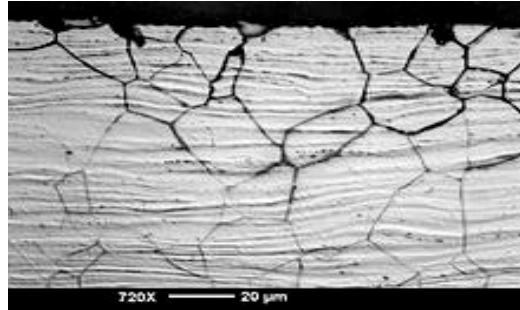


Figure 3: Intergranular corrosion.⁹

2.4.1.1 Exfoliation Corrosion

Exfoliation corrosion is a form of intergranular corrosion which lifts up the surface grains of metals. This effect is often rare and is an extreme case of intergranular corrosion. The force of expanding corrosion products occurs at the grain boundaries just below the surface. Materials most often affected are extruded sections where grain thickness is relatively small.¹⁰ Figure 4 shows a case of exfoliation corrosion where a section of material has been severely damaged. It is clear that material has been pushed to the edge and created a mass on the side of the structure by formation of corrosion products.

⁹ Antkyr

¹⁰ Calle



Figure 4: Exfoliation corrosion.¹¹

2.4.2 Pitting

Pitting corrosion is a type of corrosion that is formed on an unprotected or exposed part of an alloy that is previously coated by a film. These pits can have various depths, an example is shown in Figure 5.

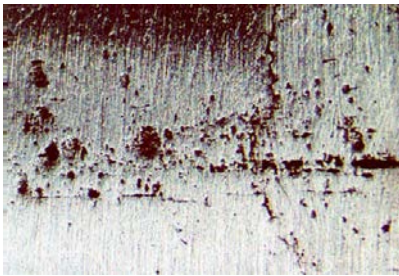


Figure 5: Pitting of various depths.¹²

Pitting corrosion is also influenced by many other parameters including environment, potential difference, temperature and metal composition, all factors that are involved in predicting corrosion rate or intensity. Pitting is considered to have various levels including: film breakdown, metastable pitting, pit growth, and pit death. The process will not start unless the

¹¹ NASA

¹² NASA

film breaks down, and a stable condition of growth of the pitting occurs for a short while before the actual pit begins to form. Metastable pitting occurs just after film breakdown where pit formation has begun, but has not developed a fully stable system. During metastable pitting the film may still close up and again prevent pit formation. Pitting is commonly used in the study of failure predictions.

2.4.3 Stress Corrosion Cracking

Stress corrosion cracking [SCC] is a gradual process that combines an applied load or tensile stress with a corrosive environments. There are three requirements for SCC to occur: The first general requirement is that the environment must promote cracking. The next requirement is the metal must be susceptible to SCC, and finally, the applied tensile stress must be above a minimum threshold. This threshold stress requirement to induce cracking is usually small due to its long term effects. Cracks in the metals or alloys usually proliferate at a rate from 10^{-9} to 10^{-6} m/s (4×10^{-7} to 4×10^{-4} inch/s). SCC can be separated into three stages:¹³

1. The crack begins to grow
2. Steady state stage where growth is linear
3. Final failure stage

¹³ ASM V13a

An example of SCC resulting in failure is the explosions of boilers in steam driven trains.

Figure 6 is a typical branching out formation of SCC: ¹⁴



Figure 6: Stress corrosion branching.¹⁵

This year the sponsoring company decided not to focus on SCC and left this type of testing as a future addition. For this reason the fixture design has included flexibility to incorporate future SCC testing as an added benefit, but will not be a focus of the project.

2.5 Corrosion Growth in Steels

This project specifically deals with corrosion in stainless steel. The following sections describe corrosion in various scenarios more specific to steels to provide a better understanding of the processes involved.

¹⁴ Calle

¹⁵ NASA

2.5.1 Atmospheric Corrosion

Atmospheric corrosion occurs under a water film deposited by atmospheric humidity. A very thin, absorbed film of water is required for corrosion formation, often obtained by dew accumulation alone. In the presence of water, hydrated oxides form which are the principal anodic process of steel corrosion. On the opposite end, cathodic corrosion occurs by oxygen reduction. Important factors in atmospheric corrosion include: time of wetness (TOW) or relative humidity, temperature, levels of chloride deposition, and presence of atmospheric pollutants. Each of these factors relate to the effectiveness of the electrolyte to conduct ions. TOW determines a material's exposure to an electrolyte. Prolonged exposure provides greater opportunity for ion transfer. Similarly, saline particle deposition and the presence of other particles will affect surface electrolyte formation. Particles such as chlorides, ionic in nature, can enhance electrolyte performance while others may inhibit ionic transfers. The presence of pollutants in the air such as sulfur and nitrogen oxides, which increase the acidity of precipitation, can also accelerate the corrosion process. Figure 7 shows an atmospheric corrosion system. This complex system all occurs in a single water droplet on the surface of the material and does not require much humidity for corrosion to begin.

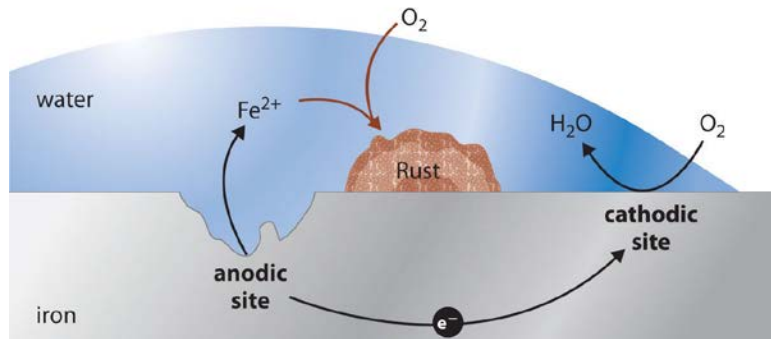


Figure 7: Mechanism of atmospheric corrosion.¹⁶

2.5.2 Aqueous Corrosion:

Aqueous corrosion is subject to the same operations as atmospheric corrosion with the difference of increased electrolyte availability. With the material submerged there is the potential for flow velocity which provides a sufficient supply of oxygen for stable oxide formation, accelerating corrosion. The largest difference between atmospheric and aqueous corrosion is that complete submersion provides a nearly infinite supply of ions and oxygen for the system to feed on. Much like in aqueous corrosion, pH can affect growth due to hydrogen evolution as a cathodic reaction.

2.5.3 Pitting in Stainless steels

Stainless steels are able to resist generic oxidation corrosion by the formation of a thin passive surface film. Pitting is a specific case of corrosion commonly found in stainless steels that undermines the protective layer through localized corrosive attacks, which produce pits. The propagation of pits involves the dissolution of metal and the maintenance of a high acidity at the

¹⁶ Flatworldknowledge

bottom of the pit by the hydrolysis of the dissolved metal ions. Figure 8 displays the formation of a pit system. The process begins within the surface defects of the steel where Chloride ions break down the oxide layer of the steel, and concentrate in the existing defects. A balanced system is composed of an anodic metal dissolution reaction at the bottom of the pit with a cathodic reaction on the adjacent surface. The system produces acid, which in turn propagates the pre-existing defect. Pit formation depends on maintenance of acid levels in the bottom of the pit, making the process extremely susceptible to circulatory flows.

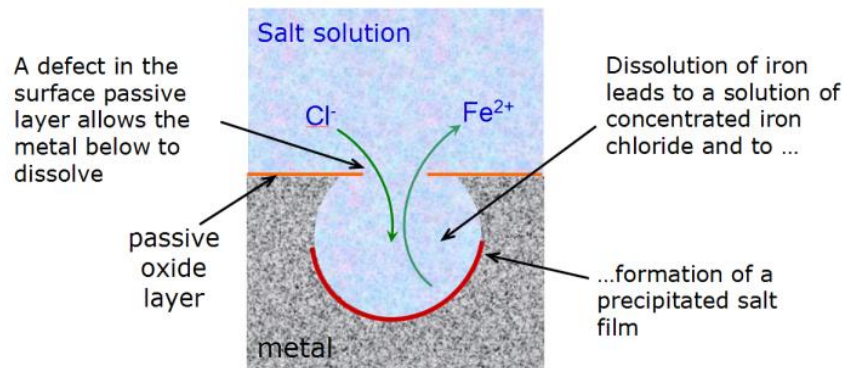


Figure 8: Pitting corrosion system.¹⁷

2.6 Types of Corrosion Tests

2.6.1 Immersion Testing

Immersion corrosion testing is the most commonly used testing methods to determine the corrosion rate of various metals in different environments. This testing method involves the complete immersion of the metal or alloy into an aqueous solution for a selected period of time. The immersion test can be changed by creating specific fixtures that can test for various

¹⁷ Davenport

parameters such as: SCC, resistance to pitting, hydrogen embrittlement, and galvanic corrosion while the samples are still immersed.¹⁸

2.6.2 Cabinet Testing

Cabinet testing, also known as salt spray testing, has been used for about 100 years to test the rate of corrosion of metals, and the resistivity of certain coatings applied to the metals. There has been extensive discussion of the salt fog test since its inception because of the reproducibility variances and the questionable correlation of results as related to actual “in-service” performance. Although many industries do not prefer the test, as it is not always applicable, changes have been made to the testing system creating more expansive and reliable results. The improvements made include tolerance limits for the test variables, which help in the production of reliable results, new test fixtures, and new procedures. However, there are still variables and different specifications that need to be implemented in the process so that test standards can be improved and better adapted to different applications.

The most commonly used salt spray test is the ASTM B 117, which yields amount and type of corrosive activity in a certain metal or alloy to compare to standards. Parameters of the test are shown in Table 1.

¹⁸ ASM V13a

Table 1: Solution composition

Test Method	Designation	Content	Specific gravity	pH	°C	°C	Duration
Salt Fog	ASTM B 117	5% NaCl	1.0255– 1.0400	6.5–7.2	35	95	24h/Cycle

2.6.3 Electrochemical Testing

Corrosion involves oxidation and reduction reactions, and therefore electrochemical tests can be conducted to study the corrosion mechanisms of metals and alloys. ASM Volume 13a has provided Table 2, which summarizes the electrochemical tests that can be used.

Table 2: Electrochemical test methods

Category	Test method
No applied signal	Open circuit or corrosion potential
	Dissimilar metal corrosion (galvanic corrosion)
	Electrochemical noise analysis
Small-signal polarization	Polarization resistance (linear polarization)
	Electrochemical impedance spectroscopy
Large-signal polarization	Potentiostatic and galvanostatic polarization
	Potentiodynamic and galvanodynamic polarization
Scanning electrode techniques	Potential scans
	Current scans
	Electrochemical impedance spectroscopy scans
Miscellaneous tests	Hydrogen permeation
	Anodized aluminum corrosion test
	Electrolytic corrosion test
	Paint adhesion on a scribed surface
	Impedance test for anodized aluminumodized
	Critical pitting temperature

2.7 Corrosion Control

Corrosion control has long been the goal of engineers to prevent the damages and costs related. As such many methods have been developed over the years to prevent corrosion. Whether it is by heat treatment or coatings, it is important to gain an understanding of the measures used to control corrosion before analyzing corrosion damage. Corrosion control in steel is the focus since that is the material under consideration.

2.7.1 Iron Carbon Alloy Crystalline Structure

In Iron-Carbon alloys, such as steel, there are several microstructures that should be understood when discussing corrosion. Each structure has different grain boundaries and properties that affect corrosion. The different structures include: fine and coarse pearlite, spheroidite, bainite, and martensite. For all but martensite, there are two phases present in the material.¹⁹ A fine crystal structure is a stronger material, but a coarse structure has a higher ductility and toughness. With a highly ductility the material can undergo greater plastic deformation without failure.

2.7.1.1 Sample Material

The examined samples were provided by the sponsor company. The information provided states that both large and small samples share the same composition. Both sample types are a 400 grade stainless steel, with a 0.6 [wt %] carbon and 12-13% composition by weight chromium. The number in front of the stainless steel is the AISI number used to identify the metal and its

¹⁹ MullenDore

properties. The first number identifies the types of steel, the second indicating if there are any alloying elements. The last two digits represent the carbon percentage of the metal. The AISI number of the steel involved in testing will not be given due to proprietary reasons, so 400 grade stainless steel was assumed. The 400 grade means that the samples are either a ferritic or martensitic structures. This lines up perfectly with the samples that are being evaluated and allows the use of phase diagrams to not only evaluate the structure and chemical make-up of the samples, but the effects that these will have on corrosion as well.

2.7.1.2 Phase Diagrams

Phase diagrams describe the crystal structure transformation of metals under specific conditions. During the heat treatment phase, the steel is raised to 1130°C to initially form an austenite structure. From there the structure is altered in the cooling stage to martensite, which is seen in Figure 9, the 0.6 [wt %] carbon means that the samples started in the pearlite region.²⁰ These regions are important for corrosion damage, each type of crystalline structure has various impacts on the corrosive growth of the sample. These effects of the crystalline structure on the corrosion are discussed in a further section.

The cooling phase is another important aspect of the stainless steel creation process. Cooling is a factor that affects how the crystalline structure forms. The rate at which the steel is cooled, temperature, and medium should all impact the final result. The crystalline structure formed as a result of cooling is the final structure that the metal will have. While the structure can change during the heating process, the cooling process is what the solid version of the metal

²⁰ Callister

will have. Therefore, getting the steel to the right temperature in the right amount of time is very important. A benefit of alloying the material of steel is that it decreases the critical cooling temperature of the steel. This in turn makes it easier to form martensite in the material and in thicker cross sections. This is useful as martensitic structures have numerous benefits, and have a unique relationship with corrosion compared to other microstructures²¹.

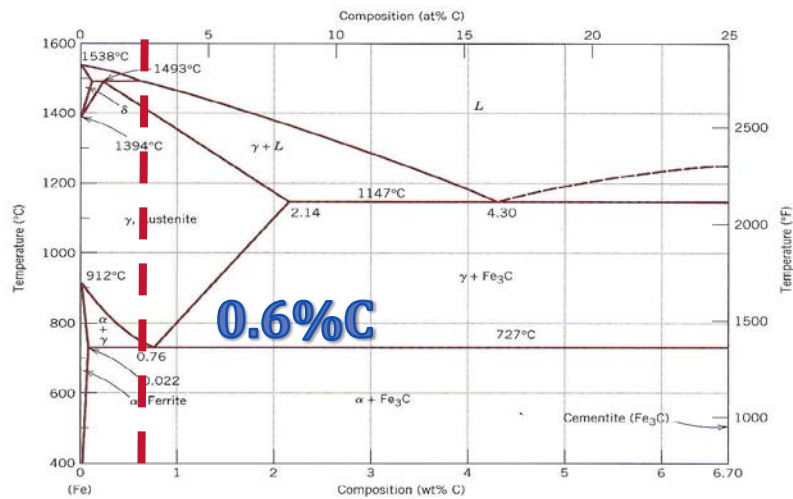


Figure 9: Stainless steel phase diagram.²¹

The cooling process is important in the overall corrosion process, due to the cooling influence on the metals. When looking at the cooling graphs of the stainless steels, the curves that indicate the transition of the metal into different structures rely on the rate of cooling. The charts are based on the time and temperature and can be seen in Figure 10.

²¹ Callister

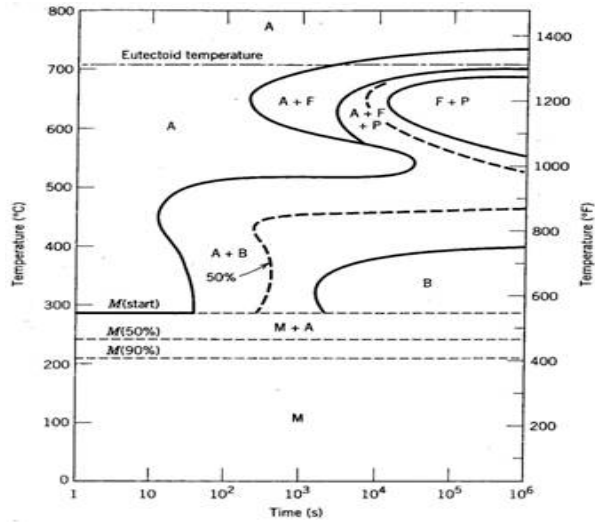


Figure 10: Isothermal transformation for 400 steel.²²

The martensite structure only forms when the cooling temperature rate reaches 120°C/s in approximately 1 seconds. What this means is that the rate of cooling on each metal influences its final phase type. Hence from our known samples, we can roughly estimate the minimum cooling rate required to produce the conditions that are under observation. From this, confirmation about the structure of the samples can be made when combined with images from the microstructural analysis.

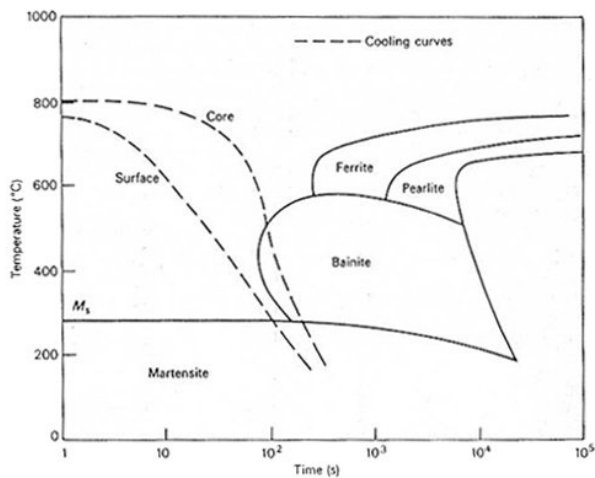


Figure 11: Stainless steel cooling chart.²³

²² Callister

²³ Materials Knowledge: Hardenability of Steels

It should be noted that alloyed steels have a slightly different cooling curve than normal iron-carbon diagrams. The additional elements involved in the alloying process can create multiple differences in the cooling diagram. These variations can range from, but aren't limited to the following: shifting to the longer nose of the austenite to pearlite transformation, and the formation of a separate bainite nose. These alterations to the cooling diagram mean that different cooling rates can be used to result in different structures when compared to the normal chart. The charts are often represented in terms of log time, so careful evaluation of the time taken during the cooling process is essential when determining the minimum time and temperature rate change to achieve a certain structure. This is important as with the samples under review, only a small portion of the composition is known. Therefore, the closest possible charts are used as a best estimate of the composition.

2.7.1.3 Pearlite

Pearlite is a microstructure that forms when there is an increasing amount of Fe_3C in a steel alloy. If this occurs while holding all other elements constant, then the result is a harder and stronger material. This also results in a higher tensile and yield strength, along with a Brinell hardness increase. However, as the carbon content of this structure increases, it suffers a decrease in both ductility and toughness. Pearlite has two phases, ferrite and cementite, which influence the mechanical properties of the material. While cementite is strong and rigid, it also restricts the deformation of the material.²⁴

²⁴ Bhadeshia

2.7.1.4 Spheroidite

Of all the steel alloys, spheroidite microstructures are the weakest and softest. In turn for this weakness however, they are the most ductile.²⁵ Alloys that contain a pearlitic microstructure have greater strength and hardness than those with a spheroidite microstructure. Pearlitic alloys also have less boundary area per unit volume than in spheroidite. However, spheroidite has boundary structures that are not nearly as constrained. They are also very tough as cracks only encounters a very small fraction of the brittle cementite phase, making propagation difficult. The crystalline structure of spheroidite is that of rods and spheres. Figure 12 shows the magnified microstructure of spheroidite where these spherical cementite phases are generally seen.

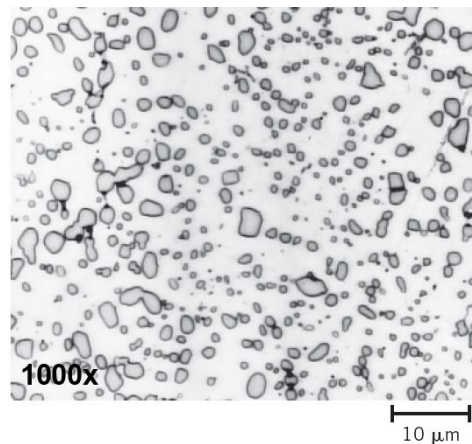


Figure 12: Spheroidite microstructure.²⁶

2.3.1.4 Bainite

Bainite is a very useful class of steel as its structure is generally finer, stronger, and harder than those of the pearlite microstructure.²⁷ They have a desirable combination of strength and ductility, which makes them an ideal material structure for many tasks. The bainite grain

²⁵ Mullendore

²⁶ Callister

²⁷ Mullendore

boundaries are similar to martensite boundaries, only smaller and deformed due to nucleation.²⁸

Figure 13 shows the fine grain formation in bainite where grains are smaller and closely packed together giving the material higher strength.

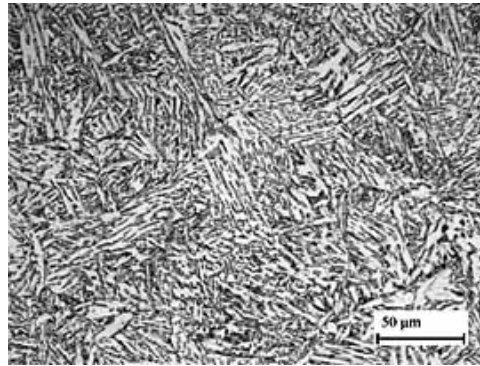


Figure 13: Bainite microstructure.²⁹

2.3.1.5 Martensite

Martensite is the strongest and hardest microstructure in iron-carbon alloys and is also the most brittle (it has negligible ductility).³⁰ The overall hardness of the martensite structure depends more on the carbon content, rather than on the microstructure. Instead, the properties are attributed to the interstitial carbon atoms, which hinder dislocation motions and relations to slip systems. When failure occurs, the structure is forced apart on the atomic level, meaning slips systems are the means on which the material fails. The presence of carbon atoms inhibits damage from progressing through the iron crystal structures. The structure of martensite is plate shaped.³¹

²⁸ Bhadeshia

²⁹ Callister

³⁰ Mullendore

³¹ Bhadeshia

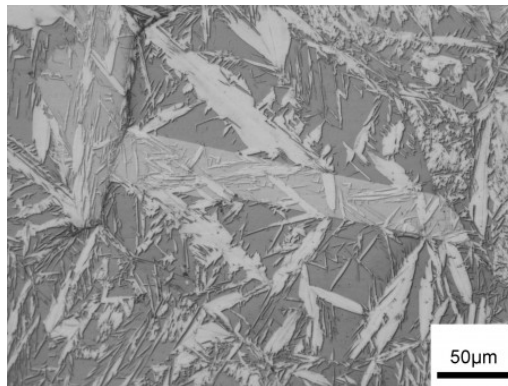


Figure 14: Martensite microstructure.³²

Microstructures of iron-carbon alloys

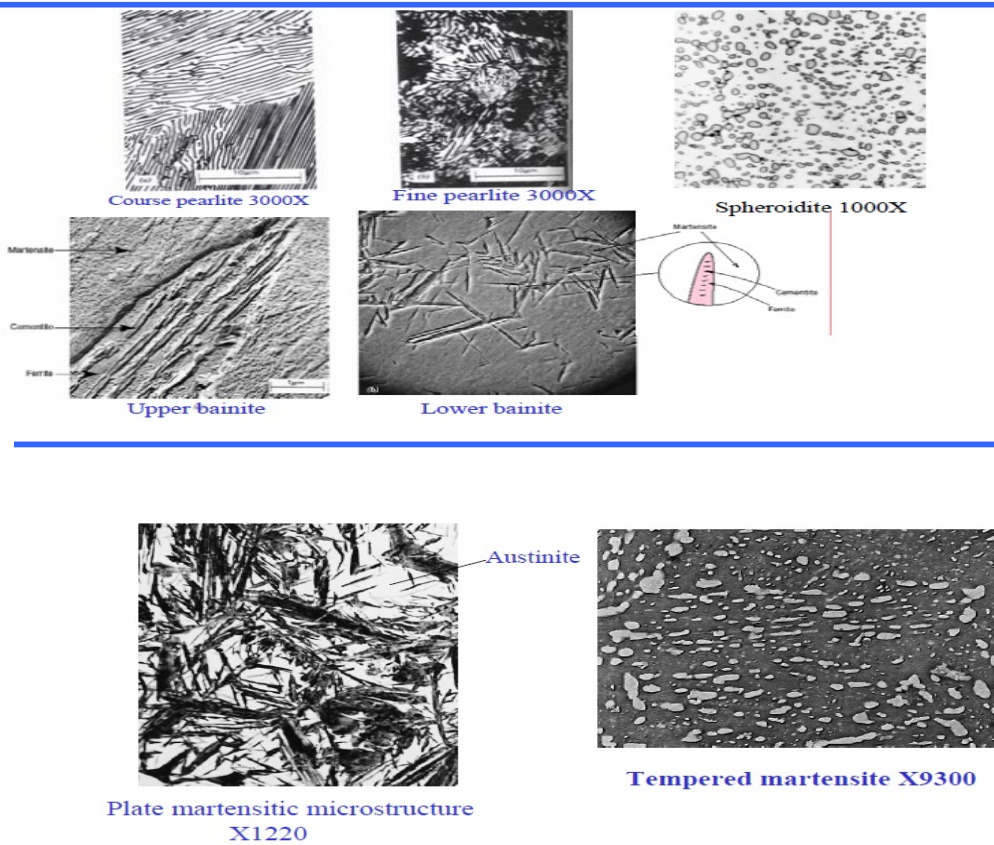


Figure 15: Various microstructures occurring in Fe-C alloys.³³

³² Hero-m

³³ Callister

2.7.1.6 Effects of Crystalline Structures

Each of the previously described structures result in different grain boundaries for the material involved. Due to the fact that intergranular corrosion attacks along the grain boundaries, the corrosive effect varies according to each crystalline structure. The larger the grain boundary, the more effect corrosion has on the sample. Due to this factor however, martensitic structures are less resistant to corrosion than other grades of steel.³⁴ In terms of corrosion resistance, austenitic steels have the highest resistance, with ferrite next in line. Austenite has the highest corrosion resistance due to its high chromium percentage with a mixture of nickel.

2.7.1.7 Cooling of Samples

Figure 16 is a representation of the cooling rate of a 400 grade stainless steel. The necessary cooling rate to maintain a completely martensitic structure must be high enough to completely avoid the lower nose. Due to this general restriction, parameters of the cooling rate equation can be determined. It should be noted that any equations given in the following section are solely based on the maximum or extreme case of just avoiding the nose. It is entirely possible the cooling rate is more extreme and accomplished in a shorter time, hence altering the suspected equations. The overall results however, would be the same in accomplishing a fully martensitic structure.

³⁴ Stainless Steels

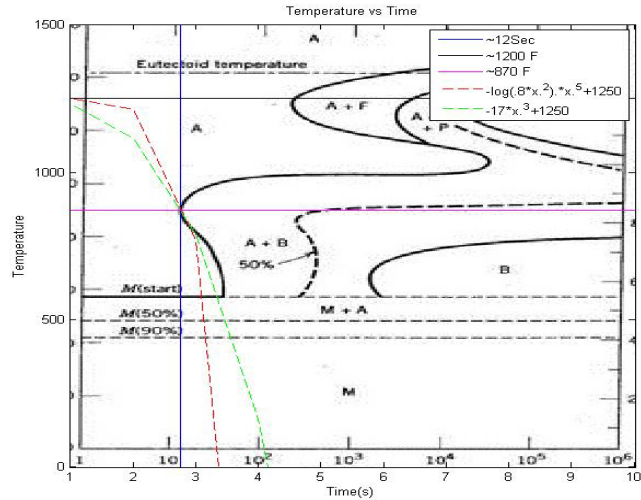


Figure 16: Equations on cooling temperature. (altered from [35])

The alterations have been made to indicate the known values and estimates. It is known that the samples used undergo an initial heating up to a temperature of 1200°C. Slight estimation and adjustments have been made to adjust for the image variation due to book scanning. Using the chart that was provided in the book, taking into account the logarithmic x-axis of graph and a constant y, the equations were estimated. The equations that are used in Figure 16 are not based in the logarithmic scale, but they can be translated roughly to the book's graph. Once the general shape of the equation is known, other guesses can be attempted in relation to the curves.

Figure 17 shows the first attempt at an equation curve that could represent the cooling rate. Using the known starting temperature and estimating the furthest point of the nose at around 12 seconds, a decay equation was found.

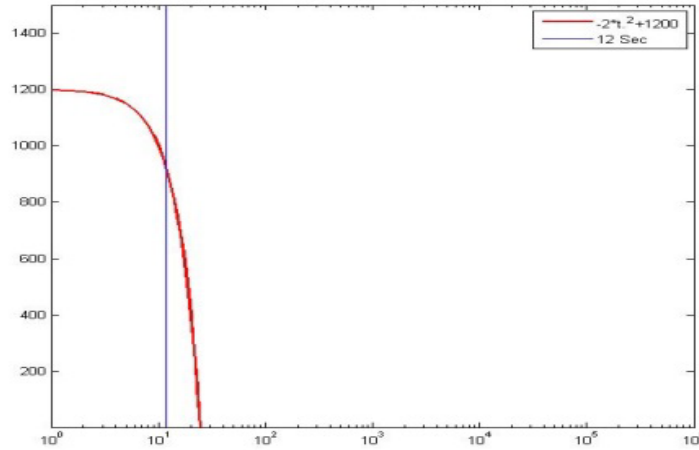


Figure 17: Cooling rate on a logarithmic time scale.

Another method to evaluate this is to look at the cooling method used to cool the samples. Using heat transfer, known equations, and the known variables allows for the determination of the temperature change and conditions constituting the temperature change. Due to the sample sizes, the first equation that should be considered is the equation to determine the Biot number of the sample.

$$B_i = \frac{h}{k} L_c \quad [10]$$

Here L_c is the characteristic length of the sample, the ratio of volume over area. Estimating a convection coefficient (h) of 100, which is a very plausible value in the range of water, and a thermal conductivity (k) of stainless steel, the Biot number for our sample is much less than 0.1. As a result of this, the small answer means that the lumped capacitance method of heat transfer can be used as shown in Eq [11]. If the value were greater than 0.1, then this method would not be practical.

$$\frac{T_f - T_\infty}{T_i - T_\infty} = \exp\left(-\frac{h}{\rho c L} t\right) \quad [11]$$

$$T(t) = (T_i - T_\infty) \exp\left(-\frac{h}{\rho c L} t\right) + T_\infty \quad [12]$$

For Eq. 12, the ρ is density in kg/m^3 and c is the specific heat of the material. T_∞ is the temperature of the surroundings, and the T_i is the initial temperature of the sample. Using the measured dimensions of the sample, along with the use of Matlab to evaluate the results, the cooling rate was determined.

The measured length of the sample was 0.035 meters, the width was 0.005 meters, and the thickness was 0.01 meters. The k value for stainless steel is 15.1 and the specific heat is 480. The density value used was 8055 kg/m^3

Since there is an estimated time and temperature for the phase change bulge, the equation for temperature as a function of time can be created. From this, the relationship of the multiple variables can be evaluated and the effects on the cooling rate determined. Figure 18 shows the results of these estimations. Comparisons can be drawn in regards to the interactions and the points of interests of the temperature change. It also allows for the estimation and speculation as to what fluid is used in the cooling process and what temperature the fluid may be at, allowing for an overall assessment of the material under speculation. Even with the assumptions being made, this equation provides a reasonable assessment of the overall cooling equation of the samples, as the cooling rate is not linear, but exponential over time.

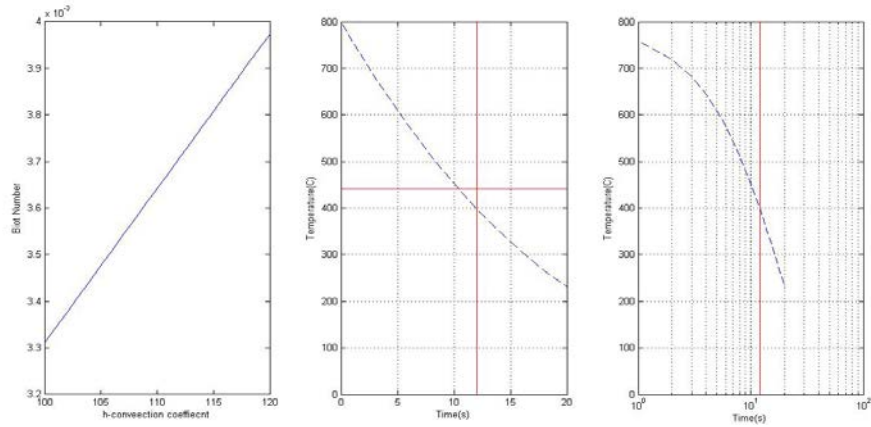


Figure 18: Cooling rate coefficient comparisons.

2.7.2 Heat Treatment of Steels

The heat treatment of steel is about one thing, producing martensitic steel. This is accomplished through the continuous and rapid cooling of an austenitized specimen.³⁶ During heat treatment, the material's structure undergoes various changes to ideally create a stronger metal. Most companies focus on the formation of high content martensitic steel. A sample of steel that has been successfully heat treated results in the formation of a steel with a predominantly martensitic microstructure. A high degree of martensite in the structure, not only means that there is primarily martensite on the surface, but that there is a strong presence throughout the interior of the specimen as well. There are three requirements which include:

1. Composition of the alloy
2. Type and character of the quenching medium
3. Size and shape of the specimen

³⁶ Mullendore

Heat treatment also has a factor in the hardenability. Hardenability is the influence of alloy composition to transform to martensite in a particular quenching treatment. It's important to note that hardenability is not true hardness. Hardness describes the resistance to indentation while hardenability represents the depth to which a material is hardened during heat treatment.

When heat treatment is performed on steels, the severity of the quench is another factor that must be taken into consideration. Severity of quench is the term used to indicate the rate of cooling.³⁷ The more rapid the cooling of the steel, the more severe the quench is. When cooling steels, the three most common mediums used are water, oil, and air. In terms of severity of quench, water has the most severe quench, followed by oil then air. During the cooling of metals, simple thermodynamic properties have to be taken into account. An example is that the velocity of the cooling media influences the cooling rate of the metal.

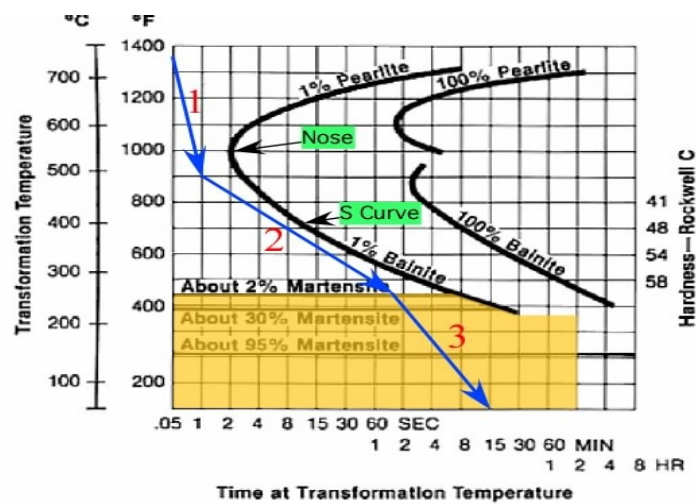


Figure 19: Quenching chart.³⁸

³⁷ Mullendore

³⁸ Callister

The purpose of these methods is to protect the metal from corrosion. The heat treatments focus on the diffusion method of corrosion. Martensitic crystal formations have interstitial carbon atoms, which occupy the space of iron atoms in steel, hindering diffusion. The presence of interstitial carbon atoms does not prevent corrosion completely but slows down the process of corrosion through diffusion. This diffusion process is known as interstitial diffusion, where atoms migrate from one interstitial position to a neighboring one that is empty.

Heat treatment must be used with caution some about materials. While heat treatments may help prevent corrosion of some types, it leaves the material vulnerable to other attacks. An example of this situation is shown in stainless steel. Normally, chromium carbides form on the grains and help prevent growth, whereas some heat treatments may remove the carbides and leave the metal more susceptible to corrosion.

2.7.2.1 Annealing

Annealing is the process of exposing the metal to high temperatures for an extended period of time and then controlling the cooling process to slow it down.³⁹ Heat treatment is performed to prevent vacancy diffusion. Vacancy diffusion occurs when there are atomic gaps in crystalline structures lattice sites. Vacancy in these lattice sites mean that atoms can migrate from one location to another. Annealing is used to primarily affect three aspects of steels:

1. Relieve stresses
2. Increase softness, ductility, and toughness
3. Produce specific micro structures

³⁹ Mullendore

When performing annealing, there are three stages that need to be considered: the initial heating to the desired temperature, the “soaking” or holding the metal at temperature, then slowly cooling the metal.

2.7.2.2 Normalizing

Steels that have been plastically deformed often consist of grains of pearlite, which are irregularly shaped, relatively large, and substantial in size. Normalizing refines these grains, decreases average size, and produces a more uniform and desirable size distribution.⁴⁰

Normalizing is accomplished by holding the temperature of the sample to at least 55°C above the critical temperature for transformation, and allowing time for complete transformation into austenite. Finally, the cooling process is done by air cooling.

2.7.2.3 Full Annealing

Full annealing is often utilized in low and medium carbon steels. For this, the alloy is treated by heating to a temperature of about 50°C above critical temperature. The metal is furnace cooled and will have a pearlite structure. Furnace cooling means that the furnace is turned off, and the metal is left inside to cool at the same rate as the furnace. This results in small and uniform grain boundaries.⁴¹

⁴⁰ Mullendore

⁴¹ Mullendore

2.7.3 Material Selection

One of the most important considerations in corrosion control is the material selection. For example take an alloy of two metals alpha and beta. Between those two metals there will be one that is more active and one more passive to corrosion. As a result when corrosion begins, the more active metal will corrode and more passive metal will not. As such, by using a material with a majority of passive metals, it will only face limited corrosion by its active sections. This gives engineers some control over the formation of corrosion. It is important to keep in mind that single phase alloys still have better corrosion resistance than two phases.⁴²

2.7.4 Passivity

When a metal undergoes corrosion, a chemical reaction occurs on the surface. As a result of this chemical reaction, corrosive products are left over. Engineers have been able to use the chemical reaction formula to determine the type of product that will result from the corrosion reaction and utilize it. This is a passive protection from corrosion. As the corrosion starts to occur the solution and sample are in contact. Corrosive products form from this process, and stay attached to the surface of the sample. Overtime, the surface of the metal will be completely protected from the solution by a layer of corrosive product. This is one of the reasons that stainless steel, which is highly resistant to corrosion, is an iron–chromium alloy. Since the sample and solution is no longer in contact, the corrosion reaction ceases, which stops the corrosion of the surface. From this, engineers have applied films to the surface of the metal to

⁴² Mullendore

prevent any corrosion to begin with. While they do their job, the films are often extremely thin, some on the order of angstroms (10^{-10}m).⁴³

2.7.5 Films/Coatings

While some materials form a protective layer via the passivity method, sometimes metals are coated in a proactive layer to prevent any kind of corrosion. These films are employed when other methods are inappropriate or economically impossible.⁴⁴ These coatings and films are normally paints, based on alkyd and epoxy resins. They are applied as liquids which subsequently polymerizes onto hard surfaces, such as that of metals.⁴⁵

Other more inexpensive metals that require film protection may also be coated in a thin layer of corrosion resistant material. Although metals are the most common coating material, there are organic options as well, such as silicon. Resistant metals are often expensive, which is why they are used sparingly. Resistant metals are often applied by the process of electrode position. This method is important as it is for the study of stainless steels. Due to the large percentage of chromium located in stainless steels, when corrosion occurs, the film method takes place. During the corrosion of stainless steels, chromium forms a passive film of chromium oxide on the surface of the metal. This film creates a barrier between the metal and oxygen, which in turn stops the corrosion process. This also has another benefit as the corrosion is

⁴³ Callister

⁴⁴ Talbot

⁴⁵ Talbot

prevented for spreading into the interior structures of the steel, which would cause major damage or possible failure of the structure over time.

2.7.6 Metallic Coated Steels

Metallic coatings provide a barrier between the steel and electrolytes. There are two categorizations of coatings: noble coatings, and sacrificial coatings. Noble coatings are comprised of noble metals in the galvanic series. These coatings fail in areas with surface defects or porosity where galvanic current accelerates attack of the base metal, which will eventually undermine the coating. Sacrificial coatings create an anodic surface to steels. At the pores, the direction of galvanic current through electrolytes moves from coating to base steel. As a result of this movement, the base steel becomes cathodically protected.

2.7.7 Cathode and Anode Protection

Corrosion is a cycle that continues as long as the cycle path is completed. In an electrochemical corrosion cell, there are four main parts that must be present for corrosion to occur. These are the anode, cathode, an ionic path through the solution, and electric path through the metals. This is a very destructive process over time, so engineers have found that by interrupting the process, corrosion can be halted. This is done by cathodic protection. Cathodic protection occurs when an external source supplies electrons to the anode, making it a cathode and reversing the corrosion process. Since the anode, which usually gives up electrons to corrode, no longer loses its electrons, the process of corrosion oxidation ceases. Figure 20 displays a basic functioning corrosion system between a cathode and anode. This process of cathodic protection in some way breaks the cycle and transfer of ions.

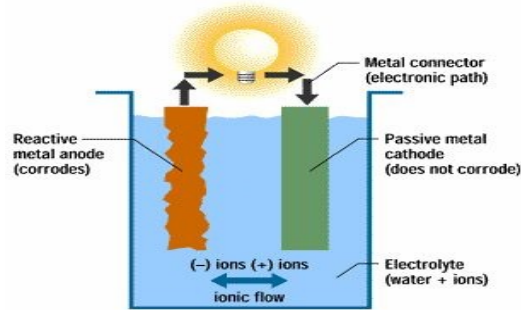


Figure 20: Anode and cathode current flow.⁴⁶

2.8 Background Test Types

2.8.1 Types of Corrosion Tests

This section investigates various methods for testing and ultimately quantifying corrosion growth. Testing types range dramatically in terms of difficulty and produced values. Whether a complex electrochemical examination or a simple optical test is conducted, these measures provide valuable information regarding corrosion. When examining corrosion, each test provides a piece of information to a varying degree of accuracy. These tests have been developed and improved over the years to aid engineers and scientists in evaluating the effects of corrosion. The following tests are believed to have potential to be involved with the experiment. From this initial research, a series of several tests will be chosen to effectively quantify results. The end goal of this project is to provide numerical analysis accurately describing the corrosive effects observed. Consider this, the following topics were studied:

2.8.1.1 Visual Observation

Visual observation is one of the simplest corrosion test procedures. This method involves simply viewing the specimen by eye to ascertain the results of the test. While this test works well

⁴⁶ Principles of Corrosion

in combination with other tests and is very simple to complete, it still suffers from several factors. Commonly it is used for comparative analysis, but offers no numerical or individual description. There is no way to get a quantitative result from this test and the results are subject to human error and individual judgment.

2.8.1.2 Loss/Gain in Weight

Loss/gain in weight experiments are a valuable and relatively simple test when analyzing the physical effects of corrosion. The test requires only a laboratory scale and are relatively simple. By measuring the gain or loss of mass over time, the damage can be measured quantitatively. A large number of test specimens are required for this test type and can suffer from measurement errors. For this specific study, a measurement of relatively high accuracy is required. Specifically, the scale used must be accurate to 4 decimal places.

Instead of measuring mass loss, sometimes the gain in weight is measured. This method assumes that all the corrosion products that formed on the sample stay on the surface and that the chemical stoichiometry is known. Although mass gain measurements are used, the most common change in mass measurement is weight loss.

After the data for weight loss experiments has been recorded, Eq. 13 can be used to calculate the corrosion rate:

$$CR = \frac{K*W}{A*T*D} \quad [13]$$

In the Eq. 13, K is a constant used to ensure proper units, W is the mass loss in grams, A is the area in cm², T is the time of exposure in hours, and D is the material density in g/cm³. If K is set to 3.45*10⁶, the answer will be in mils per year (mpy), and if K is 8.76*10⁴ then the

solution will have units of millimeters per year (mm/y). For most steels and stainless steels, the density is around 7.9g/cm^3 .⁴⁷

2.8.1.3 Change in Electrical Resistance

Electrical resistance tests play a major role in measuring the growth of corrosion via intergranular attack. The idea behind electrical resistance (ER) monitoring is that once a sample is exposed to a corrosive environment, the surface area decreases and results in an increase in resistance. The change in resistance is related to the change in surface area or depth, and can be used to determine a corresponding corrosion rate. This test is very useful in that it does not disturb the specimen during testing, so a single specimen can be tracked over time. The response from electrical resistance monitoring to localized corrosion is limited, and this leads to the production of a relatively easy time curve.⁴⁸ Though there aren't many drawbacks with this testing type, there is the issue that the type of attack cannot be determined from this test.

The change in electrical resistance monitoring technique was recently used in a study to determine corrosion rates. The study was conducted on concrete samples that were tested by periodically wetting and drying the samples. Figure 21 shows the results for the comparison of the ER and the electrochemical noise (EN) method of corrosion monitoring.

⁴⁷ Vander

⁴⁸ Legat

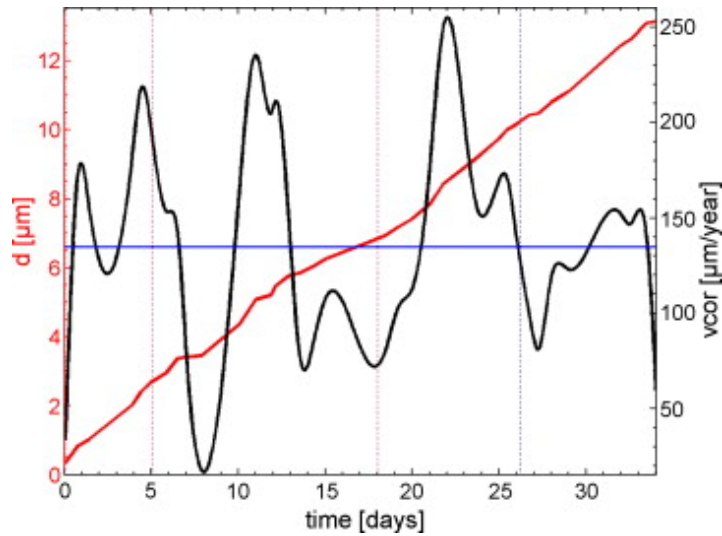


Figure 21: Comparison of EN and ER corrosion monitoring methods.⁴⁹

This study confirmed that the ER probes were able to reliably measure the cumulative as well as average corrosion rate.

2.8.1.4 Hydrogen Evolved/Oxygen Absorbed

The hydrogen evolved test focuses on the hydrogen evolved from the corrosion process into the solution. This test allows for the easy creation of time curves as the hydrogen can be measured without disturbing the specimen. The test is useful in that it examines the solution the specimen is in, but it does not help examine the distribution of the attack.

The oxygen absorbed test follows many of the same steps as the hydrogen test, where the solution is tested and the specimen remains undisturbed. The reading is done with a DO probe, which is a device that measures the percentage of oxygen dissolved in the solution, so the results

⁴⁹Legat

can be tracked over time. As the samples corrode, the relations of the oxygen dissolved rate will allow for the evaluation the corrosion rate.

During both tests the samples cannot be disturbed. That means that once the samples are set and the test begins, they cannot be moved. As such any movement of the apparatus or disturbances could potentially influence the results, so precautions should be taken to ensure accurate results.

2.8.1.5 Depth of Pitting

Depth of pitting allows for the examination of the corrosive effects at a microscopic level. The examination of the pitting is adaptable to determine the total attack of the corrosion. It also allows for the measurement of corrosion penetration by all methods except intergranular attacks, which occur not as localized sites but follow grain boundaries. This testing method does have drawbacks such as the need of multiple testing samples, and a difficulty in gaining accurate measurements. However, as more samples are taken, any possibilities for errors will be minimized as an average will be taken for all the samples. Figure 22 displays the cross section of various pit types that can be measured by their depth, but also in other ways. Pits may also be described by the average size (in diameter) or by the average density of pit occurrence (in number of pits/area).

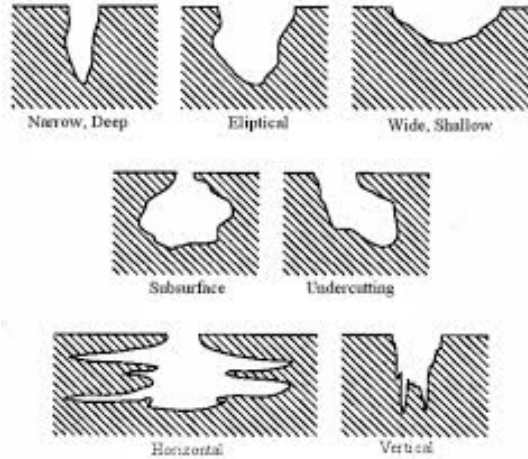


Figure 22: Pitting types.⁵⁰

2.8.1.6 Microscopic

Microscopic testing allows for the determination of the type of corrosive attack affecting the sample. This testing allows for measurements of pitting and the study of the initiation of the corrosion attack. It serves the purpose of supplementing the results of other tests, but otherwise does not offer many other benefits. It also suffers from the fact that it cannot be used for quantitative measurements.

2.8.1.7 Change in Physical Properties

This test method focuses on the structural properties of the specimen. Tests involving the change in physical properties range in many degrees because there are many physical properties. The physical properties that are most valuable to the project at hand however, are not of a quantitative use if tested. As such, any physical property changes would be worth the effort

⁵⁰ Corrosion Clinic

required when there are other tests that would reveal more information about the nature of corrosion.

2.8.1.8 Electrochemical

a. Single Electrode Potential

Electrochemical testing provides several methods for corrosion testing. Single electrode potential is a method that focuses on the study of film formation and breakdown. This type is useful with other tests to determine the total corrosion of the sample. Single electrode potential allows for the determination of film surface stability, though it is difficult to interpret and does not measure the amount of attack to be expected.

b. Potential Difference between Two Dissimilar Metals

Measuring the potential difference in the sample allows for the opportunity to study the galvanic effects that are occurring in the test specimen. This test helps to determine which metal will be more severely corroded due to the effect of the solution that is used. This test primarily helps to determine which metal will corrode more severely. The issues with this test are that results are not quantitative, and polarization characteristics (described in the section anodic and cathodic polarization) are more valuable for the purpose of corrosion analysis.

c. Film Resistance Measurements

The film resistance test focuses on determining the penetrability of the surface films of the specimen when in contact with various solutions. This test gives a quantitative measurement of the influence of anions on the probability of the breakdown of films. This test has difficulties when performed, as the voltage used must be standard. Also, other reactions must not occur

when this test is being performed, as these reactions can interfere with the measurements recorded.

2.8.1.9 Electrometric

Electrometric testing focuses on measuring the thickness of the film surface. This is a simple and accurate method for determining these quantities, and therefore provides quantitative results. It is however, limited to samples that have adherent, thin surface films on certain metals.

2.8.1.10 Influence of Metal on the Environment

This series of testing revolves around completely qualitative factors of the sample following testing. Intended for the investigation of effects the sample would have on the environment or its duty following corrosion, it has very few quantitative purposes. One purpose is to examine whether the corrosion products have a detrimental effect to the quality of a product. It is also often used to determine what metal should be used in a product. However, such measurements don't reveal any relevant information into the nature of the corrosion attack. That being said, there is still a purpose that can be employed, provided only as supplementation to other, more quantifiable tests. It may be employed by visual means such as the naked eye, or any magnification of such.

2.9 Predictive Models

2.9.1 Mechanical Models

Scientist and engineers have often attempted to model the nature of corrosion; however, this modeling depends on a multitude of variables. There are a few basic models that are commonly consulted to determine the nature of corrosion. This section describes models based on the mechanisms of corrosion growth. The first of these is the Pourbaix diagram.

2.9.1.1 Pourbaix Diagram

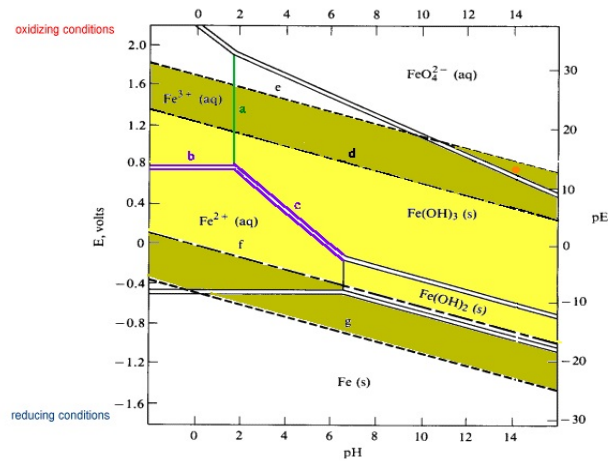


Figure 23: Pourbaix FeO.⁵¹

The Pourbaix model maps the stable phases for aqueous solutions. This in turn allows for predictive expectations as to when corrosion will take place between an aqueous solution and a sample. As seen in Figure 23, when a potential is applied to a sample submerged in a particular aqueous solution, the pH levels give an indication as to whether or not corrosion will occur. From this information the minimum potential that must be present to begin corrosion can be determined, or what pH level is needed for prevention.

Simplifying the Pourbaix diagram for certain materials and solutions can produce graphs that display the passivity, immunity and corrosive states of the metal in the solution. Needless to say this is a powerful tool for those investigating corrosion, as knowing when the combination of potential and pH level will result in corrosive growth is vitally important. However, it should be noted that these diagrams are not universal. Each diagram changes depending on the aqueous solution and the material being considered. The environment of the aqueous solution must also

⁵¹ Pourbaix Diagrams

be taken into account, specifically the right vertical scale in Figure 23. This scale is used to determine whether the solution is more aerated (oxidization) or composed of organic wastes (reducing).⁵² It is meant to show the concentration of the standard reducing agents and electrons. Lower values mean the solution is more disposed towards reduction.

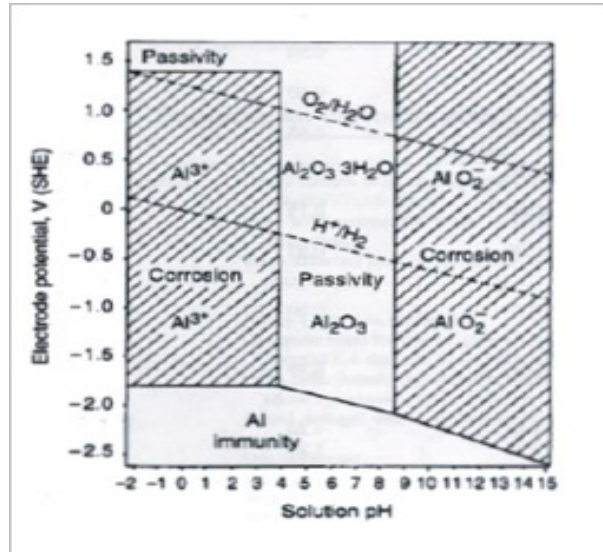


Figure 24: Corrosion section Pourbaix.⁵³

The potential-pH diagram also shows that certain combinations allow for the determination of corrosion type. The graph type allows for the determination of general corrosion, pitting and a combination of the two. General corrosion, along with pits, form mostly along crevices of the metal.

2.9.1.2 Pitting Modeling

Analysis of pitting can provide a more qualitative analysis of corrosion. This analysis commonly relies on visual inspection and results can vary from test to test based on who is

⁵² Pourbaix Diagrams

⁵³ Luo

conducting the measurements. Though the measurements can be variable, methods and charts used to evaluate are standardized. Blistering, pitting and flaking are assessed using charts to help quantify them.⁵⁴ These charts provide a guideline used to assist in the classification of number of pits and size of the pits. Similar charts are utilized when looking at cracking which, instead of looking at number and size, investigate spacing and width.

There are several other model types that have been developed over time in regards to pitting. One of these models is meant to describe the probability that no stable pits form at the given time t . Stable pits are those that will continue to grow as time elapses. The following equation was developed by the Shibata and Takamiya in 1986.⁵⁵

$$\ln[P(0)] = -\lambda a(t - \tau_c)e^{-\mu\tau_c} \quad [14]$$

Here, lambda represents the frequency of nucleation of metastable pits per unit area, mu is the probability of repassivation and τ is the critical age beyond which the metastable pit becomes stable.⁵⁶ Parameter a represents the sample's surface area. This approach was used by Henshall in 1992 to predict the growth of stable pits in 304 stainless steel.

⁵⁴ Ailor

⁵⁵ Sridhar

⁵⁶ Sridhar

Another model created involves the critical potential required for pit nucleation (growth) and bulk chloride calculation. The following equation was derived by Lin, Chao, and McDonald in 1981.⁵⁷

$$E_p = \frac{4.606RT}{\chi F \alpha} \log \frac{J_m}{J^0 u^{-\chi/2}} - \frac{2.303RT}{F \alpha} \log a_{Cl^-} \quad [15]$$

In this equation, the χ is used to represent the charge of the cation. The F is the faraday constant and α is the charge transfer coefficient. J_m is the submergence rate of the cation vacancies into the metals, J^0 is the migrational flux of cations, u is a preexponential term associated with the chloride-oxygen vacancy at the solution-film interface.⁵⁸ T represents temperature, and a_{Cl^-} the activity of the chloride ion in the solution.

2.9.2 Electrochemical Models

General corrosion rate is given in Eq. 16.⁵⁹

$$R = \frac{KW}{AtD} \quad [16]$$

R=corrosion rate [mm/yr]

K=constant

t=time of exposure [hours]

W=weight loss [g]

A=area [mm²]

D=density [g/mm³]

Electrochemical Mass Loss⁶⁰

⁵⁷ Sridhar

⁵⁸ Sridhar

⁵⁹ Sedriks

⁶⁰ Baboian

$$W = \frac{I_{ox}tA.W.}{nF} \quad [17]$$

W=mass loss [g]

$I_{ox}t$ =Product of current and time [A·s]

A.W. =Atomic weight of the of the electro active species

n=number of electrons transferred

F=Faraday's constant [C/mol]

When electrochemical corrosion occurs, and there is no applied potential influencing the corrosion, oxidation and reduction of the sample occur simultaneously at the metal/electrolyte interface.⁶¹ In this situation, the net current density applied to the sample is zero, with finite corrosion rates on the anodic surface. The mixed-potential theory allows for the corrosion process to be divided into half-cell oxidation and reduction reactions as discussed later.⁶²

Electrochemical corrosion rate is given in Eq. 18 and Eq. 19:⁶³

$$CR = \frac{3.27 \cdot 10^{-3} i_{ox} E.W.}{\rho} \quad [18]$$

$$E.W. = \frac{1}{\sum \frac{n_i F_i}{A.W._i}} \quad [19]$$

CR=corrosion rate [mm/yr]

E.W=equivalent weight

ρ =density [g/mm³]

⁶¹ Baboian

⁶² Baboian

⁶³ Baboian

f_i = the mass fraction of the i^{th} component of the alloy

$A.W._i$ = the atomic weight of the i^{th} component of the alloy

N_i = the number of electrons transferred or lost when oxidizing the i^{th} component element

i = the number of component elements in the alloy

The electrochemical corrosion rate is gained by altering the mass loss equation due to electrochemical corrosion. Rearrangement of the mass loss equation allows for a corrosion rate when I_{ox} (current) is uniformly distributed over the surface area, or the corrosion can be classified as localized in area A.

*Film Thickness*⁶⁴

$$C = \frac{\epsilon\epsilon_0 A}{d} \quad [20]$$

C = film thickness [mm]

A = surface area [mm²]

d = dielectric thickness [mm]

ϵ_0 = the electric permittivity of a vacuum [F/mm]

ϵ = the dielectric constant for the passive film or coating

Immersion Penetration

$$penetration = \frac{(Mass\ loss\ in\ mg)(C-factor)}{(area\ in\ mm^2)(density)} \quad [21]$$

C-factor = 1 for mm; or C = 0.061 for mils

⁶⁴ Baboian

Mixed Potential Theory

The mixed potential theory is based on the current distribution in a system with two metals.⁶⁵ The general idea of the theory is that when a common potential is reached, the corrosion current of the metal higher on the noble scale will be reduced, and the corrosion current of the lower noble metal will increase.⁶⁶ Therefore while the potential of two metals is the same, the current density of the two different metals will differ. Total attack depends on the proportion of the total anodic current and the relative areas of the metals.

$$i_{app} = i_{corr} \left(e^{\left[\frac{2.3(E-E_{corr})}{\beta_a} \right]} - e^{\left[\frac{-2.3(E-E_{corr})}{\beta_c} \right]} \right) + C \left(\frac{\partial E}{\partial t} \right) \quad [22]$$

$$i_{corr} = \frac{1}{2.3R_p} \left(\frac{\beta_a \beta_c}{\beta_a + \beta_c} \right) \quad [23]$$

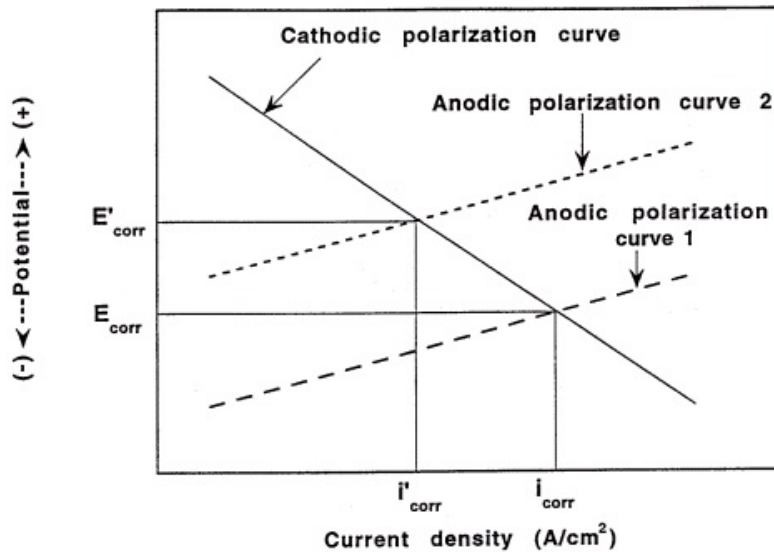


Figure 25: Mixed potential theory.⁶⁷

⁶⁵ Talbot

⁶⁶ Talbot

⁶⁷ Arenas

2.9.3 Established Models

Influence of Salt Content

$$f(S_r) = \frac{\gamma}{\varepsilon\sqrt{2\pi}(S_r+\delta)} e^{\left[-\frac{(\ln(S_r+\delta)-\beta)^2}{2\varepsilon^2}\right]} \quad S \geq 0 \quad [24]$$

$f(S_r)$ = corrosion rate factor for salinity

S_r = salinity ratio

γ = constant introduced as a magnification factor to adjust the values of the corrosion rate correction factor
($\gamma \geq 0$)

δ = constant introduced to adjust the truncated portion ($\delta \geq 0$)

β and ε

= constants corresponding to the mean value and standard deviation of the distribution

Influence of Temperature

$$f(T_r) = cT_r + d \quad [25]$$

$f(T_r)$ = corrosion rate correction factor for temperature

T_r = temperature ration

c = constant representing the slope of the $f(T_r) - T_r$ relationship

d = constant represents the $f(T_r)$ value at zero T_r

Influence of Dissolved Oxygen

$$f(O_r) = aO_r + b \quad [26]$$

$f(O_r)$ = corrosion rate correction factor for dissolved oxygen concentration

O_r = dissolved oxygen concentration ratio

a = constant representing the slope of $f(O_r) - O_r$ relationship

b = constant representing the corrosion rate correction factor $f(O_r)$ at zero O_r

Influence of Ph.

$$r = kC_H^{n+} \quad [27]$$

r = corrosion rate

C_H^+ = hydrogen concentration

n = exponent dependent on the hydrogen ion concentration

(corrosion rate increases with hydrogen ion concentration)

$$r(ph) = k10^{-(n*ph)}$$

k = constant

Influence of Water Velocity

$$f(v_r) = \lambda(1 - e^{-\eta(v-\theta)}) \quad [28]$$

$f(v_r)$ = corrosion rate factor for veolovity

v_r = folw veolovity ratio

λ = magnification factor to adjust the value of the corrosion rate correction factor

θ = constant introduced to adjust the truncated portion from the distribution

η = factor to adjust the curvature and the slop of the curve

Nonlinear Corrosion Wastage Model for General Corrosion⁶⁸

$$\frac{\partial d_{n,i}(t)}{\partial t} = \frac{d_\infty}{\tau_t} e^{-(t-\tau_c)/\tau_i} \quad t > \tau_c \quad [29]$$

$$\frac{\partial d_{n,i}(t)}{\partial t} = 0 \quad t \leq \tau_c \quad [30]$$

$$d_{n,i}(t) = d_\infty \left(1 - e^{-\frac{t-\tau_c}{\tau_i}}\right) \quad t > \tau_c \quad [31]$$

$$d_{n,i}(t) = 0 \quad t > \tau_c \quad [32]$$

The equations presented here were developed by Soares et al. for the immersion of steel plates.⁶⁹ The equations were developed for situations that are similar to what is being tested by

⁶⁸ Soares

⁶⁹ Soares

this project. Using these equations as a guideline for the development of final equation specific to this project, a baseline can be created along with multiple variations of the testing environment and other unique consideration from the test setup.

For the several corrosion rate equations that are presented in this paper, the ones that will be under the most consideration and will most likely be applied to this project are the influence of water velocity and pH levels. The paper itself is in regards to ships that are travelling through the ocean, so the comparison to this paper's testing will require some alteration. However, the relationships in the end should, in theory, be similar even once the alterations are made. All changes or variations that at implemented will be explained.

In terms of the overall corrosion waste, the equation that was developed from their paper is as follows:

$$d_{c,i}(t) = f_{i,1}(S_r)f_{i,2}(T_r)f_{i,3}(O_r)f_{i,4}(pH_r)f_{i,5}(v_r)d_{n,i}(t) \quad [33]$$

From this equation the overall corrosion waste can be determined. As stated before, due to the conflicting balance and importance of certain parameters, the functions they used will be different from the ones used in this project. Also the relations of all the functions that are being evaluated as a part of the waste function will see some rearrangement of the inclusive functions. Namely the oxygen dissolved function will feature far less prominently in the project of this paper, and as such the minimization or elimination will be taken into account. This will mainly be due to the idea that the oxygen will remain at a fairly constant level with the overall change being minimal. The same can be stated for the salt content as the solution that is being used will be constant through all tests.

3.0 Methodology

To begin, the team conducted general research about the process of corrosion. The goal of the research was to establish a complete understanding of corrosion, specifically how and why it occurs. From here research was done into the current testing methods of corrosion, and adapted to the study of this project, with the addition of the standards provided by the sponsor. After the team completed testing all of the products, analytical and numerical analysis of the data acquired was performed. The next step after the analysis was creating a mathematical model to predict the rate of corrosion with respect to time using the data that was acquired.

The project began with general research in to the corrosion problem. The intent was to firmly establish the reasons for corrosion formation, along with a general understanding of its effects. From this research, the groups was able to discuss and decide on which types of corrosion would most likely be experienced. From this point, research was directed into the current testing methods of corrosion, and utilized to develop the methods of testing applied in this project.

There were quite a few research resources available to the group members during the course of the project. In order to create a fixture for testing, the machine shop in Washburn Labs was used for the creation of several test components. The upper levels of Washburn also had chemical rooms where solutions and etchants were mixed, and samples were polished and examined. The chemical laboratories in Goddard Hall were used for accessing the chemicals needed to create the testing solutions and etchants.

3.1 Tests that apply

3.1.1 Loss/Gain in Weight

Loss/gain in weight testing is a very useful test when evaluating the effects of corrosion on a sample over time. By exposing the sample to a corrosive solution for a period of time, the gain in weight caused by the corrosive product allows for an evaluation of the chemical reaction occurring on the sample. Alternatively, by removing the loose corrosive product from the sample, a weight difference can reveal the chemical process that occurred over time as well. As such the two tests are very similar with only how the sample is handled at the end of corrosion induction process being the major difference. The testing apparatus allows for the testing of multiple samples at the same time in the same solution, which helps to minimize unexpected variables that may interfere with future measurements. However, the drawback to these tests is the number of samples required to get an accurate graph of mass vs. time is much larger than some other tests available.

3.1.2 Cross-sectional Corrosion Damage Measurement

There are several steps required for measuring the cross-sectional corrosive damage in small samples. To begin, a clean unaffected small sample is mounted and polished. This clean sample is placed on the microscope with the 50X magnification, during which a technique called thresholding is used on this clean sample. The process of thresholding selects a specific color range on an object. For this study, the entire clean sample was selected as the threshold. After the entire sample is selected, this threshold setting is saved on the computer for later use in comparisons. In addition to saving these threshold settings, the entire uncorroded cross-section area is measured for future comparison.

Once the clean sample has been thresholded, a dried corroded sample is placed on the Nikon Eclipse MA200 microscope and properly oriented for cross-section measurements. The microscope lens is placed in the 20X magnification. In order to ensure uniform measurements, the samples are rotated on the microscope such that the tip is always towards the user.

3.1.3 Surface Area Measurement

One way to quantify the damage in the smaller samples is to evaluate of the surface area change using the Nikon Eclipse Digital Microscope. This process provides numerical values for the damaged area that is present on a smaller sample. Each sample is taken and placed flat onto the microscope, and an un-corroded threshold is loaded onto the corroded sample. Each sample is examined and numerically analyzed at 5 sections, to provide a complete picture of the distribution of damage along the entire sample. The same procedure is followed with all other samples to gather as much data as possible to avoid any inconsistencies. Using the NIS-Elements program (Optical Analysis Program), data that is seen and logged is then easily transferred to an excel sheet where loss in area could be seen. The area of the damaged or corroded area is subtracted from the original undamaged area to provide the final remaining area.

3.2 Current Testing Standards

The sponsoring company provided the group with confidential documents describing their current testing for corrosion along with the ASTM G44-99 (2013) Standard Practice for Exposure of Metals and Alloys by Alternate Immersion in Neutral 3.5% Sodium Chloride Solution.⁷⁰ The company had based its testing procedures from this ASTM standard, which

⁷⁰ ASTM Standard G44-99

provided the basic outline for the procedures. Though the company procedure is commonly used for SCC testing, it is often used for other forms of corrosion testing such as: uniform corrosion, pitting, intergranular, and galvanic corrosion. The testing practice can be applied as a guideline for existing tests or used for a unique testing process, keeping in mind that strict test conditions are stipulated for the assurance that variations in results are due to variations in the test material and not the procedure.

The alternate immersion test is an all-purpose test that produces valid comparisons for most metals. While it is an accelerated test and is considered to be representative of certain natural conditions, it is not intended to predict performance in specialized chemical environments where a different mode of corrosion may be operative. The test utilizes a one hour cycle that includes a 10 minute period in the aqueous solution followed by a six hour drying period outside of the solution. This cycle is continued 24 hours a day for a time period recommended for the particular material, which can be from 20 to 90 days or longer depending on corrosion resistance.

3.2.1 Important specifications

The following test specifications and considerations are taken from the ASM standard G44-99.⁷¹ They are applicable to the current test methods that will be adapted for the team's testing purposes.

⁷¹ ASTM Standard G44-99

3.2.2 Solution conditions

The salt solution shall be prepared by dissolving 3.5 ± 0.1 parts by weight of NaCl in 1.5 gallons of Distilled water (DI). The pH of the salt solution, when freshly prepared, will be within the range of 6.4 to 7.2. Only diluted reagent grade HCL or reagent grade NaOH shall be used to adjust the pH of the solution which should also be kept at 40°C. The volume of the test solution should be large enough to avoid any significant change in its corrosiveness either through exhaustion of corrosive constituents or the accumulation of corrosion products. An arbitrary minimum ratio between the volume of test solution and area of specimen of 32 mL/cm² is recommended. Evaporation losses must not be replenished with the salt solution. The simplest and recommended procedure is to initially fill the solution to a liquid level line and refill to that line daily. Fresh solution shall be prepared weekly but more frequent replacement may be required. The portions of the apparatus that contact solution should be cleansed by flushing with water.

3.2.3 Current Testing Standards

These standard practices have been adapted by the sponsoring company to form two test procedures for corrosion induction. The tests vary by the duration and by the aggregation of the solution. One of these tests lasts only 48 hours, while the other takes up to two weeks to complete. The basic procedure for both tests requires immersion in a heated chloride solution. The accelerated test leaves the product in the solution for the complete 48 hours to provide aggressive corrosion induction. The other procedure utilizes alternate immersion spending 3 minutes in solution followed by a drying time of 7 hours. This test allows the specimen to dry completely in conditions that are similar to those the actual product endures.

The testing used in this project replicated the procedures currently in use, following both the sponsor company's procedure and ASTM G44-99 (2013). The testing implemented were as standardized and repeatable as possible in order prevent unintentional variables. Testing involved a combination of the two methods to develop reliable data over both short and long term testing.

3.2.4 Stirring Plate

The fixture will be placed upon an electromagnetic stirring plate to satisfy multiple needs. The first is that the stirring bar will be used to provide flow to the fixture. The stirring bar will be magnetically rotated by the magnetic field generated by the plate, which in turn creates the flow in the fixture. This flow will be important to accelerating the process of corrosion. The stirring plate also provides the source of temperature control. The base of the stirring plate will allow the solution to be raised to 40°C, and the temperature probe will keep the solution at the predetermined degrees with minimal variation. Therefore, the stirring plate plays a valuable role in the overall conductance of the testing procedure.

3.3 Fixture

The fixture for this project had several goals it must satisfy. The fixture must hold 45 specimens at one time for testing, and also must be able to hold a corrosive solution without suffering any side effects that are detrimental or intrusive to the testing procedure. Finally the fixture must be able to withstand a temperature greater than 40°C without any damage or effects detrimental to the tests or the fixture itself. To this end the following apparatus was designed to satisfy these needs.

3.3.1 Apparatus

Any suitable mechanism may be used to accomplish the immersion provided that: (1) it achieves the specified rate of immersion and removal, and (2) the apparatus is constructed of suitable inert materials. The rate of immersion and removal should be as rapid as possible without jarring the specimens. For purposes of standardization, an arbitrary limit was adopted such that no more than two minutes elapse from the time the first portion of any specimen is immersed, until it is fully covered by solution. Materials of construction that came in contact with the salt solution shall be such that they are not affected by the solution to an extent that they can cause contamination of the solution and change its corrosiveness. The specimen holders should be designed to electrically insulate samples from each other and from any other bare metal. The shape and form of the specimen supports and holders should:

- Avoid any interference of free contact of the specimen with the salt solution
- Not retain a pool of solution in contact with the specimen after immersion
- Avoid specimens contacting each other

3.3.2 Initial Fixture Design

The fixture was designed to meet the conditions of the ASTM Standard Practice for Exposure of Metals and Alloys by Alternate Immersion in Neutral 3.5% Sodium Chloride Solution while satisfying additional testing requirements. The fixture must hold multiple small samples at once while still providing accurate testing conditions. Basic requirements include that this fixture must expose test samples uniformly to solution, facilitating alternate immersion techniques in an environment that will not interfere with corrosion development.

Additional functional requirements of our apparatus ask that it can support the heating and circulation of solution while able to test various types of specimens. The team have added the circulation of solution to accommodate for the size of the apparatus and to ensure localized environments do not develop. Solution circulation helps to maintain the accuracy of testing and to accelerate the growth of corrosion. SCC testing is not a major concern for this project, but the designs should be mindful of future SCC test development in such a manner that there is room to accommodate such a change.

3.3.2.1 Material Selection

The material used in apparatus construction is extremely important to the validity of testing. To recall requirements outlined by ASTM G44-99 (2013) the apparatus must be constructed of suitable inert materials. Materials that come in contact with the solution shall be such that they are not affected by the corrodent to an extent that they can cause contamination of the solution and change its corrosiveness. The largest constraint is to avoid any metal materials in construction, which leads to the use of either a polymer or glass for tank construction. Glass provides excellent chemical resistance but is difficult to work with and was therefore limited in use. Polymers are ideal to use a single material in apparatus construction. Acrylic is a promising material that was selected for the fixture. It displays excellent chemical resistance in much more reactive environments while also providing rigidity, ease of manufacturing, high temperature resistance and translucent options. The Borosilicate glass however, had a much higher thermal conductivity, which is why it was selected for the base component where heat transfer was most important.

3.3.2.1 Physical Design

Initial designs featured a rectangular tank with a removable lid, opening from the top. Attached to the lid would be the support for an insertable rack allowing specimens to be organized and placed in the assembly when outside of the apparatus with ease. The rack would then be slid in the supports and lowered into the solution. This design provides ease of load up and handling, is able to keep the specimens in the rack while drying, and has space for up to 15 samples. The preliminary apparatus design developed using SolidWorks modeling is displayed in Figure 26, and the independent rack can be seen in Figure 27. Several rack designs could be implemented to accommodate for various test products, each fitting into a standard support. The downfall of this design was in the implementation of solution flow. The rectangular tank would inhibit flow while the linear placement of samples in the rack introduced non-uniform exposure to solution circulation.

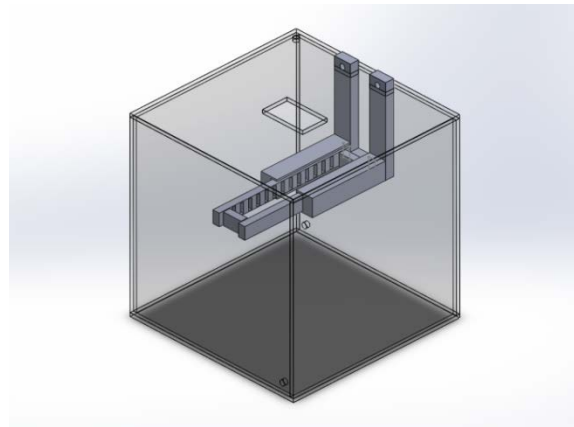


Figure 26: Primary fixture design.

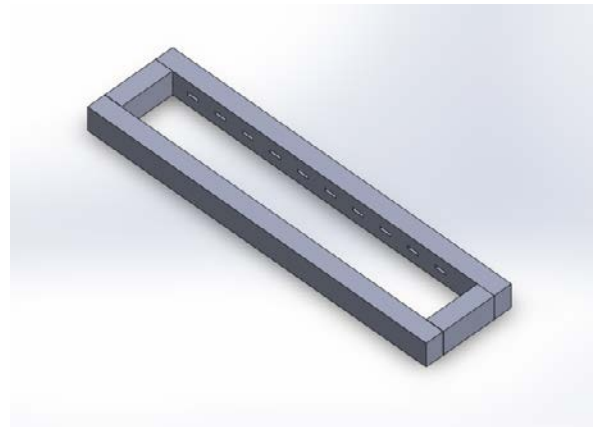


Figure 27: Independent rack design.

3.3.3 Secondary Fixture Design

The secondary design set out with the goal to better accommodate for uniform flow patterns and specimen exposure. In designing this fixture, all components were dependent on a

circular flow design. The cylindrical tank allows the solution to circulate uniformly. Test samples are attached to the sides in equal configurations in order to maintain that each experiences similar flow velocities. The objective was to include nine test mounts, one for each sample, that adjust vertically and can adapt to various product dimensions. Vertical adjustment allows the selection of the ideal placement for exposure to solution circulation, which may vary with height.

For analytical purposes, the fixture was designed as a basic cylindrical tank with nine test fixtures simulating the size and shape of the design. Each fixture is about two inches in width, based on a product width of 1.5 inches. The tank itself is 16 inches in diameter, allowing for the specimens to sit four inches from both the exterior wall and center of the tank, avoiding wall boundary effects and the development of stagnancy in the center caused by circular flow effects. Figure 28 displays the design model used to test flow circulation using SolidWorks FloXpress. Several different configurations were tested by altering inlet and outlet positions. The initial design placed the inlet and outlet ports at the bottom of the cylinder, opposite of each other, seen in Figure 29. This provided sufficient circular flow on the tank bottom but neglected the top and center of the apparatus. Secondly, the team placed the inlet at the top of the tank, keeping the outlet position. This configuration provided a better distribution of circular flow along tank walls but continued to create stagnancy in the center, displayed in Figure 30. The final design brought the most uniform flow patterns by placing the inlet at the top of the apparatus and the outlet in the center of the base. Simulations show that this developed the best circular flow pattern on the edges of the cylinder while reducing stagnancy in the center. Figure 31 shows the flow pattern for this design.

As a final consideration, research was done in to use of magnetic stirring and heating plates. This proved to be a useful alternative to circulation by an external pump. The plate has the advantage of stirring the solution using a magnetic stirring stick placed in the apparatus. It would alleviate the need for an external pump, which may introduce solution contamination while providing consistent mixing. The test apparatus could simply be placed on this plate serving the dual purpose of a heater and a stirrer. Two constraints may limit the stirring plate: available plate size and conduction of heat through apparatus material. However, research into the available plates allowed the team to find an appropriate sized one for this project.

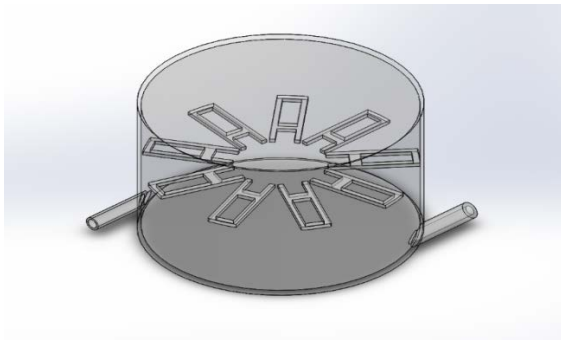


Figure 28: Circular flow apparatus design configuration.

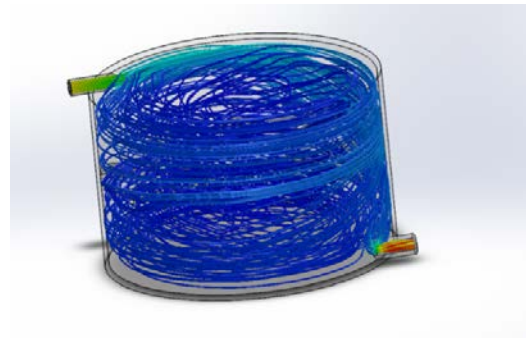


Figure 30: Alternate inlet configuration.

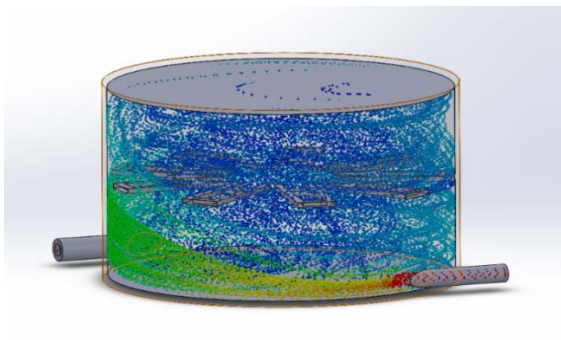


Figure 29: Initial inlet and outlet.

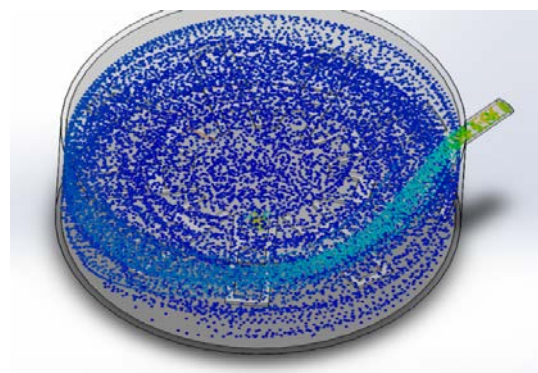


Figure 31: Final flow configuration.

3.3.4 Final Fixture Design

3.3.4.1 Considerations

To satisfy the requirements of the tests that were conducted, the team designed the final fixture accordingly. A circular tank was chosen to achieve uniform conditions for each test specimen. The circular shape allows each sample to be equally distant from both the outer walls, and the tank center. The shape accommodates for the introduction of flow to the system as well, providing the capability to use a stirring platform for uniform agitation. The stirring platform was chosen as a means to heat and mix the solution because it offers a single piece of equipment with control of mixing speed and temperature through a thermal sensor placed in the tank. The tank size was determined by considering the available stir/hot platform sizes along with the position of sample fixtures. Final dimensions of the tank were 12 inch I.D. by 10 inch height, providing enough space for 5 fixtures, and a total of 45 specimens to be placed in the tank and allowing for a reasonable solution height of 8 inches. The complete assembly is displayed in Figure 32.

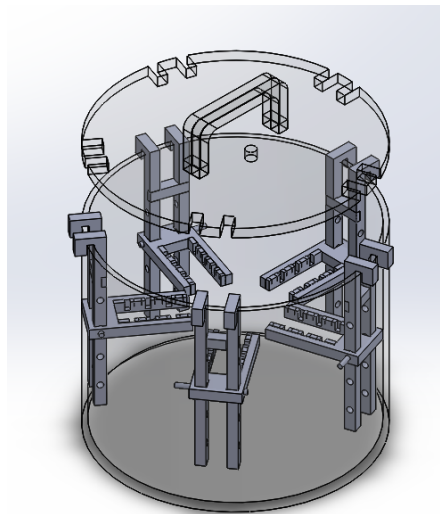


Figure 32: Complete assembly.

3.3.4.2 *Material Selection*

Acrylic plastic and “SCHOTT BOROFLOAT 33” Borosilicate glass were chosen for the material of the tank components due to their inert properties and capability to be operated on in the shop on campus. The Acrylic plastic was used for the racks, smaller components of the tank that hold the samples, and the circular body of the tank. The majority of the components were cut from sheets, using a laser cutter providing the accuracy and capability to produce small slot widths (.010 inches) needed for small sample testing. Bonding of various parts was easily accomplished using a chemical bonding agent, which physically bonded the two pieces of acrylic into one. The initial strategy to manufacture the tank was to form a thin acrylic sheet into a ring, then bonding it at the seam to a flat base. Due to the various challenges this method could introduce, it was determined that the best solution was to build the tank by bonding an acrylic tube to a flat base. This strategy increased material costs but provided a reliable tank for future testing. The base of the tank was made of the Borosilicate glass, and was chosen due to its high chemical resistance and thermal conductivity. Since heat was going to be introduced to the tank for testing purposes, a material that was strong enough to withstand the pressure of the solution on top and the heat had to be chosen, which the Borosilicate glass accomplished.

3.3.4.3 *Sample Fixture*

The fixture was to be capable of holding two types of samples, both small, and large products. From there, racks were designed with slots where either size can rest at any given time, shown in Figure 33. Slot sizes alternate to provide the most compact design. Based on the testing strategy, the apparatus needed to hold at least 30 of the small samples at once, specifically intended for the characterization of corrosion growth over time. Each fixture is able to house six

small products and three large products, which provided a total of 30 small products and 15 large products among the five sample fixtures within the tank. Each rack was horizontally positioned to provide the most uniform solution environment. Sample placement was designed to provide adequate spacing on either side from the sidewall, or the center of the tank.

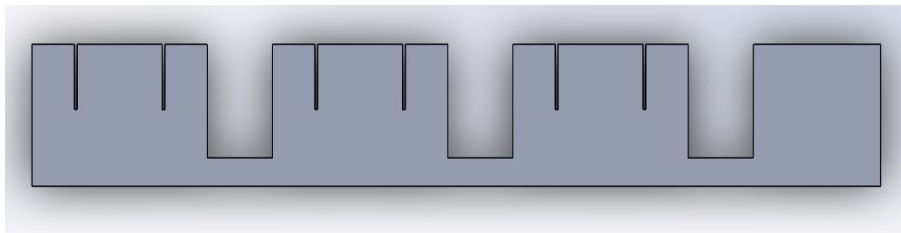


Figure 33: Slot placement.

3.3.4.4 Vertical Adjustment

A requirement of each fixture was to be able to adjust the vertical rack placement, allowing for optimization based on mixture effects. A pin system was developed to lower or raise the samples to multiple heights. The rack itself is attached to two vertical supports that hang from the top of the tank shown in Figure 34. The sliding mechanism provides rigidity to the fixture relying on the pins strictly for vertical placement. Figure 33 displays the slot features of the rack component that the vertical supports slide through. There is a through hole in the rack that allows a single pin to pass through both vertical supports and the rack, maintaining vertical placement.

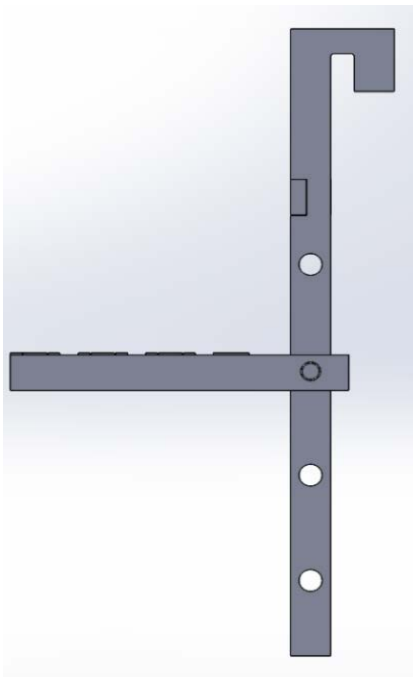


Figure 34: Tank support rack.

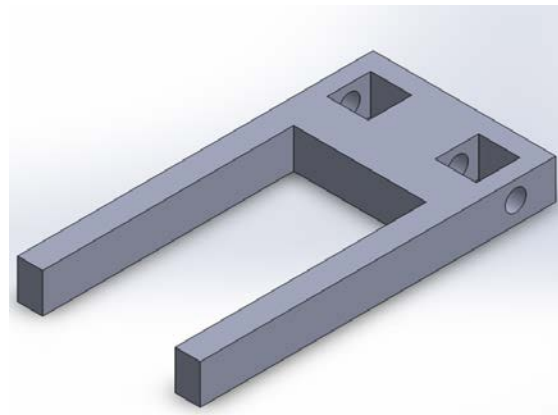


Figure 35: Sample rack holder.

Tank Lid

Since some tests were conducted with heat, a lid was designed to fit over the rack hooks in order to contain vapors and help maintain solution temperature. The lid is important in preventing the evaporation of water from the tank, which could potentially increase the concentration of sodium chloride in the solution. As for accommodations for the thermal sensor that was inserted in the tank, a hole was cut into the lid to tightly fit a rubber seal and the thermal sensor. A series of notches were cut in the tank lid allowing for the top of each fixture to protrude through. The lid was made of half inch material to provide substantial weight, creating a better seal.

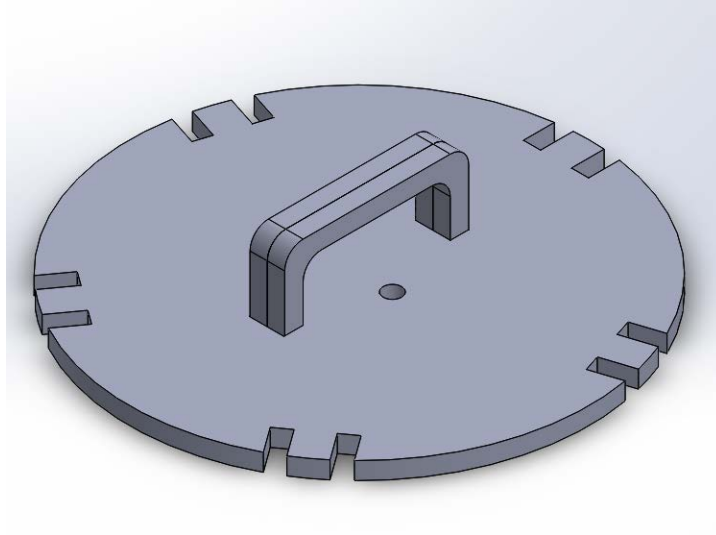


Figure 36: Tank lid with notches.

3.3.5 COMSOL Simulation

Before a design for a fully functional testing tank could be finalized, certain precautions were taken to ensure the apparatus will provide a suitable environment. One concern was the involvement of an agitation bar to stir solution during corrosion induction. The team wanted to ensure that agitation was uniform throughout the tank. If any area were to receive a significantly different agitation rate then testing results would be skewed and not properly represent natural corrosion formation. The following sections describe the process by which tank conditions were simulated with the software package COMSOL to ensure these requirements were satisfied.

3.3.5.1 Geometry

The model used in this study is based on the COMSOL Multi-physics sample model titled “Laminar Flow in a Baffled Stirred Mixer”.⁷² The model is designed as a cylindrical tank with four fixtures along the edge. A screen shot of the model geometry is shown in Figure 37.

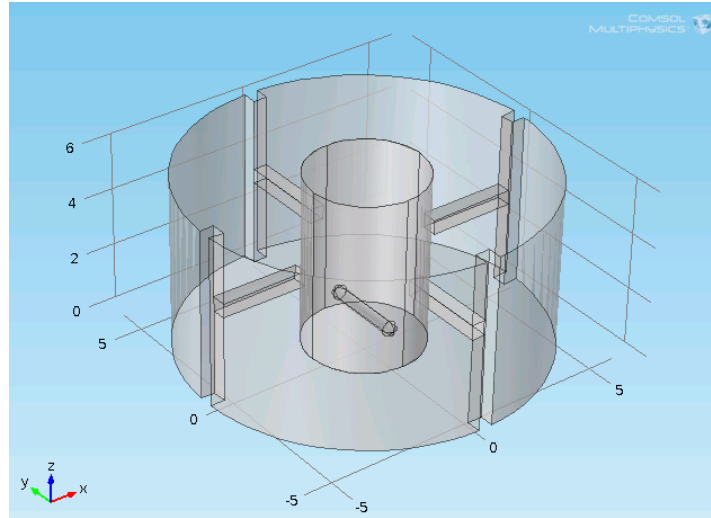


Figure 37: COMSOL model geometry.

The tank has an overall diameter of 12 inches and a height of six inches to model the water level. The fixtures divide the circumference into four sections of equal length, and touch the side of the tank. Each section of the fixture that extends into the tank center has a height and width of 0.5 inches and extends into the center for three inches. The actual experiment setup has five fixtures, each with two fixture pieces extending into the center. This simulation was created with only four fixtures in order to simplify the design. It is important to note that this model does not perfectly resemble the actual setup and is meant as an approximate guide to determine the sample and solution height. The stir bar is 2.5 inches in length and has a radius of 0.25 inches.

⁷² COMSOL

The smooth tips of the stir bar were modeled by adding two spheres of 0.25 inches radius to the ends. The model also consists of a central cylinder with a two-inch radius, and its purpose will later be explained.

3.3.5.2 Model Design

The basis of the model is a system with two domains. The outer domain is fixed and the inner domain rotates. The inner domain is the two-inch cylinder in the center, and the outer domain consists of everything outside of the two-inch center. In order to create a model with only two domains, the entire model was created as the volume that water occupies within the system. This study is focused on the fluid mechanics of water, so none of the components in the model are made of acrylic. In order to create the outer domain, the four fixtures and inner cylinder were subtracted from the outside cylinder. The fixtures in the model represent gaps in the model of volume that water does not occupy. The inner domain was created in a similar fashion as the result of subtracting the central stir bar from the inner cylinder.

3.3.5.3. Boundary Conditions

A no-slip boundary condition was applied to most of the model surfaces. The no-slip boundary condition signifies that the fluid in contact with that surface has no velocity, and the fluids surrounding this surface have increasing velocities until the bulk velocity is reached. This condition was applied to all surfaces in the model except for the top surface and the inner cylinder surface. Flow continuity was applied to the central cylinder surface in order to signify that the flow on both sides of the boundary are the same, as the inner cylinder was only created to separate a fixed domain from the rotating domain. A symmetry boundary condition was

applied to the top surface boundary to control the flow. This condition ensured that the flow had no velocity normal to the top boundary.

3.3.5.4 COMSOL Results

Time to steady state

The first step in the analysis of the stir tank model was to determine the time required to attain a steady state. The model solution is time dependent, so each solution is different depending on the specific time elapsed. Each solution was qualitatively inspected to determine the time after which no changes appeared in the solution. It was assumed that after the time to reach a steady state was attained, the solution was identical for all time intervals afterwards. In order to accomplish this task, the model was solved for all times between zero and 20 seconds with intervals of two seconds in-between. The fixture heights were also set to 4 inches from the base. The results of this analysis are shown in Figure 38.

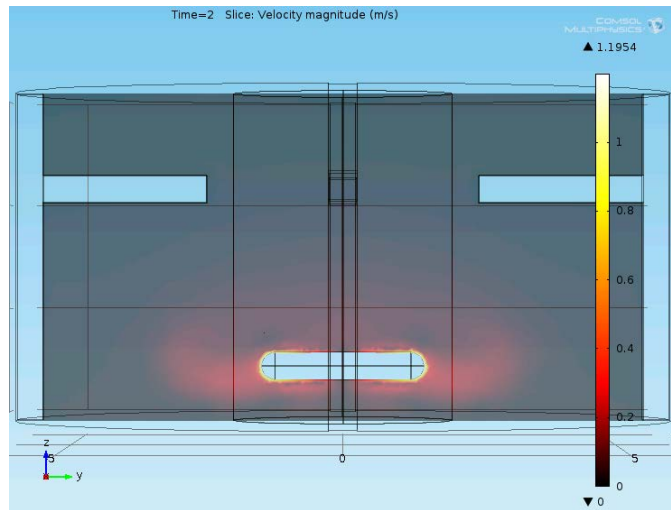


Figure 38: Velocity magnitude at t=2 seconds.

Figure 38 shows the velocity magnitude of the water after two seconds. The red region indicates areas where the velocity has increased. As expected, the areas closer to the stir bar have

a higher velocity than the regions that are farther away. The solution has clearly not had enough time to fully develop, as the red region has only spread into the center of the tank.

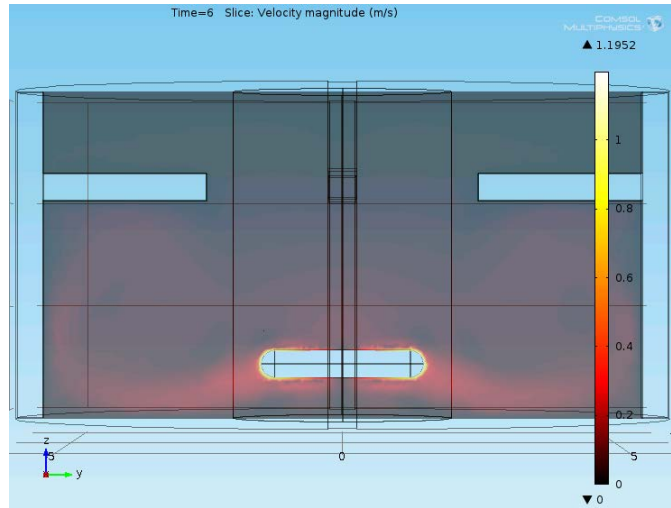


Figure 39: Velocity magnitude at t=6 seconds.

Figure 39 shows the velocity magnitude of the water solution after six seconds. The solution bulk velocity is increasing and the red region is spreading to the tank walls. However, the stirring has not yet affected the top portion of the tank.

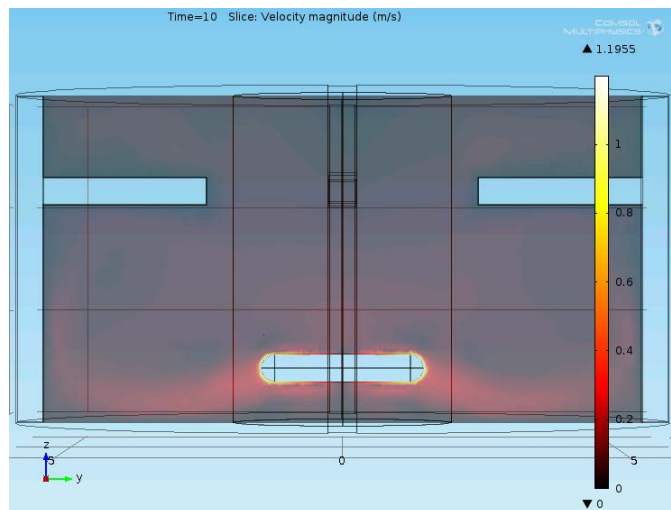


Figure 40: Velocity magnitude at t=10 seconds.

Figure 40 is for the velocity at ten seconds. After ten seconds, the fixture was assumed to be at steady state. For times after ten seconds, slight changes occur to the velocity profile but the following general trends stay the same. The red velocity region curves down and around to affect the walls. The red region is also spread to the center and region above the fixtures. Also, a small curve in the velocity profile representing a vortex can be noted at the top center. All following results are shown after ten seconds, because these velocity profiles show that steady state can be assumed.

Fixture Height

The next and key analysis of the COMSOL model was the determination of the ideal fixture height. The ideal position for the fixtures was determined based on the lowest height at which all the samples experienced uniform flow. The height of the fixtures was varied from two inches to 5 inches above the base at one-inch intervals. An ideal testing height was determined from qualitative analysis of the following results.

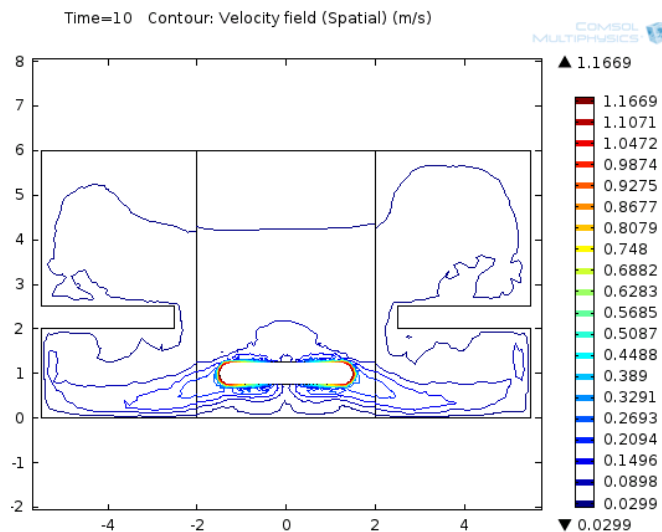


Figure 41: Velocity contour plot at 2 inch height.

Each line on Figure 41 represents a flow path with a specific velocity. The contour plot for the model at a two-inch fixture height reveals areas of concern in the tank. As shown in the figure, the right samples could experience a different flow pattern than the samples on the left region. In addition, there seem to be regions over the samples in which a different flow is passing over due to small vortexes formed.

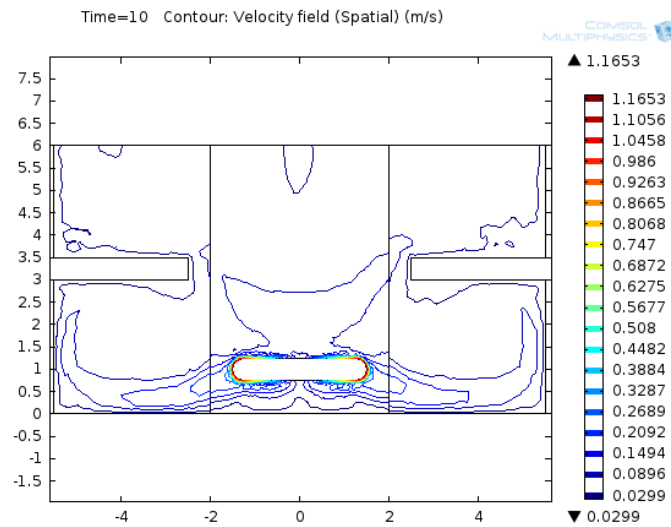


Figure 42: Velocity contour plot with 3 inch height.

Figure 42 shows results that are very similar to the previous results with minor improvements. The left side samples seem to experience more uniform solution velocity than the flow pattern on the previous graph. The right side, however, continues to show a pocket on the right side.

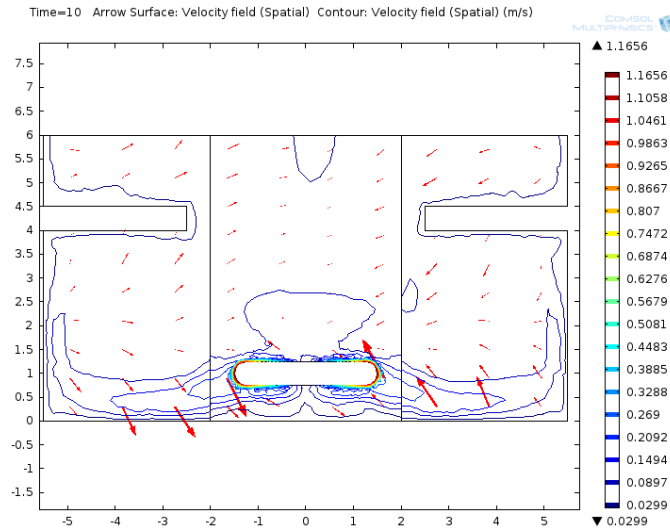


Figure 43: Contour plot and arrow surface at fixture height of 4 inches.

The final figure is for the fixture with a four-inch height, which represents the lowest height at which the samples should be placed for each sample experiences similar flow. The left and right side samples have no velocity pockets passing over them. The figure also shows the velocity vectors as red arrows. These velocity arrows show that the flow passes evenly over the samples. Also, a minor vortex is at the top, which is acceptable because it does not influence the samples.

3.4 Part Drawings

See appendix A for complete drawings of the final apparatus parts.

3.5 Corrosion Induction

The process of testing begins with general research in to the corrosion problem. An understanding of corrosion, how and why it occurs, is vital to the development process of

completion for the testing. From here there is an examination of the current testing methods of corrosion, and adapting those to the chosen test procedure. The testing procedures chosen involve three types of tests: pitting, weight loss, and change in electrical resistance of the products, conducted at specified intervals in the induction process. To prepare the metallographic surfaces for the following optical tests, the test specimens will be sectioned, mounted, polished, and etched. These steps will ease the process for observing the test specimen in optical data collection performed once the corrosion process is completed.

3.5.1 Background

The corrosion inducement procedure is one of the most important aspects of this project. Inducting corrosion onto our specimens will be accomplished by exposing the specimens to a corrosive solution, in this case calcium chloride. Corrosion will be induced in two different ways through methods labeled the soak and the Dip & Rinse test. The soak method involves a straight soak of the specimens being considered. The specimens will remain submerged in the solution for the desired duration of the test. The Dip & Rinse method involves the submerging the specimen for short duration, such as only a few minutes and then removing the specimen from the solution for set drying time. Each of these tests requires that the solution be at a different calcium chloride concentration, which will be specified by the test.

3.5.1 Pre-Test Procedure

Prior to testing, there are certain preparations were completed. Each rack in the tank was labeled from one through five. In order to keep track of each sample position in the tank, the team developed a scheme where each slot in the rack had an order. Labeling involved the type of

test so that sample one of the alternate immersion samples is distinguishable from the total immersion. The larger samples required no major preparation other than be independently placed in the numbered slots as well so that that they can be identified during the testing phase. The moisturizing strip was removed from each large sample to prevent mass influence. All samples however, were weighed for their initial mass, as the change in mass test requires it. From the initial weight of the three samples, the significant figures required to accurately measure these samples should become clear. As such, all future mass measurements should be to the same number of significant figures as determined by this pretesting phase. For the testing purposes of this experiment all mass measurements were taken to four decimal places.

3.5.2 Solution Preparation

When preparing the station to begin testing, several steps must be completed to ensure accuracy and precision among samples. The first step when preparing the tank was to rinse the inside of the tank and all holders with a small amount of deionized water. This is to remove any contaminants on or in the equipment that may or may not interfere with the testing process. Once the tank and holders have been cleaned out, then tank can be filled with the desired solution. The magnetic stir plate allows for the mixing of chemicals within the tank. While this isn't encouraged, depending on the chemicals, the mixing process can be accomplished quickly within the tank while the solution is heating to temperature.

The amount of solution used per test is 1.5 gallons. This fills the tank enough to completely immerse the samples for the duration of the test. The 1.5 gallon volume requires 197.8 g of sodium chloride to produce a 3.5% solution. When filling the tank with the NaCl

solution, the deionized water should be added slowly to prevent excess splashing within the tank. Once the necessary amount is within the tank, the stir plate should be set 20-30°C for ten minutes to prevent any thermal shock on the base of the tank. From there, the temperature can be raised to the required 40°C. During the entire heating process, the temperature probe of the plate must remain in the solution. It is important to recognize that the stir plate controls heat output based on its current temperature reading. This means if the probe is not receiving an accurate temperature reading, it will continually output large heat in an attempt to increase the temperature, which can lead to a dangerous testing environment and can potential damage the tank or equipment.

Adding the NaCl in small amounts with a stir rpm of 300 allows for a quick and equal mixing of the solution. A glass stir bar can also be used if needed to break up and chunks on the base of the tank. This should all be done while the tank is heating, to save time and assist in mixing.

3.5.3 Sample Preparation & Handling

While the solution is undergoing heating the samples can be inserted in the holders. Each sample should be inserted so that they can be easily tracked as to which sample is which. For that reason, every holder has a number 1-5 for easy identification. It is recommended that a numbered diagram of the apparatus be printed. Gloves should be worn when inserting the samples to prevent any contamination potentially affecting test results. Once the samples are inserted into the holders, each holder can then be placed into the solution granted the predetermined temperature has been reached. The lid lining of the tank has cut outs where each holder should rest with equal spacing. This is required for the lid to properly close on the tank. The holders

should be inserted slowly into the solution to prevent any damage to the holders and to make sure the samples remain firmly in place. From this point, the lid can be placed over the tank and should securely fit over the legs of each holder. This is to prevent as much loss to evaporation as possible during the test.

When removing the samples from the tank, there are a couple of steps that must be followed in order to maintain consistency among the test samples. When removing the samples from the tank, a tweezers or other small gripping instrument should be used on the smaller samples. Gloves should be worn during this portion to prevent an unnecessary damage. If a larger sample is blocking or making it difficult to remove smaller sample, the larger sample can be lifted carefully to make access to the smaller sample easier.

Once removed, all samples should be dipped in a beaker of deionized water. This is in order to remove any solution that may still be attached which could create undesired corrosion. The sample is then gently dabbed on both sides by a paper towel to remove the excess water. Once dry, the samples are individually separated and labeled for data collection.

3.5.4 Total Immersion Test

The following procedure for Total Immersion is altered based on the procedure of the sponsoring company. A 3.5% sodium chloride solution was selected for this study, however the solution may be altered in future tests. The procedures outlined in the previous two sections should be followed for solution and sample preparation. Once all samples are completely submerged in the corrosive solution the total immersion test has officially started, and the following specific procedure was used to remove the samples. Three small samples and one large

sample were removed from the fixture at every specified time interval. Three small samples were removed at a time so that an average value can be calculated for each time slot. After the four total samples were removed, they were placed on a paper towel to dry. The small samples were also carefully flipped to ensure both sides are dry. These samples were then individually stored in labeled bags for later analysis. The remaining 27 small samples and nine large samples remain immersed in the corrosive solution. Once the next specified time interval has passed, this procedure for removing samples was repeated until no samples remain in the tank.

The main difference between the Total Immersion test described in the ASTM standard and the procedure presented is the selected time intervals. The ASTM standard states the samples must be left in the solution for a minimum of six hours before removal. However, the used altered procedure does not have a minimum immersion time. This change was implemented in order to gain a better understanding of the corrosion damage at shorter time spans. The following two tables show the selected time intervals for the first and second total immersion tests respectively.

Table 3: Total Immersion Test 1 time intervals

Interval Number	Time	Small Samples Remaining	Large Samples Remaining	Total Hours Immersed
0	8:00 AM	30	10	0
1	11:00 AM	27	9	3
2	2:00 PM	24	8	6
3	5:00 PM	21	7	9
4	8:00 PM	18	6	12
5	8:00 AM	15	5	24
6	11:00 AM	12	4	27
7	2:00 PM	9	3	30
8	5:00 AM	6	2	33
9	8:00 PM	3	1	36
10	8:00 AM	0	0	48

Table 4: Total Immersion Test 2 time intervals

Interval Number	Time	Small Samples Remaining	Large Samples Remaining	Total Hours Immersed
0	3:00 PM	30	10	0
1	4:30 AM	27	9	1.5
2	9:00 PM	24	8	6
3	9:00 AM	21	7	18
4	3:00 PM	18	6	24
5	3:00 PM	15	5	48
6	3:00 PM	12	4	72
7	3:00 PM	9	3	96
8	3:00 PM	6	2	120
9	3:00 PM	3	1	144
10	3:00 PM	0	0	168

3.5.5 Alternate Immersion Test

The alternate immersion (Dip & Rinse) test shares many similar features of the total immersion test. While the preparation measures are the same, such as mass measurements, the major differences arise in conduction of the test. Once all preparations are complete, the test begins with the immersion of samples for a time of 10 minutes. The immersion should not be shorter or longer than this established time. Once the time is reached, all the samples should be removed from the solution. Once removed, the samples should be removed from the features that hold them and placed on a wire rack to dry. It is important that all samples be carefully labeled so that the exact number of the sample can be know when the time comes for analysis. The samples should not be rinsed and should be left to dry on the wire rack for a minimum of six hours. Once the minimum amount of drying time has passed, the necessary sample for that time interval can be removed and labeled as such. Once the samples are labeled, the remaining

samples should be dipped into the solution again for the 10 minute time limit and the process repeated.

Table 5: Dip & Rinse time table

Interval Number	Time	Small Samples Remaining	Large Samples Remaining	Total Hours Immersed
0	8:00 AM	30	15	0
1	8:00 PM	28	14	12
2	8:00 AM	26	13	24
3	8:00 PM	24	12	36
4	8:00 AM	22	11	48
5	8:00 PM	20	10	60
6	8:00 AM	18	9	72
7	8:00 PM	16	8	84
8	8:00 AM	14	7	96
9	8:00 PM	12	6	108
10	8:00 AM	10	5	120
11	8:00 PM	8	4	132
12	8:00 AM	6	3	144
13	8:00 PM	4	2	156
14	8:00 AM	2	1	168
15	8:00 PM	0	0	180

3.6 Data Collection

A series of three collection types have been selected based on the following considerations: The goal of this project is to produce a reliable and repeatable method for quantifying corrosion. Therefore the tests are simple to complete providing the least chance of error. They are also among the quicker tests to complete and multiple can be completed with a single sample. The use of a single sample for multiple tests allows for the comparison of data between collection types, further ruling out variation. The following sections will explain the process for analyzing the tests.

Once all samples for a testing round have been collected, the use of each sample needs to be determined. Due to the fact that some testing methods pursued in this project are destructive, all non-destructive tests must be completed first. These non-destructive tests include mass measurements and surface area analysis, and should be completed before the mounting stage of test procedure.

3.6.1 Mass Measurement

When measuring the mass of the smaller and larger samples for testing, it is important that the mass measuring device provide up to four significant figures. This will be due to the small mass of the smaller samples. The larger number of significant figures is to accurately measure the difference in mass between each of the samples and the overall change of the samples after the corrosive process. When measuring the sample masses, it's important to tare the scale before each measurement. The tare will take into account anything that may have fallen on the scale and interfered with the measurements. This will be especially important after the corrosive process when the change in mass is relevant. The samples will have the possibility of losing some corrosive product while on the scale. While this would not affect that samples measurement, as the corrosive product is still a part of the change of mass, if the product stays on the scale and no tare is performed, it could adversely affect the results. Also, due to the sensitivity of the measuring device it is important that the samples be maintained in an environment that prevents the accumulation of dust or other particles on the samples. For example, after measuring the samples, each was returned to a plastic bag to keep the samples clean. This should help hold a consistent and reliable result throughout the testing process in terms of mass measurement.

The final mass of each sample should not be taken immediately following its removal from tank. This is due to several reasons, but the most important is the water weight. If weighted immediately following removal, there is a chance of water and/or solution still being on the sample. This would affect the mass, and due to the sensitivity of the measuring device and the accuracy required, the results would not be reliable or usable. As such, the mass measurement of samples should wait to the completion of the test, and the final samples removed should be given a day or so to dry completely. This is especially important for the larger samples, which have a significant amount of plastic surrounding them. The chances of solution being trapped, or stored in crevices is high and precautions should be taken to prevent this occurring in the measurements.

3.6.2 Surface Area Analysis

Following the completion of a testing cycle and following the overall mass measurement test, the next test conducted is the surface area analysis. To complete this testing method, a video microscope should be used as to provide a constant visual feedback at 5x magnification, which is necessary for this analysis process. To begin the testing process, a completely un-corroded sample must be used as a baseline for the test. It should be noted that the general lighting in the room can have an effect on the baseline threshold imaging, so if testing is stopped for an extended period of several hours, a new baseline threshold should be used.

When selecting the baseline threshold, the area selected should be the entire area of the un-corroded sample in the image. This process should be done for two certain areas of the sample. Those areas of the sample are the interior of the second cut out and main section between

cutouts. These areas are needed for the overall change that will occur in the future samples. Therefore the five total areas for analysis per sample are next to and on the hole, for both the upper and lower cut out, and the area exactly in the middle of the two cut outs. The area in the middle should be reached by taking the image of next to the cut out, and performing two screen wide movements towards the center. This should put camera in about the center of the sample for every sample that is considered. The thresholding therefore gives the initial un-corroded area and calibrates the computer for the color of the un-corroded surface.

Once the initial thresholding is completed, then the sample analysis can begin. There are 5 points to be examined per sample in order to avoid as much variation as possible. It should also be noted that the camera will be inversed, so the top of the sample in video screen is actually the bottom of the sample. The five sections that are being evaluated are then thresholded with the same threshold as the baseline and the corroded areas should not be accounted for when the image analysis takes place. This in turn grants a change of surface area for the samples, when compared to an un-corroded sample.

Once the corroded sample is thresholded, the image is then measured for the area covered by the threshold and the data exported to an excel document. This process should be repeated five times per sample, once for each of the designated areas

3.6.3 Cross Sectional Analysis

3.6.3.1 Mounting

A series of samples will be mounted for cross sectional optical analysis. Mounting is required because of the small size of the samples. A mounting machine will be utilized in order

to properly mount the sample. To begin, the sample must be cut along the surface that is to be evaluated. In this case each sample is cut in the center. A sharp cutting instrument should be used to minimize the damage to the sample during the cut. Once the cut is made, a C-clamps is used to hold the sample in place before mounting.

Once the sample is held properly, the sample will be placed on the platform of the mounting machine with the surface that is going to be observed on the bottom of the platform. The EXTEC mounting machine must be turned on from the back left corner and verified that the water supply is active. The sample is then lowered into the machine by holding the down arrow on the control panel. When at the bottom of the machine, mold powder can be funneled into the chamber using only a single scoop which is provided with the powder. For all mounted samples glass reinforced EPOXY mounting powder was used.



Figure 44: Mounting press.

The top lid of the machine must be secured by rotation and the red cover rotated over the lid. The mounting machine's pre-programmed function F-1 is used run the cycle. The cycle time should take 20-25 min to complete. Once completed, the mount removed should look like an

inch thick bottom cap. This will be a completed mount with the surface to be examined at the top of the mount. Figure 45 shows an example of the mounted sample.



Figure 45: Mounted sample.

3.6.3.2 Polishing

Once the sample has been mounted, it must be polished to a near mirror finish for optical viewing. This is accomplished by grinding the mount on increasingly higher grades of sand paper until the surface looks smooth under an optical microscope. For this project, the starting sandpaper grade was 600, which then increased as the surface was polished. The surface was examined under an optical microscope in order to evaluate the polish of the sample and determine whether it was ready for etching. Once the sample is viewed under the optical microscope and no scratches on the smaller sample can be seen, then the mount can be etched.

After mounting, polishing, and etching the predetermined samples numbers, cross-sectional analysis can begin for the samples. Each of the samples must be clearly polished as to allow for the visual distinguishing of corroded and un-corroded surface. The process that will be used to distinguish the corrosion will be the same thresholding process that was employed on the surface area. The fixed area that will be looked at is the distance of 200 microns from the tip of

the sample going towards the center. This area will be consistent for every sample as to provide a clear pattern of the penetration of corrosion. Due to the time needed to mount the samples, a single sample from each time slot was taken and mounted for the cross-sectional analysis.

3.6.3.3 Etching

Etching was specifically used in the microstructural study. It is the process of exposing a material surface to certain acids and or chemicals in order to view particular aspects of the material microstructure. In this project, etching was used for two particular reasons: to determine the microstructure of the samples and to see the effects of corrosion on the microstructure. The process for etching the samples begins with the determination of the etching solution. By etching the sample, specific particles are isolated and removed to provide a better surface for optical inspection.

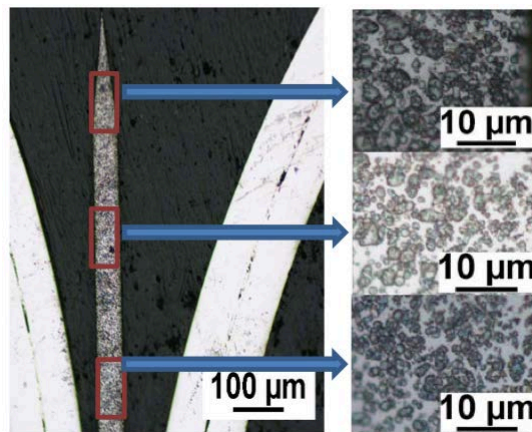


Figure 46: Etching locations and resulting microstructures.

A nital solution was chosen, which constitutes a 2% mix of nitric acid. Plastic gloves are required during any chemical handling and all procedures must occur in a fume hood as a safety

precaution. The sample needs to be placed in 2 ml of the nital for a specified period of time (in a magnitude of seconds), then quickly removed and placed in a petri dish of 2-5 ml of ethanol (enough to effectively cover the sample) to stop the reaction. For nital, the duration should be 5 seconds. Fry's reagent was also used in etching. Fry's reagent requires significantly less time, as the etchant is far stronger, and should be diluted where necessary to achieve useable results. Both etchants are aggressive acid solutions which can easily over etch the sample. Careful attention must be given to the time of reagent exposure.

Once the sample has been soaked in ethanol, it is air dried by a hair dryer or any other reasonable source for a period of 1-2 minutes. When completely dried, the mount is examined under microscope to determine the extent of the etching. If the etching is not deep enough the process should be repeated until favorable etching is seen. If over etching occurs, the sample can be repolished and etching performed again. An example of the etched material can be seen in Figure 47.

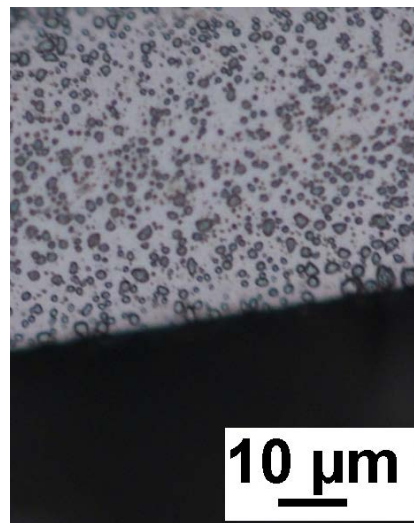


Figure 47: Microstructure of tempered martensite.

4.0 Results

4.1 Mass Data Analysis

4.1.1 Total Immersion Test 1

To begin the experimentation of this project, test 1 focused on the total immersion of the samples. Following the mass measurement guidelines, the initial mass values were taken, and once the test was complete, final mass was taken to examine the difference. For all collected mass data, see Appendix B. The final column in the appendix tables represents the average change in mass for each time interval. The first interval change average value represents the average change in mass for samples one, two, and three. The second value represents the average of samples four, five, and six, and the same pattern is followed for each of the 30 samples down the column.

From the collected data, several graphs were developed in relation to the mass loss over time. The mass vs. time graphs can be very telling in terms of their relationship and the overall effects of the corrosive process. An important calculation is the average mass loss per interval. From the first interval, the samples have continually decreasing overall masses.

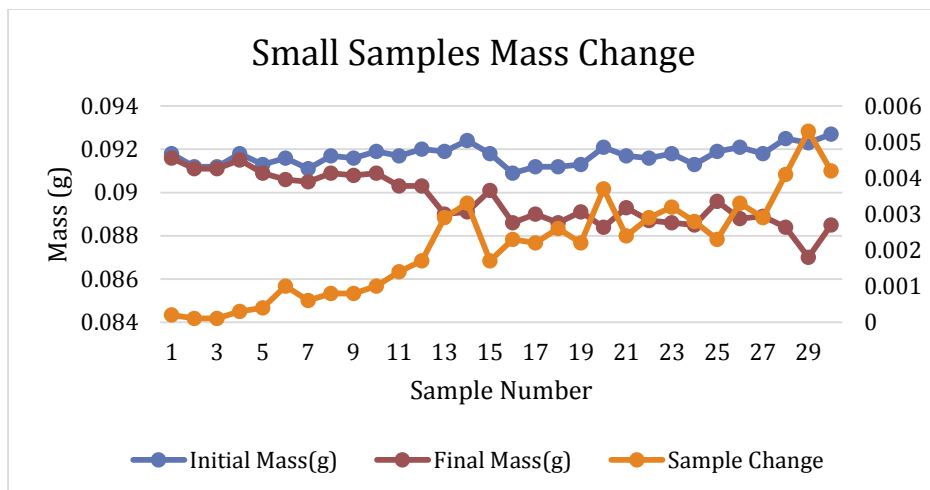


Figure 48: Small sample mass change.

Using Figure 48, the difference in mass can be seen with relation to the initial and final masses. From this figure the relationship over time is obviously one of deterioration. Though there are some variations from sample to sample, the general relation is that the longer the samples are immersed, the more mass is lost over time. By taking the average of the mass change per interval, an examination of the mass loss per interval can be made, so the time slots mass change can be seen. The data forms a fairly linear pattern with a few variations. From this it can be hypothesized that the mass loss over time follows a linear pattern for at least the first 48 hours.

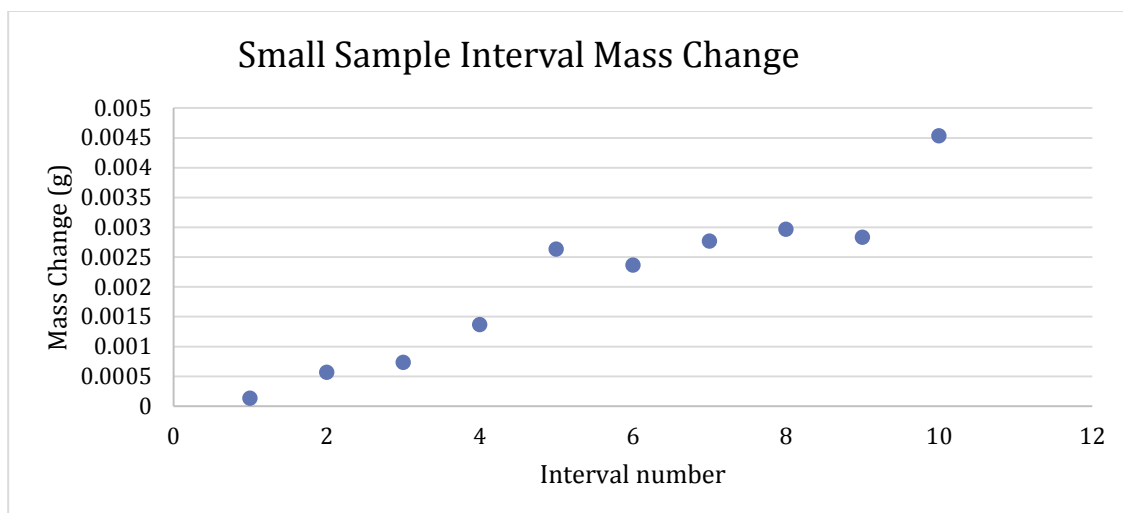


Figure 49: Interval mass change.

The final method of examination employed on the mass is the interval change in mass. This is to examine the difference between the points in the interval mass change and thus the difference of the rate of change. Using this comparison allows the view of how quickly mass changes through the intervals occurred, and what interval had the greatest change of mass. From these numbers, a period of increasing mass change from the first interval to the fourth was observed, followed by a period of constant mass increase. During the final interval, there was a rapid jump in the rate of mass change.

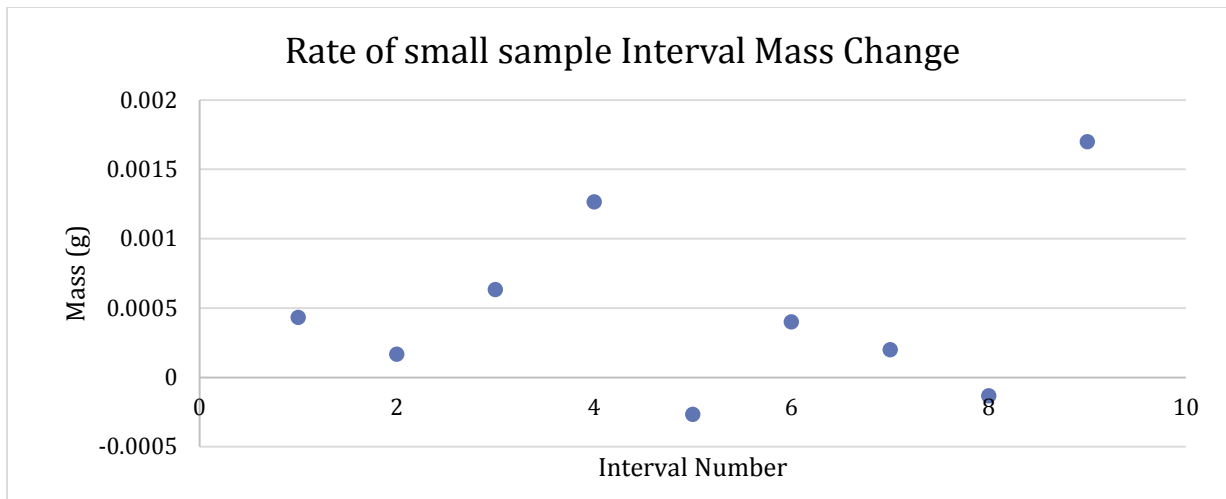


Figure 50: Rate of interval mass change.

The rate of change of the change in mass allows for some interesting analysis. From the research in the background, it is known that as corrosion occurs a film forms on the surface area. As the corrosive process progresses, particularly around the 5th interval, the film begins to form and slow down corrosion. The entire sample is still exposed to the solution, so the loss of mass continues, but at constant rate.

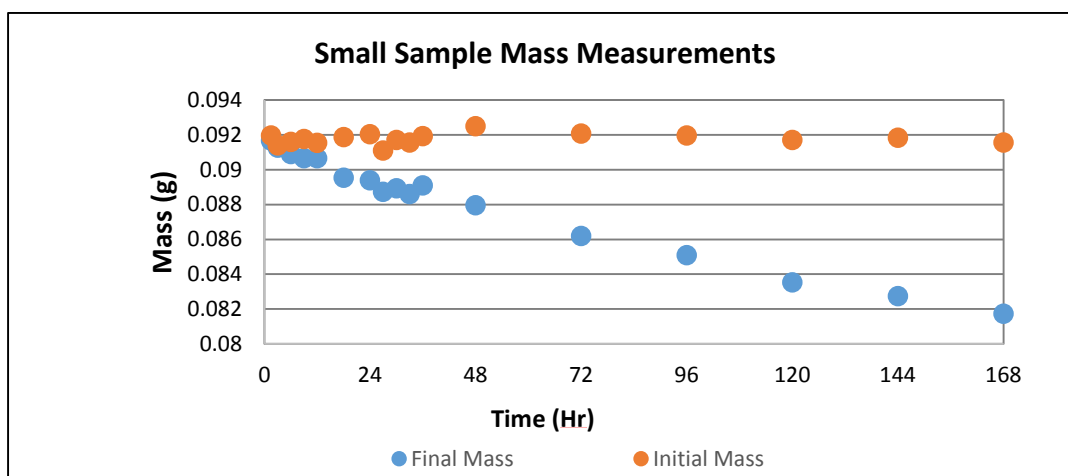


Figure 51: Small samples mass measurements.

The mass change of the large samples was not as revealing as those of the smaller samples. Still, there were a few points of interest to be noted and changes made for future tests as

a result. The mass change of the larger samples collected in the initial test will be discussed further alongside the results of total immersion test 2, as the combination of the results is more revealing.

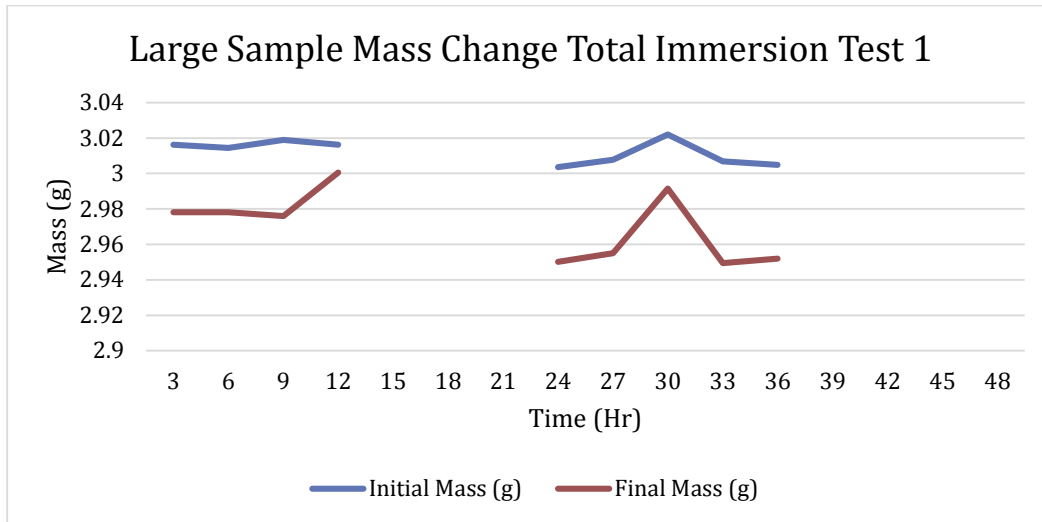


Figure 52: Large sample mass change, initial total immersion test.

4.1.2 Alternate Immersion Test 1

Following the procedure for the Dip & Rinse test, the samples were exposed to the set conditions for the selected amount of time. The masses were measured again to calculate the difference due to corrosion. The results however, were not as expected, returning a very small mass loss in the samples.

The change in mass following the 3 minutes submersion process was very small. Due to the limited exposure to the solution, there was not much corrosion during this test. The result is that the masses measured either varied very little or actually increased during the testing phase. The explanation for this occurrence is that there was so little corrosion occurring during the duration of the test that all variance can be attributed to the variance of the mass scale. Due to the

precision of the equipment, any variation may be the cause of the measurement differences. Therefore, the change in mass cannot definitively be determined a result of corrosion for this test, but rather the standard deviation of the equipment, explaining the miniscule gain and loss of mass at each interval.

4.1.3 Total Immersion Test 2

The mass results from the total immersion test 2 were completed specifically to supplement the results found in test 1. By overlapping several intervals and increasing the overall time for the test, the general pattern of corrosion begins to take shape.

It is worth first noting that the change in mass from total immersion test 1 and 2, when the time interval overlaps, are fairly similar. There are some slight differences, but the scale stays the same and the slight variation is to be expected as corrosion cannot be completely controlled to replicate results. Still these similar results reinforce the fact that the corrosion pattern is being repeated and the overlapping numbers support each other.

When combining the two total immersion test results, the average interval mass provides a pattern over the course of the 168 hours of immersion. The following can be seen in Figure 53.

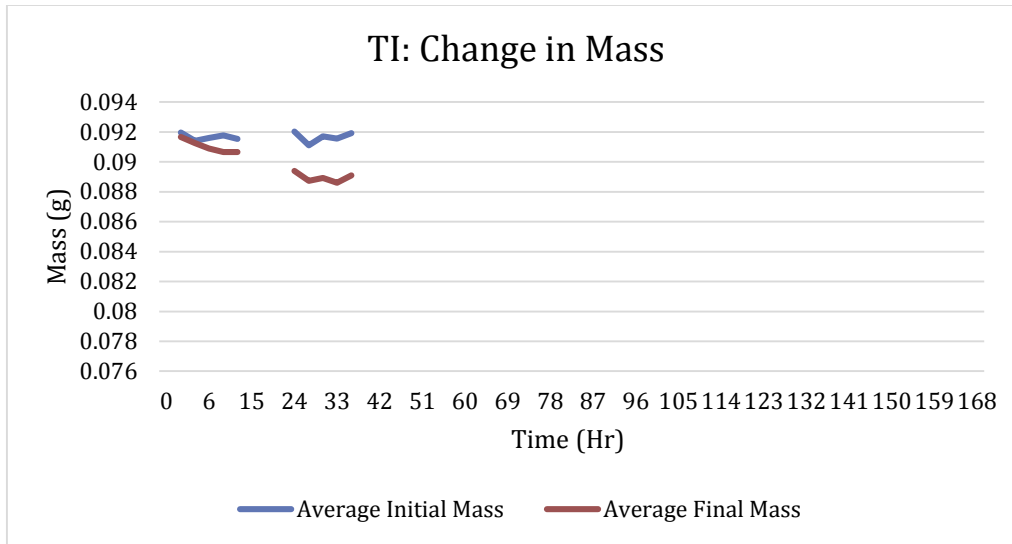


Figure 53: Total Immersion Test 2 small sample mass measurements.

From this graph, the general formula of the corrosion can be determined. The pattern shows that the expected corrosion equation follows the pattern of an exponential decay. From this, the baseline and starting point of the overall equation can be formed. However, it also allows for some hypothesis revolving around the point where corrosion may in fact stop. This point is in reference to the point in which the sample may stop losing noticeable amounts of mass and appear to show a mass change of around zero. By fitting the data points, an equation for this estimation can be found.

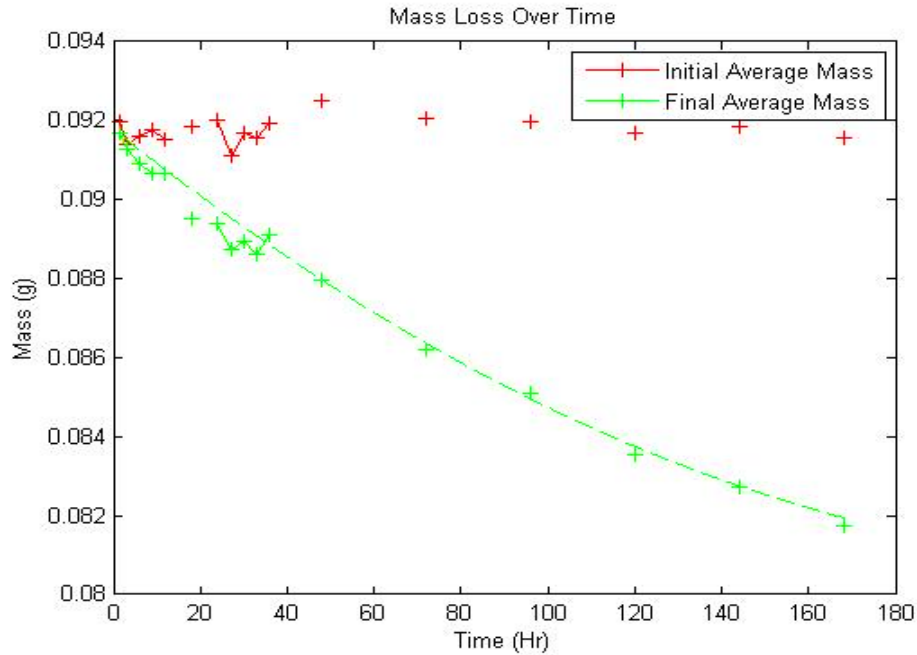


Figure 54: Mass loss over time.

This line was found using the following equation:

$$y = 1.75e-7 * t^2 - 0.000088 * t + 0.0918; \quad [34]$$

From this equation the derivative is taken to find the zero point of the slope.

$$\frac{dy}{dt} = 3.5E - 07t - 0.000088 = 0 \quad t = 251.42 \text{ Hr} \quad [35]$$

$$y(251.42) = .08073 \text{ Mass change/Hr} \quad [36]$$

This answer is plausible, though unlikely, as that result suggests only a 13% mass loss occurred before the corrosion process stopped completely. Still, it is a useful estimate and could be a testing point for future tests that take the time duration longer than the duration tested here.

When looking at the larger samples, it is easier to consider the combination of the two total immersion tests due to a similar method to the smaller ones. To start, combining the initial and final mass measurements of all the larger samples are shown in Figure 55.

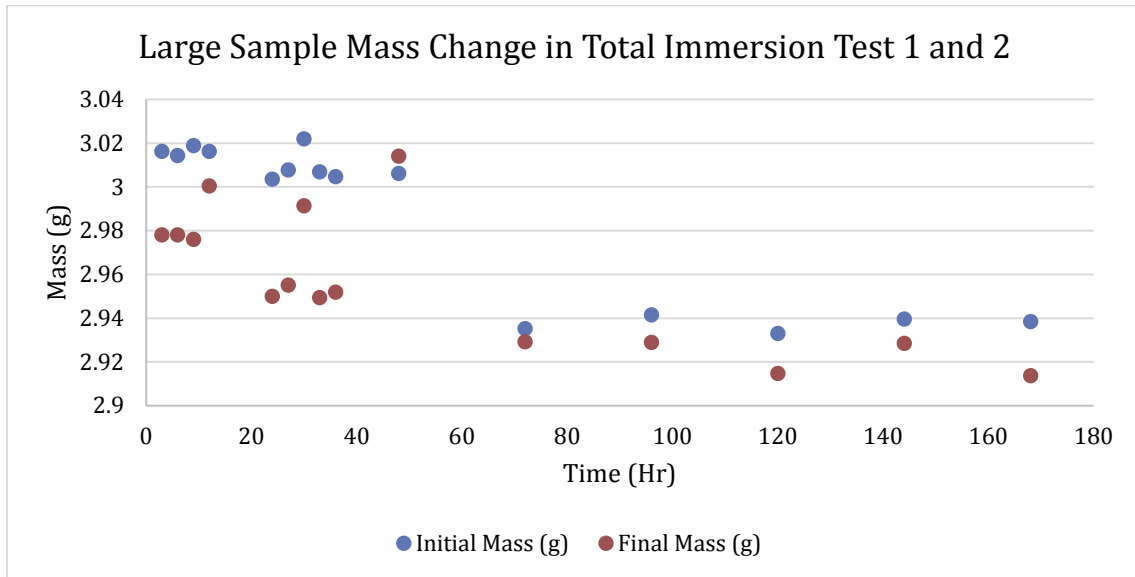


Figure 55: Combination of large sample mass change in Total Immersion Test 1 and 2.

It should be noted that the initial masses of the samples from the first total immersion test were greater as a component of the sample was left attached for that test. It was later discovered to absorb water and hence interfere with mass measurements. This explains why earlier the mass varies so much, as the component was removed for the second total immersion test.

The first part of this graph that stands out is the fact that the first two samples end with larger masses than they started with. The explanation for this is that the samples have a case of plastic surrounding multiple metal segments. As such, any immersion will result in some of the solution being left behind in between these surfaces. Though precautions are taken to limit the

effects, the earlier samples were measured sooner, and hence there was most likely still solution in the cases that influenced the mass measurements.

Still, the mass results of these samples are not as informative as the smaller samples. This is mainly due to the plastic structure around the samples. This plastic makes up a majority of the sample mass. Relative to this weight, the metal samples within have a very small mass. Therefore, even when corrosive effects are present, mass loss is minuscule when compared to the rest of the sample. From this it is safe to assume that the most reliable results for mass change come from the smaller samples.

4.1.4 Alternate Immersion Test 2

Results seen from the final alternate immersion trial mirror the results seen in test 2. The numbers show a minimal change in mass, even when the immersion time was increased more than threefold to try and induce more corrosion. Due to the lack of useable data, this section will focus on discussing the possible changes to this test to get actual corrosion results in this time period.

The original Dip & Rinse test resulted in very little mass change and the second test experienced the same pattern as the original test. Increasing the immersion time did not affect the results, so another possible method of influencing the corrosion rate seems to be other changes to the test procedure. Instead of changing the immersion time, each sample should be left to dry in between tests in a more humid setting. Since the goal of the test is simply to induce corrosion, the humid setting should not, in theory, influence any of the future test results. The rise in humidity may slow the drying rate of the samples leaving moisture on the samples, and continuing the corrosion process. Since the samples that have run their time in the solution will

be stored in a separate environment, there is no fear of influencing the results by making this change.

4.1.5 Change in Mass after Sample Removal

It should be noted that corrosion will continue to occur to a sample exposed to excess oxygen. To counter this effect, all samples were stored in air-tight bags as soon as they were removed from the solution and during times when tests were not being conducted. To confirm that the masses of the samples did not change from the original measured values, several samples were measured again over a month after the original mass measurement. The results found the masses were almost exactly the same as initially measured. As a result, the assumption that no additional corrosion or change to the mass occurs once the samples are removed from the solution can be made.

4.2 Surface Area

After the samples were corroded, the surface area damage was measured by visual thresholding. During the two total immersion trials 30 small samples and 10 large samples were corroded with the 3.5% sodium chloride solution. The first total immersion test was conducted for two days. In order to increase the scope of the results, the second test was conducted for a full week. The second test time intervals were strategically chosen to fill in gaps in the results.

4.2.1 Total Immersion Test 1

The results for the surface area damage for the first total immersion test are shown in Figure 56. The ten data points shown each represent an average of three numerically ordered

samples. As shown in the figure, there is an upward trend as time increases. The corrosion relationship appears to be linear, however this relationship cannot be stated with certainty as the results represent a limited time range.

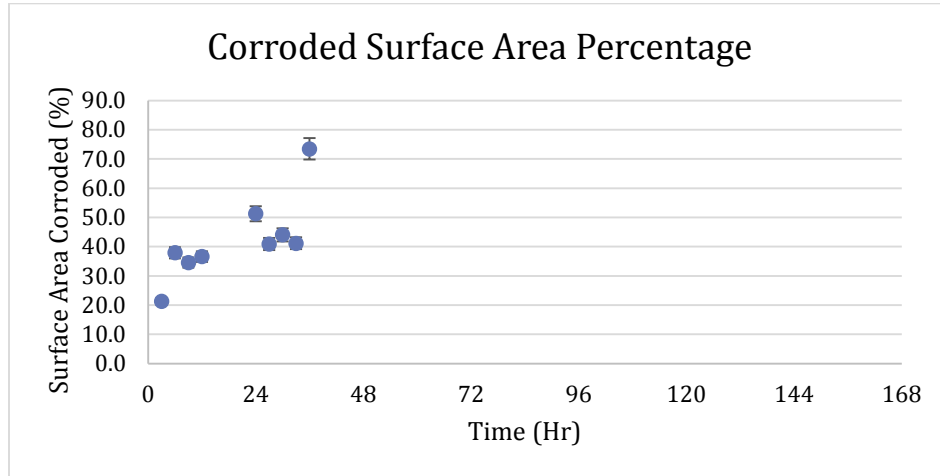


Figure 56: Total Immersion Test 1 surface area corrosion damage.

4.2.2 Total Immersion Test 2

After total immersion test 1 was conducted, the total immersion test was repeated for a longer time range of 168 hours to develop a better understanding of corrosion growth behavior.

Figure 57 shows the combined results for the second total immersion test as well as the initial results.

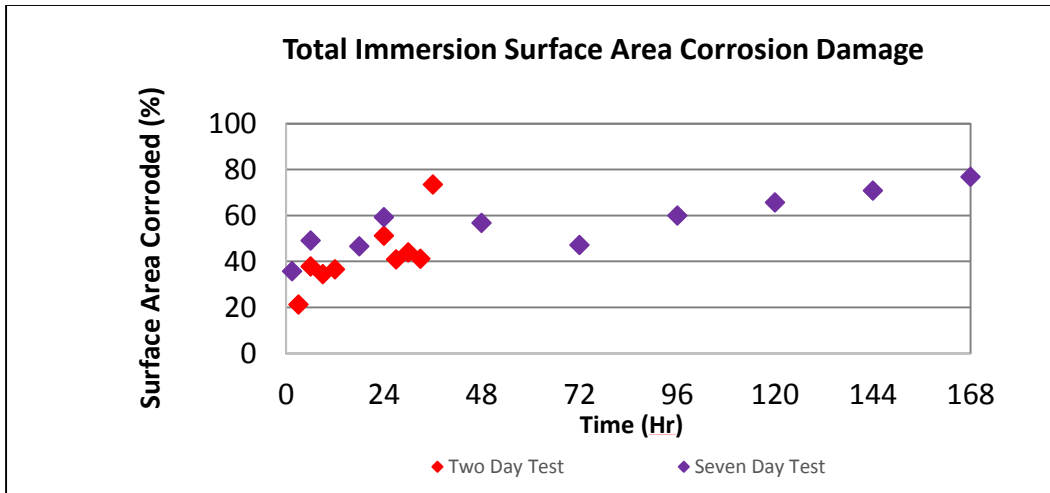


Figure 57: Combined Total Immersion Surface Area Corrosion Damage.

Similar to Figure 56, each of the ten new data points in Figure 57 represents the average of three damaged results. This figure corresponds more with what is expected. In comparison to the first total immersion test, which showed a linear relationship, this figure shows a more asymptotic relationship. It is expected that the corrosion damage reaches an asymptotic value, as the samples are stainless steel, which creates a layer of oxides covering the surface and blocking corrosion over time.

With the exception of the final data point from total immersion test 1, the data fits fairly well with the results from total immersion test 2. In general, the surface area test produces more reliable results at a larger time scale. Early on in the corrosion process, corrosion grows from the sample tip outwards in a seemingly arbitrary fashion, so some of the early variation in the results can be included in the noise. As the damage progresses, a thicker layer of oxides is formed on the surface, which produces a more pronounced and consistent product.

Pictures were taken of the surface area damage for a group of the small samples. Afterwards, these representative samples were used as part of the cross sectional analysis for this project. Figure 58 shows surface area images for the total immersion test 1.

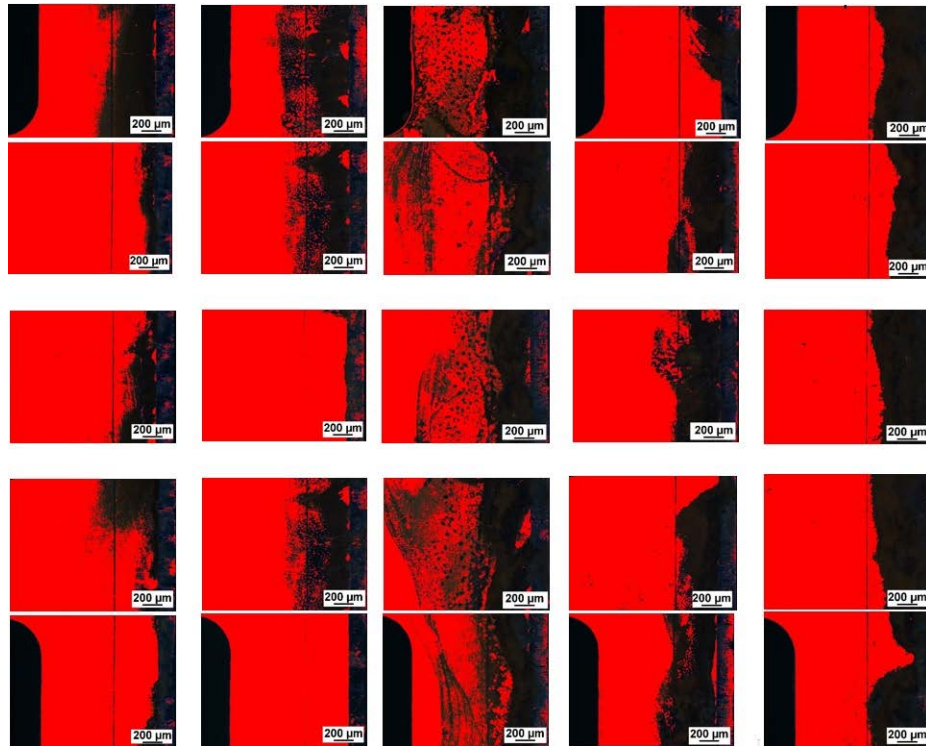


Figure 58: Surface area of damage of Total Immersion Test 1.

The images represent the surface area of damaged results for the total immersion test 1. The images are separated into five columns, each of which represents a sample. The red area shows the area selected by the threshold software and represents the un-corroded area. From left to right, the images represent samples at 6, 12, 24, 30, and 36 hours of exposure to the corrosive solution.

Although the damage does seem to get progressively larger from left to right, these results can be influenced at early stages by the drifting of corrosion products over the surface. As is shown in the third column (24 hour sample), it is expected that the damage to this sample would be less. However some corrosion products have drifted to the left and may have led to a higher surface area of damage measurement. A potential solution to this issue is to carefully wipe the surface of each sample with a solution that will not cause further damage or influence the corrosive film. Figure 59 shows the surface area of damage results for the total immersion test 2.

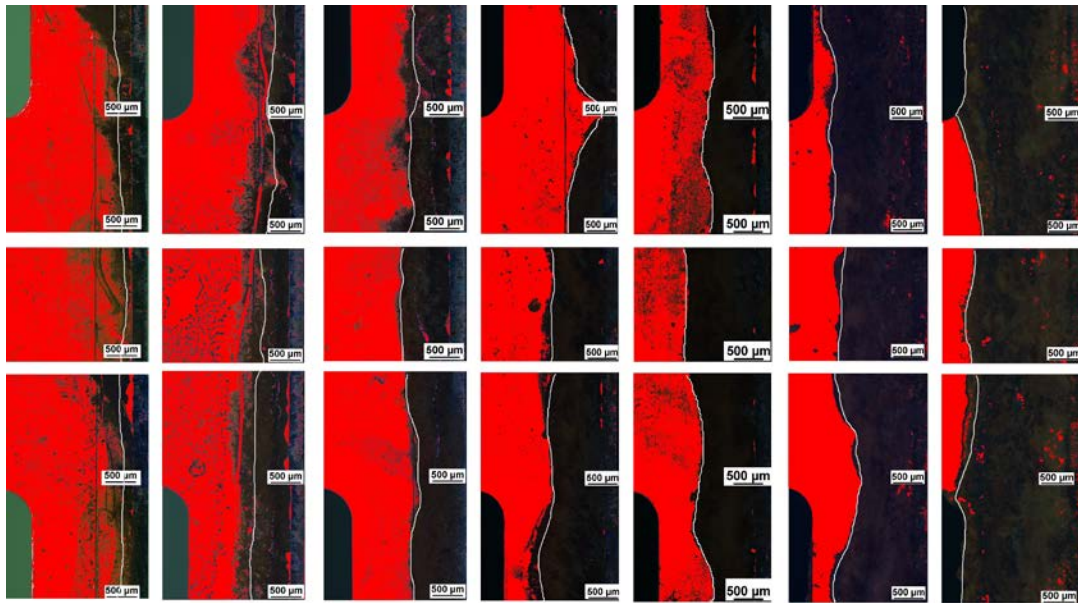


Figure 59: Surface area of damage for Total Immersion Test 2.

Each column represents a sample with a different exposure time. From left to right, the pictures represent 1.5, 6, 24, 48, 96, 144, and 168 hours of exposure. From these images is clear that the damage progressively increases as time passes. An interesting note is that the damage originates at the sample tip (right side of pictures) and progresses to the center. Although it can be seen that some of the earlier samples have slightly higher results due to surface products

drifting to other areas, this interference is much less for the later time period samples where the corrosive film is more pronounced.

4.3 Cross Section Analysis

Cross sectional analysis of the samples offer a view of the internal effects of corrosion growth. Figure 60 shows progressing penetration of corrosion with increasing time from left to right. Throughout the project a consistent attack was observed internally. The following sections describe the data collected on this growth.

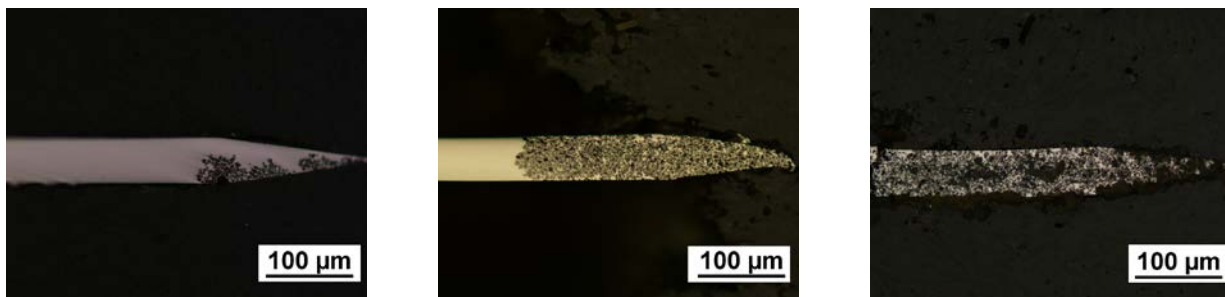


Figure 60: Cross section of samples.

4.3.1 Total Immersion Test 1

A graph was constructed from the cross sectional data acquired by optical thresholding from the first total immersion test, shown in Figure 61. From this a slight pattern in regards to the interior cross-section corrosion was observed. The steady decline indicates the possibility of an equation defining the process of interior corrosion such as this. Following the analysis of total immersion test 1, several points of discussion came up, which will be addressed in the third tests analysis section.

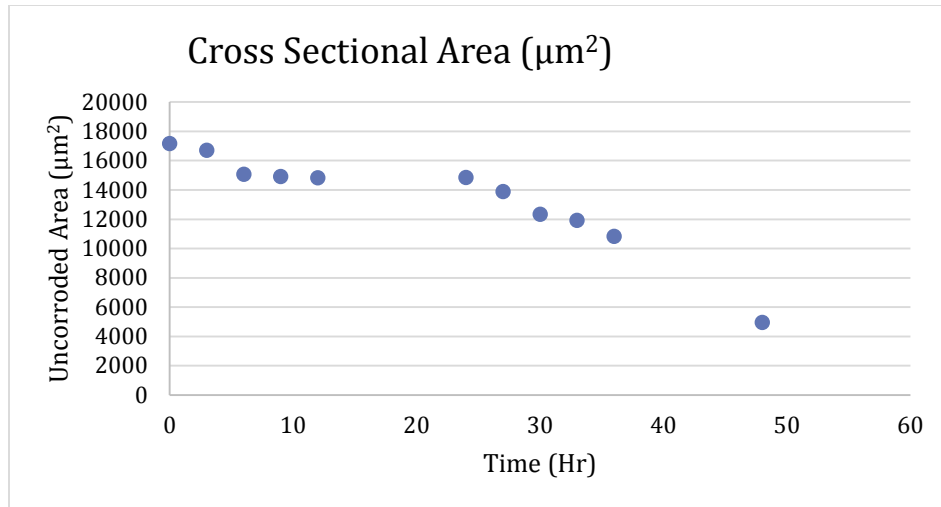


Figure 61: Cross sectional area for Total Immersion Test 1.

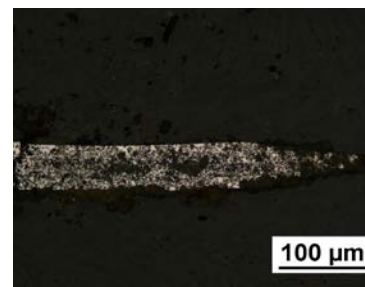
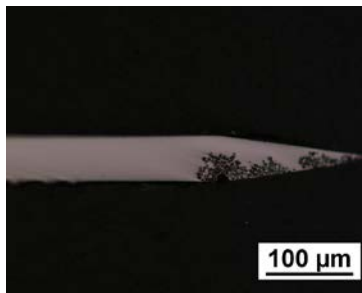
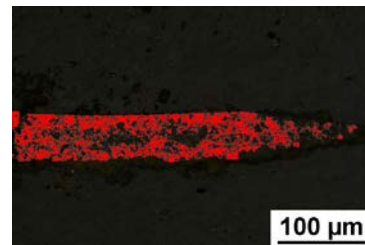
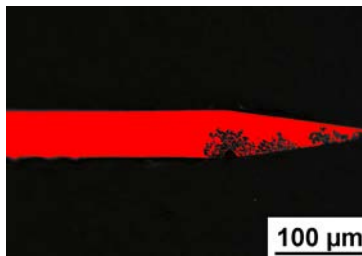


Figure 622: Cross-sectional thresholding at different time steps during Total Immersion Test 1. (Left 6 Hr)(Right 48 Hr)



4.3.2 Total Immersion Test 2

The cross section analysis on the samples from total immersion test 2 were performed with the original intention of supplementing and reinforcing the results from that test. However, when comparing the cross sectional graphs for each test, there are several inconsistencies.

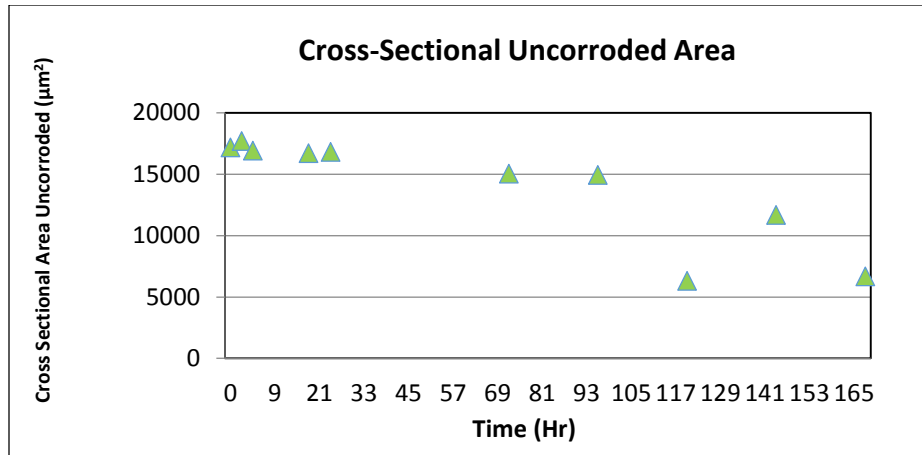


Figure 63: Cross sectional area for Total Immersion Test 2.

The main inconsistency and primary concern is that fact that the cross-sectional area of the first test showed a significantly faster corrosion rate than samples of total immersion test 2. The differences weren't a small rate, but rather a rather drastic change. As a result, it is necessary to try and determine the reason for this major difference. When looking at the mass changes of these two tests, changes occur on a fairly similar level at similar time intervals, meaning that the exposure and mass loss were similar. To understand this inconsistency, the units of each was compared and it was found that the scaling of the program had changed between the tests. This resulted in the variation of data that was seen. However, by making a few assumptions regarding how the scaling changed, it is still possible to get viable data from the results.

To try and explain the causes behind this internal corrosion rate, the most likely possibility is to focus on the thresholding method as the main issue. While the thresholding method is sound in theory, the likely cause of this issue is the lack of precision on the instrument used. The main issue therefore is the computer's ability to distinguish the small corroded particles in a cross-section. This can be seen in the results later during the third test, where the

cross section area is very small. On several of these samples, the depth of penetration was significantly larger than the previous samples, yet the cross-section selected by the program was often off, requiring manually alteration to try and align the results. Therefore, the programs limitation lead to human factors in the data collection process, which in the end is the most likely cause for these results.

The general lighting was another source of potential error for this test. The thresholding measurement relies on optical methods which isolate specific colors and shades of the material. Therefore, this process requires an extremely consistent lighting environment during the measure of all test samples. However, due to the time necessary to completely measure samples, the lighting could change due to the time of day or even shadows through a window.

Still, the method brings up several factors that could be considered for future tests. One is that a smaller focus area may be needed in order to pursue this method of analysis. The tests here were done on a 200X magnification, on a very small sample as well. Therefore, larger samples or a larger magnification may help solve the calibration problems that were faced by the project team.

4.4 Equation Formulation

A primary goal of this project was in the development of a corrosion rate equation based on the data collected. By using the established corrosion equation Eq. 16, we took the next step of determining what the value of the constant K_1 would be.

Established Corrosion Model

$$R = \frac{k * W}{\rho * A * t}$$

R=Rate of corrosion [in/yr]
 W=Weight loss [g]
 ρ=Density [g/m³]
 A=Corroded Surface Area [m²]
 T=Time [Hr]
 k=Corrosion constant

Predictive Volume Corrosion Model

$$V = \frac{K_1 * W}{\rho * A * t}$$

V=Rate of corrosion [m³/hr]
 W=Weight loss [g]
 ρ=Density [g/m³]
 A=Corroded Surface Area [m²]
 T=Time [Hr]
 K₁=Corrosion parameter [m²]

Looking at the comparisons of the known literature equation and the teams' representation of the volumetric equation, the similarities are fairly close. This is due mainly to the fact that the volumetric is based off of the literature equation. Since the established model focuses mainly on a length per time model, by expanding this to be m³ per time, the volumetric form could be evaluated. All that remained was to find the functions that represented the measured data of W, A, and V.

To begin the process to determine the necessary functions, the change in mass was determined. By plotting the change over time, it is possible to fit an equation, which will effectively function as the W term in the predictive volume corrosion model.

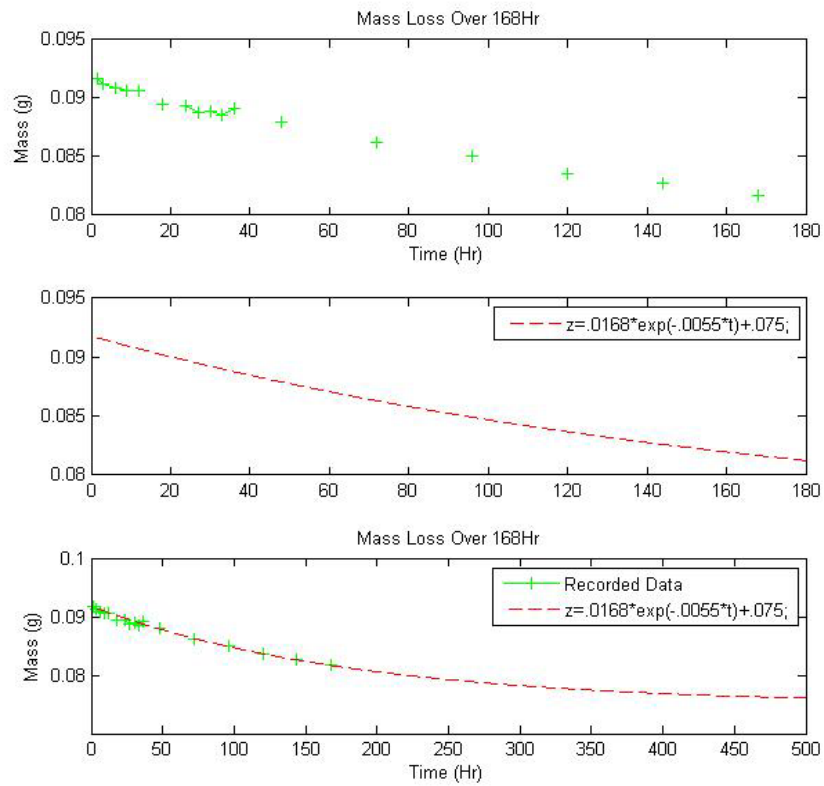


Figure 64: Mass loss over 168 hours.

Using this function, which can clearly be seen in Figure 64, the function of time for mass loss can now be inserted in the corrosion equation. This process is repeated for surface area data as well.

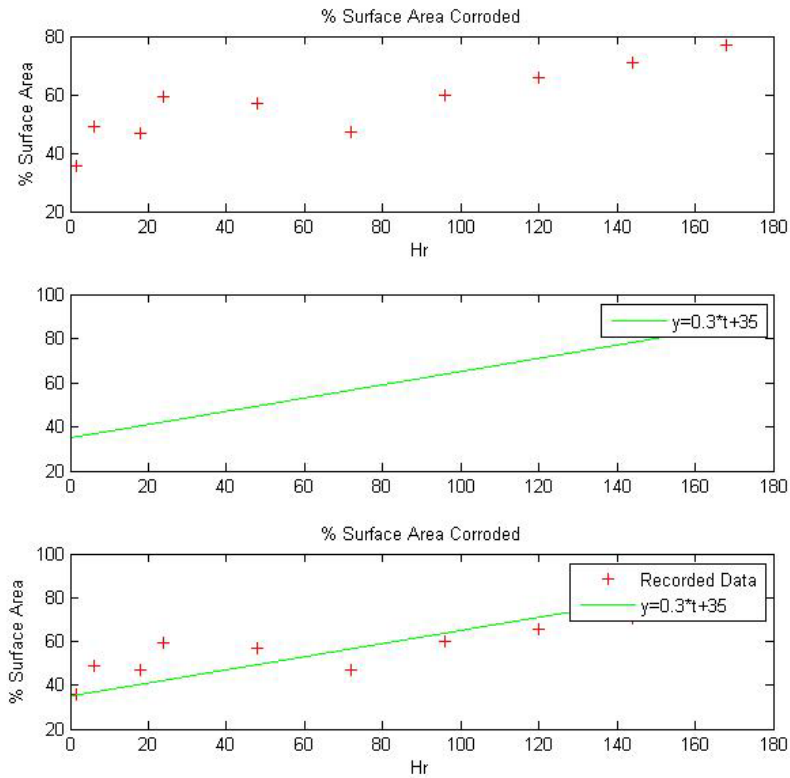


Figure 65: Surface area corroded (%).

It's important to note here that the surface area is represented in un-corroded percentage values. Therefore, to get the necessary value of A, the percentage was changed to one minus the un-corroded percentage given by the equation. This grants the corroded surface area percentage, which when multiplied by the surface area grants the necessary variable.

The final variable is the corrosion rate R, which is normally given in length over time units. However, the formulation attempted by the project alters the R to a volume related variable. To achieve this from the data, the cross section corrosion area was fitted over time like the previous variables.

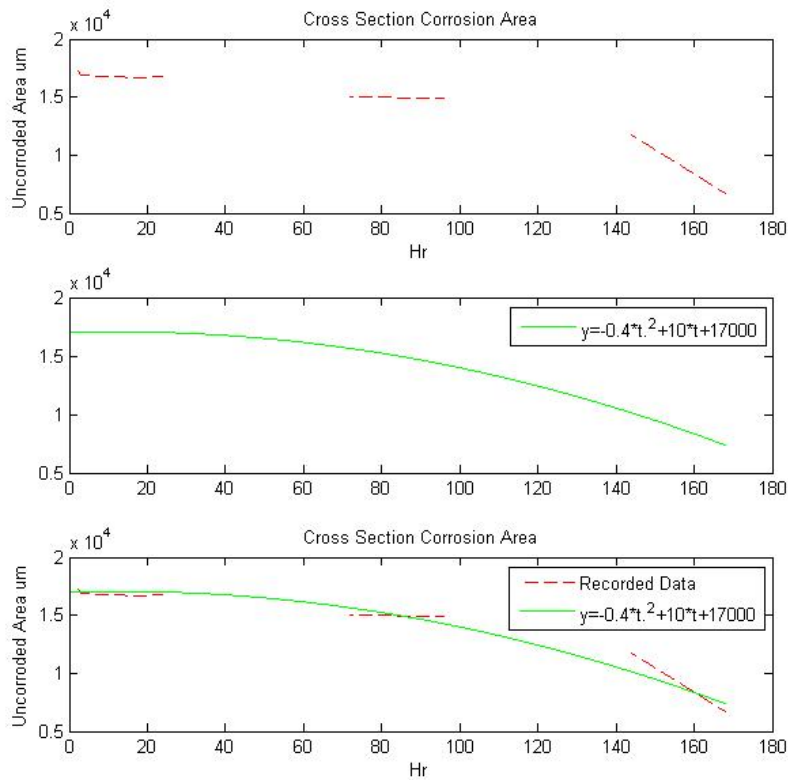


Figure 66: Cross section corrosion area.

Since it was determined that the corrosion through the samples was fairly uniform from a cross sectional view, multiplying the cross section by the length gives the sample's volume change. Since the exact measurements of the samples can be measure, this makes determining the volume and corrode volume fairly simple. The exact density is unknown, but because of the material, a reasonable estimation can be made. By checking the units and converting to the necessary units, the variable K_1 was solved for.

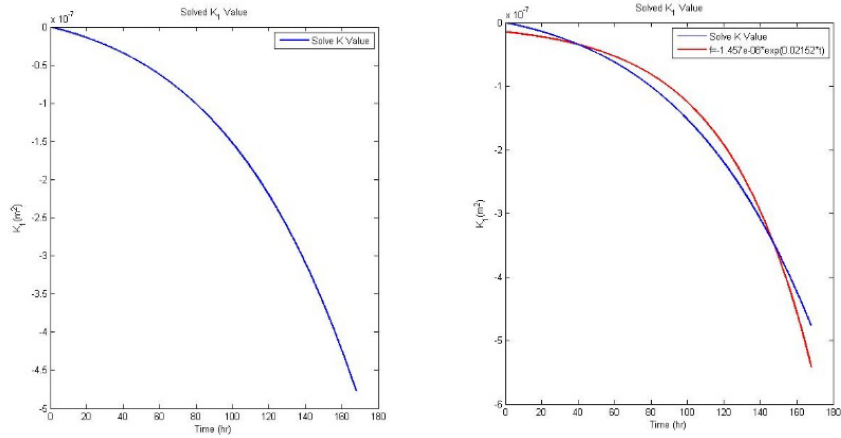


Figure 67: Solved K_1 parameter value.

It should be noted here that K_1 is a function of time that has the units of m^2 . However, this K_1 depends on the multitude of variables that affect corrosion, and were not tested in this project. Still, by fitting the K_1 curve, estimations on where certain variables would fit can be made. For example, known effects of fluid velocity, temperature, and salinity have been researched in the background of this paper. Taking the general form on the K_1 equation, which is shown in Eq. 37, allows for these variables placement.

$$-Ae^{(bt)} \quad [37]$$

For example, it was researched that the effect of temperature was linearly related to the corrosion process. As temperature increases, corrosion rate does so linearly as well. Therefore, the variable placement can be made to reflect that knowledge. The same can be done with the other variables, resulting in the following proposed equation. Eq. 38:

$$-K_2 \frac{F(v)}{F(S)} e^{(F(T)t)} \quad [38]$$

where $F(v)$ is the velocity factor, $F(T)$ is the temperature factor and $F(S)$ is the salinity factor

The K_2 is a representation of all the corrosive factors that aren't currently being tracked or have a known measured effect. This includes factors such as humidity or solution contamination, which may influence the corrosive rate. As such, if the equation for the effect of humidity over time was found, then it would be possible to know exactly how that factor would influence the rate of corrosion based on where it would be fit in Eq. 38. While this project doesn't go into the exact locations of many of these variables, it allows for future research to be done to predict exactly where certain factors should be located and their effect on corrosion, based on the representative mathematical model of that factor.

5.0 Conclusions and Future Work

The goal was to develop a reliable test method and quantitative procedure for analysis of corrosion damage in samples. These deliverables can be applied to the sponsoring company's products for numerical evaluation of samples. To begin with, the design of a specific apparatus to provide a standardized testing environment for the samples was created. This apparatus controls multiple variables that affect the growth of corrosion during induction and can be easily modified in future testing. As an effort to expedite the testing process, the apparatus was designed to contain multiple samples at once. Temperature, solution, and agitation can be modified to change the rate of corrosion or provide an alternate environment if needed.

Two corrosion induction procedures have been adapted from the sponsoring company procedures and ASTM standards to provide reliable standardized methods and to fit the purposes of this project. The total immersion test involved a complete immersion of the samples for an extended period of time. The alternate immersion test method involved short periods of immersion followed by long drying periods.

The samples were analyzed using mass measurements, surface area, and cross section of damage measurements. In terms of the mass measurements, each sample was measured for initial mass before corrosion growth and final mass after corrosion occurs. Using optical methods, the surface of the samples were analyzed to determine the surface area of corrosion growth. With a similar optical method, the cross section of these samples was measured to determine the extent of internal corrosion damage.

Analyzing the data, the change in mass showed an asymptotic decrease, whereas surface area damage increased asymptotically. As for cross sectional corrosion damage, a similar increase in area of damage was observed. Taking each of these measures with respect to time, the team combined those equations with a known corrosion rate equation to relate each of these measurements to the change in volume. An original K_1 parameter was developed to account for the known relations from the predictive volumetric corrosion model. This final equation comes with a corrosion parameter K_2 that is a function of all non-stated corrosive variables. The variable K_1 was modified to account for the contributions of additional corrosion factors of the variable K_2 . Future tests with more parameters will improve the known relationship with K_2 based on the factors' corrosive mathematical models.

6.0 Recommendations

For future projects the team has several recommendations to make regarding equipment and procedures. When conducting corrosion induction the team noticed that a significant amount of corrosion product can accumulate in the testing solution. This product may or may not affect the growth of corrosion going into longer sample periods. The salinity of the solution is another concern. Monitoring the salinity of the solution throughout tests to see whether it remains constant may be useful in determining more accurate results. This topic may require some investigation going further to verify whether it is in fact an issue. Something else to consider during corrosion induction is the humidity of the room. During this project the team had no methods of monitoring or control the humidity of the room in which tests occurred.

After each test the samples should be kept in a desiccator, with fresh desiccant in the bottom to absorb any moisture present and prevent further corrosion growth. This will help to maintain the accuracy of all analysis. During surface area analysis it was noticed that longer exposure times to solution provided a better picture of growth over time. It was also noticed that on the surface of these samples were hard corrosion product and a film of similar color left behind by products in the solution. This film tints the surface in a way that may affect image analysis which is color dependent. A suggested solution to this would be to remove the film by either use of a solution or another physical method taking care not to remove actual corrosion products.

7.0 Acknowledgements

The group would like to extend a special thank you to the following people and departments who assisted in the successful completion of this project:

The Sponsoring Company

Professor Diana Lados

Professor Cosme Furlong

Anthony Spangenberger

Professor Boquan Li

Paula Moravek

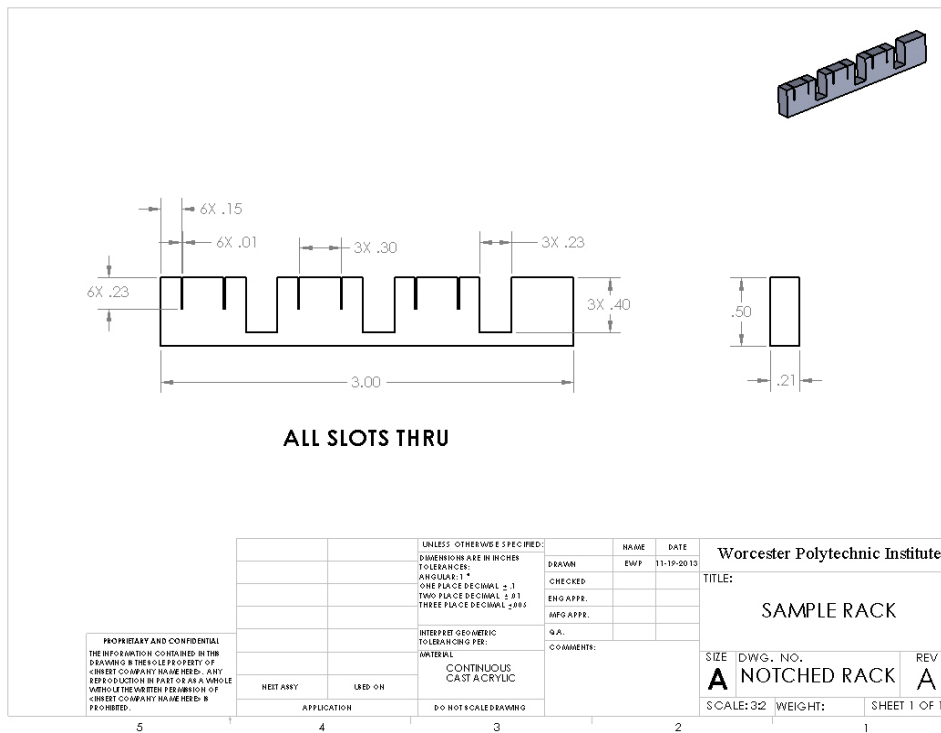
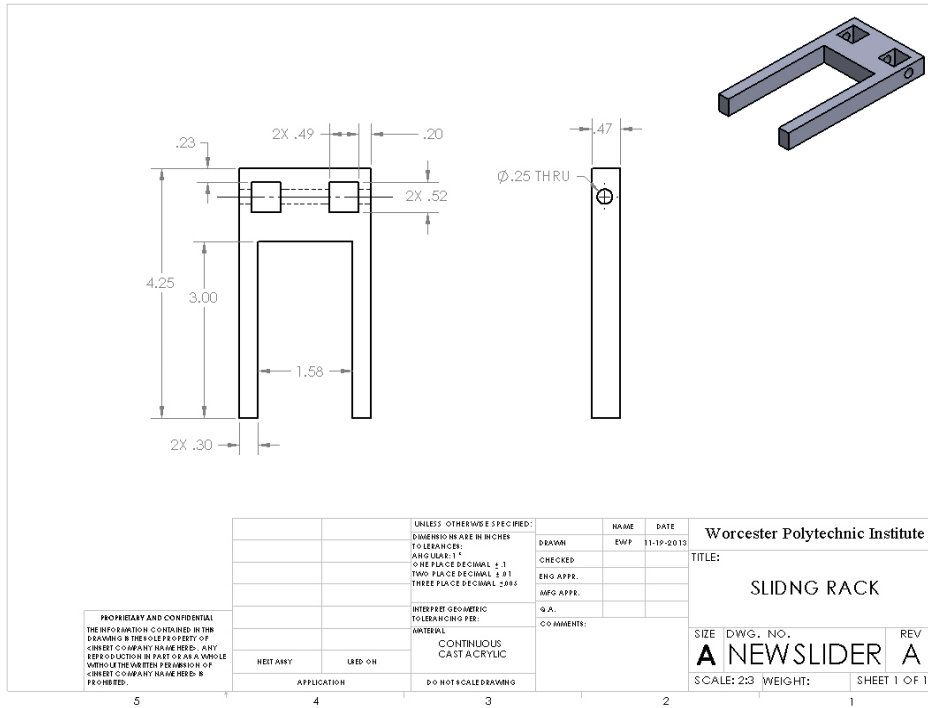
Chemistry Stockroom

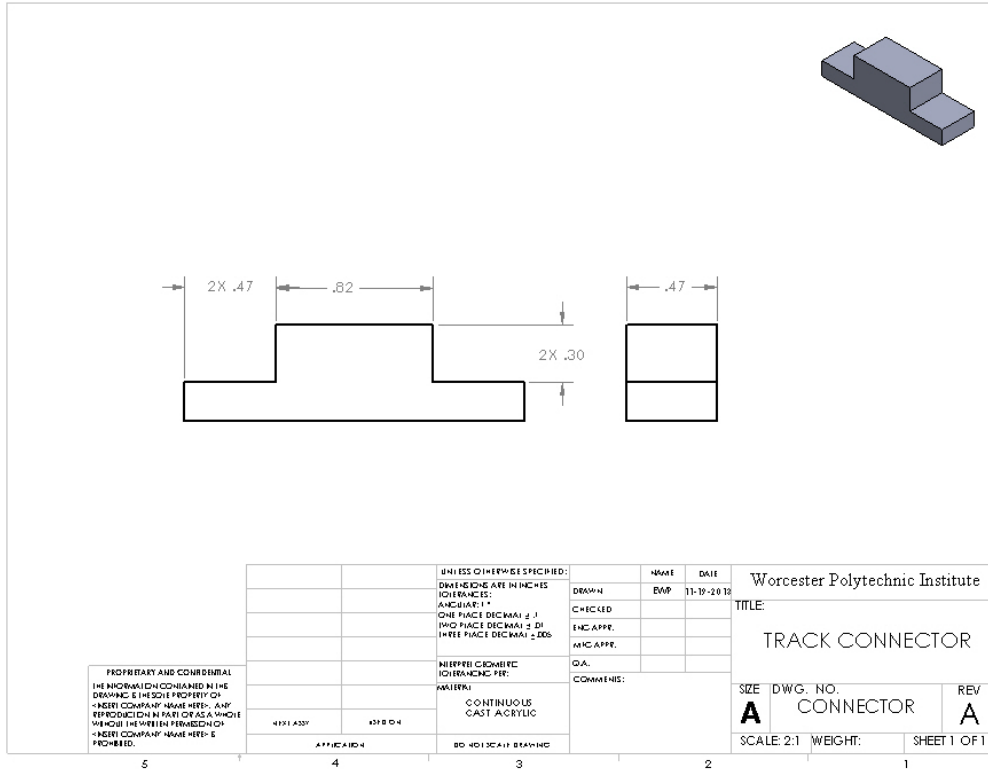
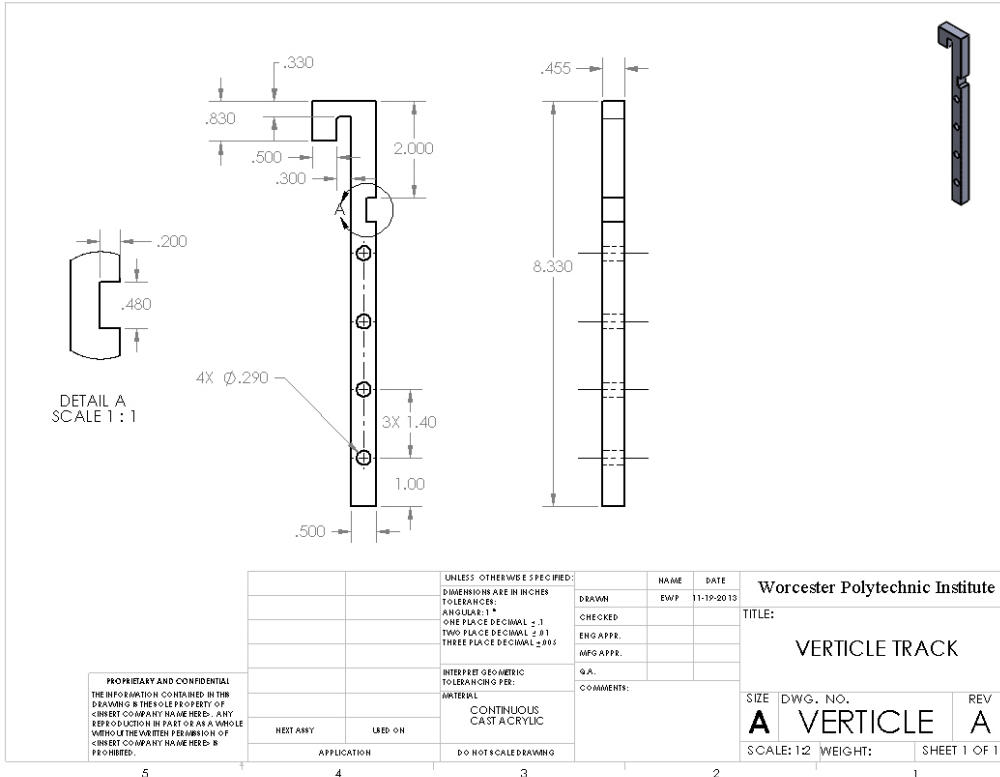
Physics Department

Washburn Shops

Ultimate Plastics

Appendix A: Part Drawings





Appendix B: Mass Measurement Data Tables

Table 6: Total Immersion Test 1 mass measurements small samples

Small Samples #	Initial Mass(g)	Final Mass(g)	Mass Change (g)	Interval Change Average
1	0.0918	0.0916	0.0002	0.0001
2	0.0912	0.0911	0.0001	0.0005
3	0.0912	0.0911	0.0001	0.0007
4	0.0918	0.0915	0.0003	0.0013
5	0.0913	0.0909	0.0004	0.0026
6	0.0916	0.0906	0.001	0.0023
7	0.0911	0.0905	0.0006	0.0027
8	0.0917	0.0909	0.0008	0.0030
9	0.0916	0.0908	0.0008	0.0028
10	0.0919	0.0909	0.001	0.0045
11	0.0917	0.0903	0.0014	
12	0.092	0.0903	0.0017	
13	0.0919	0.089	0.0029	
14	0.0924	0.0891	0.0033	
15	0.0918	0.0901	0.0017	
16	0.0909	0.0886	0.0023	
17	0.0912	0.089	0.0022	
18	0.0912	0.0886	0.0026	
19	0.0913	0.0891	0.0022	
20	0.0921	0.0884	0.0037	
21	0.0917	0.0893	0.0024	
22	0.0916	0.0887	0.0029	
23	0.0918	0.0886	0.0032	
24	0.0913	0.0885	0.0028	
25	0.0919	0.0896	0.0023	
26	0.0921	0.0888	0.0033	
27	0.0918	0.0889	0.0029	
28	0.0925	0.0884	0.0041	
29	0.0923	0.087	0.0053	
30	0.0927	0.0885	0.0042	

Table 7: Total Immersion Test 1 mass measurements large samples

Large Sample #	Initial Mass (g)	Final Mass (g)	Mass Change (g)
1	3.0163	2.9781	0.0382
2	3.0144	2.9781	0.0363
3	3.019	2.976	0.043
4	3.0163	3.0005	0.0158
5	3.0035	2.9501	0.0534
6	3.0078	2.9551	0.0527
7	3.022	2.9915	0.0305
8	3.0069	2.9494	0.0575
9	3.0048	2.9519	0.0529
10	3.0062	3.0141	-0.0079

Table 8: Dip & Rinse Test 2 mass measurements large samples

Large Samples	Initial Mass (g)	Final Mass (g)	Mass Change
1	3.0128	3.0199	-0.0071
2	3.0134	3.1289	-0.1155
3	3.012	3.0149	-0.0029
4	3.0109	3.022	-0.0111
5	3.0156	3.0233	-0.0077
6	3.0106	3.0187	-0.0081
7	3.0031	3.0261	-0.023
8	3.0055	3.0172	-0.0117
9	3.0123	3.0186	-0.0063
10	3.0081	3.0246	-0.0165

Table 9: Dip & Rinse Test 2 mass measurements small samples

Small Samples	Initial Mass (g)	Final Mass (g)	Mass Change	Interval Change
1	0.0924	0.0926	-0.0002	-0.0002
2	0.0922	0.0925	-0.0003	-0.0003
3	0.0924	0.0925	-0.0001	-0.0001
4	0.0919	0.092	-0.0001	-0.0001
5	0.0918	0.0922	-0.0004	-0.0001
6	0.0912	0.0916	-0.0004	1E-04
7	0.0926	0.0922	0.0004	-3.33 E-05
8	0.0921	0.0926	-0.0005	-0.0006
9	0.0915	0.0917	-0.0002	3.33 E-05
10	0.0918	0.0918	0	0.0003
11	0.092	0.0916	0.0004	
12	0.0915	0.0922	-0.0007	
13	0.0924	0.0928	-0.0004	
14	0.091	0.0916	-0.0006	
15	0.0928	0.0923	0.0005	
16	0.0916	0.0912	0.0004	
17	0.0914	0.092	-0.0006	
18	0.0916	0.0911	0.0005	
19	0.0921	0.0922	-0.0001	
20	0.0918	0.0925	-0.0007	
21	0.0922	0.0915	0.0007	
22	0.0918	0.0924	-0.0006	
23	0.0912	0.092	-0.0008	
24	0.0918	0.0922	-0.0004	
25	0.0922	0.0921	0.0001	
26	0.0913	0.0918	-0.0005	
27	0.092	0.0915	0.0005	
28	0.0923	0.0924	-0.0001	
29	0.0923	0.0919	0.0004	
30	0.0922	0.0917	0.0005	

Table 10: Total Immersion Test 2 small samples

Initial Mass(g)	Final Mass(g)	Mass Change (g)	Interval Mass Change
0.0921	0.0917	0.0004	0.0003
0.0923	0.092	0.0003	0.0010
0.0915	0.0913	0.0002	0.0023
0.0924	0.0912	0.0012	0.0025
0.0918	0.0909	0.0009	0.0040
0.0921	0.0913	0.0008	0.0059
0.0918	0.0891	0.0027	0.0069
0.0922	0.0904	0.0018	0.0082
0.0916	0.0891	0.0025	0.0091
0.0923	0.0898	0.0025	0.0098
0.0915	0.0891	0.0024	
0.0917	0.089	0.0027	
0.0917	0.088	0.0037	
0.0915	0.0876	0.0039	
0.0919	0.0874	0.0045	
0.0922	0.0864	0.0058	
0.0924	0.0862	0.0062	
0.0916	0.086	0.0056	
0.0922	0.0851	0.0071	
0.0917	0.0855	0.0062	
0.092	0.0847	0.0073	
0.0913	0.0823	0.009	
0.092	0.0842	0.0078	
0.0918	0.0841	0.0077	
0.0916	0.0832	0.0084	
0.0923	0.0825	0.0098	
0.0916	0.0825	0.0091	
0.0915	0.0825	0.009	
0.0911	0.0804	0.0107	
0.0921	0.0823	0.0098	

Table 11: Total Immersion Test 2 large samples

Sample #	Initial Mass (g)	Final Mass (g)	Change in Mass
1	2.9362	2.9386	-0.0024
2	2.9375	2.9432	-0.0057
3	2.9302	2.9296	0.0006
4	2.9281	2.9261	0.002
5	2.9319	2.9278	0.0041
6	2.9353	2.9293	0.006
7	2.9416	2.929	0.0126
8	2.933	2.9148	0.0182
9	2.9397	2.9285	0.0112
10	2.9385	2.9137	0.0248

Table 12: Alternate submersion Test 2 small samples

Sample #	Initial Mass (g)	Final Mass (g)	Change in Mass	Interval Change
1	0.0916	0.0914	0.0002	0.0002
2	0.0924	0.0922	0.0002	5E-05
3	0.0911	0.0911	0	0
4	0.0924	0.0923	0.0001	0.0002
5	0.0922	0.0922	0	-0.0003
6	0.0925	0.0925	0	-0.0004
7	0.0924	0.0922	0.0002	-0.0005
8	0.0921	0.092	0.0001	-0.0006
9	0.0922	0.0923	-1E-04	
10	0.0918	0.0923	-0.0005	
11	0.0921	0.0927	-0.0006	
12	0.0917	0.0918	-0.0001	
13	0.0919	0.0924	-0.0005	
14	0.0923	0.0928	-0.0005	
15	0.0908	0.0916	-0.0008	
16	0.0917	0.092	-0.0003	

Works Cited

- ASM Material Information*. (2013, December 11). Retrieved from ASM International:
<http://products.asminternational.org.ezproxy.wpi.edu/hbk/index.jsp>
- ASTM Standard G44-99, Standard Practice for Exposure of Metals and Alloys by Alternate Immersion in Neutral 3.5% Sodium Chloride Solution. (2003). West Conshohocken, Pennsylvania: ASTM International.
- Baboian, R. (1995). *Corrosion Tests and Standards*. Philadelphia: ASTM.
- Bhadeshia, H. (n.d.). *Interpretation of the micro Structures of Steel*. Retrieved October 29, 2013, from Graduate Institute of Ferrous Technology:
http://cml.postech.ac.kr/2008/Steel_Microstructure/SM2.html
- Calle, L. M. (2013, September 28). *Corrosion technology Laboratory*. Retrieved from
<http://corrosion.ksc.nasa.gov/index.htm>
- COMSOL. (2013, January 10). *Laminar Flow in a Baffled Stirred Mixer*. Retrieved from
http://www.comsol.com/shared/downloads/models/cfd_baffled_mixer.pdf
- Cost of Corrosion Study*. (n.d.). Retrieved October 18, 2013, from NACE International:
<http://www.nace.org/Publications/Cost-of-Corrosion-Study/>
- Davis, J. R. (2000). *Corrosion: Understanding the Basics*. Materials Park: ASM International.
- Helmenstine, A. M. (n.d.). *Chemistry*. Retrieved November 14, 2013, from About.com:
<http://chemistry.about.com/od/imagesclipartstructures/ig/Science-Clipart/Steel-Phase-Diagram.htm>

History and Facts. (n.d.). Retrieved October 18, 2013, from Willis Tower:
<http://www.willistower.com/building-information/history-and-facts/>

Kaesche, H. (2003). *Corrosion of Metals: Physiochemical Principles and Current Problems.* Berlin: Springer.

Legat, A. (2007). Monitoring of Steel Corrosion in Concrete by Electrode Arrays and Electrical Resistance. *Electrochemical Methods in Corrosion Research, Vol. 52, Issue 27, 7590-7598.*

Luo, D. R. (n.d.). *Advanced Electrochemistry and Corrosion Prevention.* Taiwan: Industrial Technology Research Institute.

Mario Arenas, G. W. (n.d.). *Aqueous Corrosion Study of Melt-Spun NdFeB Ribbons with TiC Additions.* Tuscaloosa: University of Alabama.

Mechanistic Corrosion Models. (n.d.). Retrieved October 30, 2013, from Corrosion-Doctors:
<http://www.corrosion-doctors.org/Corrosion-Models/Mechanistic.htm>

Metals Knowledge: Hardenability of Steels. (2013, October 14). Retrieved from
<http://news.alibaba.com/article/detail/metalworking/100190133-1-metals-knowledge%253A-hardenability-steels.html>

Mullendore, J. (1951). *Elements of physical Metallurgy.* Addison-Wesley Press.

My Scopetraining for Advanced Research. (2013, Januaray 29). Retrieved from Office of Learning and Teaching: <<http://www.ammrf.org.au/myscope/sem/background/>>.

Pourbaix Diagrams. (2013, November 19). Retrieved from Western Oregon University:
<http://www.wou.edu/las/physci/ch412/pourbaix.htm>

Principles of Corrosion. (2013, October 25). Retrieved from Metallurgy & Material Engineering:
<http://met-engineering.blogspot.com/2009/06/principles-of-corrosion.html>

Sedriks. (1996). *Corrosion of Stainless Steels*. Princeton: Wiley-Interscience.

Soares, C., Garbatov, Y., & Zayed, A. (2005). *Non Linear Corrosion Model for immeresed Steel Plates Accounting for Enviromental Factors*. Jersey City: Society of Naval Architects and Marine Engineers.

Stainless Steels. (2013, January 25). Retrieved November 14, 2013, from Material Engineers:
<http://www.materialsengineer.com/E-Stainless-Steel.htm>

Stainless Steels. (2013, September 2). Retrieved from Materials Engineer .com:
<http://www.materialsengineer.com/E-Stainless-Steel.htm>

Talbot, D., & Talbot, J. (1998). *Corrosion Science and Technology*. CRC Press.

Uhlig, H. H. (1971). *Corrosion and Corrosion Control*. New York: Wiley.

Vander, V. G. (2004). *Metallography and Microstructures*. Materials Park: ASM International.

William D. Callister Jr., D. G. (2010). *MAterials Science and Engineering: An Introduction*.
John Wiley and Sons.